Tisk této publikace byl podpořen z projektu:
„Tvorba mezinárodního vědeckého týmu a zapojování do vědeckých sítí v oblasti nanotechnologií a nekonvenčního tváření materiálu“, reg. č. CZ.1.07/2.3.00/20.0038
podporovaného Operačním programem Vzdělávání pro konkurenceschopnost, spolufinancovaného z Evropského sociálního fondu a ze státního rozpočtu České republiky.

Autor:	kolektiv autorů
Pracoviště:	VŠB-Technická univerzita Ostrava Fakulta strojní
Název:	Sborník příspěvků z workshopu „What I can to offer“
Místo, rok:	Ostrava, 2014
Počet stran:	94
Vydala:	Vysoká škola báňská – Technická univerzita Ostrava, FS, Katedra mechanické technologie

Za obsah příspěvků odpovídají jednotliví autoři.

Vysoká škola báňská – Technická univerzita Ostrava, 2014

ISBN 978-80-248-3473-3

Nanotým VŠB – TU Ostrava
CZ.1.07/2.3.00/20.0038

INVESTICE DO ROZVOJE VZDĚLÁVÁNÍ

Nanotým VŠB – TU Ostrava

CZ.1.07/2.3.00/20.0038

WORKSHOP

„What I can to offer“

2. – 4. února 2012

Sborník příspěvků

Hotel Ráztoka***, Trojanovice, Česká republika
2012

Project name:	Creation of an international team of scientists and participation in scientific networks in the sphere of nanotechnology and unconventional forming material.
Program:	Operational Programme Education for Competitiveness
Priority Programme:	2 - Tertiary Education, Research and Development
Support area:	2.3 - Human resources in research and development
Registration number:	CZ.1.07/2.3.00/20.0038
Project start date:	1. June 2011
Project closing date:	31. May 2014
Project applicant:	VŠB - TU Ostrava
Project partner:	COMTES FHT a.s.
Administrative team:	Main project manager – prof. Ing. Stanislav Rusz, CSc.
	Project coordinator – Ing. Jan Kedroň
	Finance manager – Ing. Stanislav Tylšar

Nanoteam VSB – TU Ostrava
CZ.1.07/2.3.00/20.0038

WORKSHOP
„What I can to offer“

Proceedings

2nd – 4th February 2012
Hotel Ráztoka ***
Trojanovice, Czech Republic

VŠB – Technical University of Ostrava, Faculty of Mechanical Engineering, Department of Mechanical Technology, 2014

evropský sociální fond v ČR
EVROPSKÁ UNIE
MINISTERSTVO ŠKOLSTVÍ, MLÁDEŽE A TĚLOVÝCHOVY
OP Vzdělávání pro konkurenceschopnost
INVESTICE DO ROZVOJE VZDĚLÁVÁNÍ

SUMMARY OF RESEARCH AND DEVELOPMENT ACTIVITIES IN THE RANGE OF STEEL STRIP AND EXAMPLES OF RESULTS

Josef BOŘUTA [a], Vladimír DĚDEK [a], Tomáš KUBINA [b]

[a] *MATERIAL AND METALLURGICAL RESEARCH Ltd., Pohraniční 693/31, 706 02 Ostrava – Vítkovice, CZ, josef.boruta@mmvyzkum.cz;* [b] *VŠB - TU Ostrava, 17. listopadu 15, 708 33 Ostrava - Poruba, CZ,*

Abstract

In the institute MATERIAL AND METALURGICAL RESEARCH Ltd. originaly creating a part of the company VÍTKOVICE and now independent, a branch of forming research has already been existing for almost 60 years [1]. Technological methods of testing hot formability of steel, such as the impact of bending and upsetting tests, developed and used during the sixties, enabled a study of the effects of base deformation conditions, such as temperature, heating, degree and rate of deformation and stress condition, on formability and sensitivity to hot shortness. In those days it was possible to perform even interrupted torsion tests with longer between individual deformations. At the present time the plastometer SETARAM have the second generatin of control computer. Possibilities of plastometric tests will be demonstrated on the simulation of hot rolling steel strip for to achieve a very fine microstructure.

The main part of this article is based on complete processing of 25 grades of carbon and low-alloyed steel strip by cold rolling to the limit options determined by cold formability. Also will be described methodology of evaluation of formability of cold formed steels. In the field of cold formability of steel testing the conventional tensile test is mostly used in normal practice. Other aspects of changes of mechanical properties of strain hardened steel and also classification and charakteristics of tested strip steels according to their cold formability will be shown.

Keywords

Material and metallurgical research, forming research, torsion plastometer, steel strip, cold strip, microstructure, mechanical properties, cold deformation, cold formability.

1. INTRODUCTION TO TORSION TEST

Micro alloyed and thermo-mechanically rolled steel grades are already standardized according to EN10149-2 with minimum yield strength values from 315 to 700 MPa. However, further intensive research is underway. According to [2] it is generally accepted that at currently used technologies of thermo-mechanical forming the achieved grain size of 4 - 5 micrometers is optimal for requirement of certain minimum plastic properties.

Plastometric test are made on plastometer SETARAM at accurate and controlled thermo-dynamic conditions. This is possible thanks to the many changes including the upgrading the control computer. For a better understanding of plastometric tests we differ four basic test made

under different condision. Continual torsion test is made under constant temperature and strain rate to fracture Isothermal interruption torsion test (IITT) is made under constant temperature and strain bat with interruption between the same deformations. Anisothermal interruption torsion test (AITT) is simillar to isothermal interuptions test, temperature after first deformation isn't control by computer and during the test temperature naturally decreases Last is Plastometric simulation - here each deformation is defined by temperature, strain and strain rate. Also dwell between deformations may be different.

2. PHYSICAL SIMULATION OF DIFT FORMING

2.1 Use of anisothermal interruption torsion test to prepare physical simulation

For our example of physical plastometric simulation using plastometer SETARAM-MMV we used inspiration [2] of deformation-induced ferrite transformation (DIFT). The trials were performed on material for shipbuilding sheets grade 1.0583.

In case of the steel that we tested we first needed to specify optimum temperature for DIFT, since the steel that we investigated had higher carbon content. That's why at first we used earlier-developed procedures of anisothermal interruption test (AITT) in order to determine characteristic points of transforming austenite to ferrite, co-effected by previous forming.

The test was performed after reheating with holding time of 5´at temperature of 1200°C, cooling down to first deformation temperature of 1000°C with one minute holding time. After the first deformation the AIT was performed without reheating regulation, i.e. temperature dependency was influenced especially by the state of structure and thermal-mechanic testing parameters – however, these were maintained at constant levels – deformation of 0.2 and deformation speed of 0.5 s^{-1}, intermissions 5 s – natural cooling. The trial ends when samples' formability under current conditions is spent - fracture, or an interruption can be scheduled to analyze the achieved structural state.

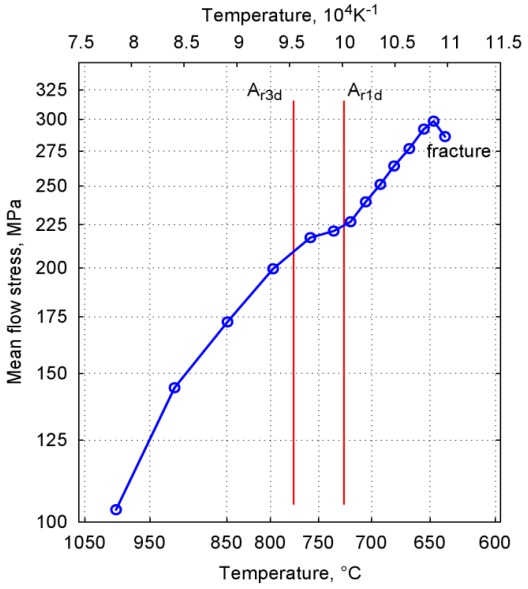

Fig. 1 Evaluation of AIT shown on previous picture, marking deformation-affected transformation points.

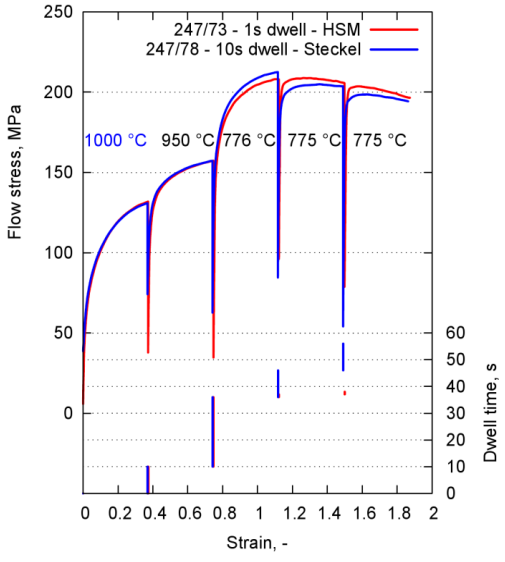

Fig. 2 Detailed comparison of physical simulation outputs of DIFT for HSM and STECKEL

2.2 Physical simulation in the area of dual-phase structure states – DIFT physical simulation

For our example of plastometric simulation using plastometer SETARAM-MMV we used inspiration [2] of deformation-induced ferrite transformation (DIFT). In order to achieve state of dissolving microalloying elements, material was first reheated to 1200°C with holding time of 5 minutes. The purpose of the first reduction at approximately 1000°C is to refine austenitic grains by re-crystallization – this should have a positive impact on DIFT. The purpose of the second reduction at temperatures of 950 - 930°C is to utilize the fastest course of precipitation (Nb, V)(C, N), that should, at the same time, accelerate kinetics of DIFT. At last, three reductions at 820°C are considered [2] a DIFT rolling. However, based on Fig.1 it is clear that temperature for DIFT has to be lowered to approximately 780°C. On Fig. 2 is direct compare the curves of flow stress at different dwells in DIFT forming area (HSM – 1s, STECKEL – 10s). Nature of curves in fourth and five deformation is different. For continuous rolling and one second dwell, curve has not marks of softening between deformations. Some marks of little softening between deformations has simulation of reversions rolling (STECKEL).

3. METHODOLOGY OF EVALUATION OF FORMABILITY OF COLD FORMED STEELS

For evaluation of cold formability in the particular process a production forming test performed on the given production equipment up to the limiting state of material formability is the most advantageous. Such a test respects both entire properties of the formed material and also peculiarities of the technological process, e.g. friction, stress condition, etc.

For general evaluation of cold formability of steel, mostly resulting values of mechanical properties or other variables found out from the initial material by means of simple cold tensile test, conducted at the ambient temperature of +20 °C, are used.

As a very suitable criterion of formability of steel in cold state K_{ts} parameter according to the following relation between elongation and yield strength was introduced [3]:

$$K_{ts} = \frac{A_{10}}{R_{p0,2}} \tag{1}$$

where the value of A_{10} is elongation in % and the value of $R_{p0,2}$ yield strength in MPa. At carbon and low alloy steels with different C content and ferritic structure K_{ts} values vary from 0.01 to 0.14, whereas in steels with austenitic structure this criterion fluctuates around the value of 0.3.

Tab. 1 Classification and characteristics of tested strip steels according to their cold formability

Steel Grades		K_{ts} [%MPa^{-1}]	α_{FR} [°]	ε_{FR} [%]	character of cold formability
A o	Low-Carbon, rimmed and semi-killed, max 0.20 %C	0.118 - 0.162	180	90-95	excellent to very good
B Δ	Low-Carbon, killed, max 0.20 %C	0.091 - 0.130	180	85-95	
E ■	Higher-Carbon plain, soft annealed, 0.45-0.85 %C	0.043 - 0.097	180	70-85	very good to difficult
F ♦	Higher-Carbon low-alloy, soft annealed, 0.50-0.80 %C, 3% Σ alloy max	0.035 - 0.070	180	45-80	
C □	Higher-Carbon plain, not heat treated 0.45-0.85 %C	0.020 - 0.065	40-140	35-70	good to difficult
D ◊	Higher-Carbon low-alloy, not heat treated 0.50-0.80C, 3% Σ alloy max	0,010 - 0.027	45-75	35-50	difficult to poor

With growth of this value cold formability of steel grows up, too. An advantage of this criterion consists in simplicity and physical justifiability because K_{ts} value includes the influence of both initial structure defects (R_e) and their interaction with dislocations at cold deformation on formability up to limiting state (represented by the value of elongation A). With decrease in Re value and increase in A value (both values feature a growth of cold formability) K_{ts} always grows.

In Tab. 1 values of limiting bending angles to fracture (α_{FR}) and also values of limiting rollability (ε_{FR}) are assigned for carbon and low carbon steels according to this criterion. In the table classifying formability of cold steel strips also a specification of particular steel groups according to similarity in deformation behavior (A, B, C, D, E, F) is given (see Tab 1).

4. CHANGES OF MECHANICAL PROPERTIES OF STRAIN HARDENED STEEL

With the growing total deformation size the strength properties of cold forming steels are gradually increasing and plastic properties decreasing. The changes are found out by tensile tests of the initial and cold formed material, performed at the ambient temperature.

Knowledge of stress – strain curves for different grades of cold formed steels and their different initial structural states has a significant practical meaning for determination of equivalent stress of the strain hardened material, needed for calculation of forming forces (forming pressures etc.) and for control of mechanical properties of the cold formed metal with the different total deformation size.

An example of the stress – strain curve for a low carbon low alloy steel with 0.2 % Mo is given in Figure 3.

For cold formed steels with ferritic structure the following Hollomon mathematical relation between values of real (actual) normal stress σ_{sk} and real (actual) cold deformation e, for the area of homogeneous plastic flow during tensile test, is valid with relatively good accuracy:

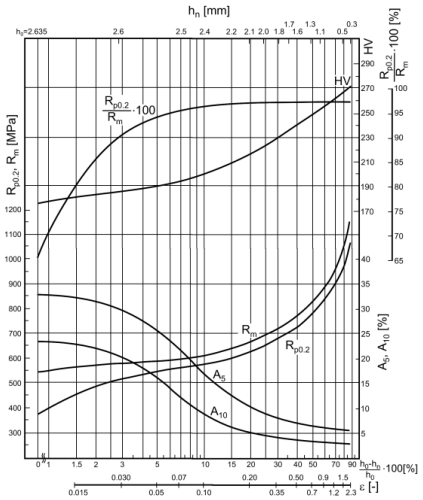

Fig. 3 Effect of cold deformation on mechanical properties of low carbon low alloy (0.2 Mo) steel. The steel strip with initial dimensions 225 x 2.635 mm rolled in non-heat treated state up to limiting possibilities.

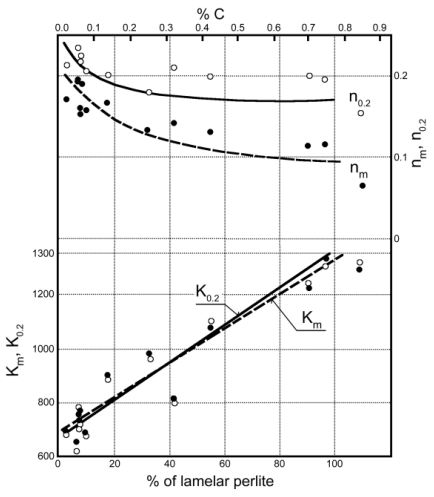

Fig. 4 Influence of wt. % of carbon and lamellar pearlite on parameters in relations (4) and (5).

$$\sigma_{sk} = K\, e^{n} \tag{2}$$

where K is constant dependent on material, and n is index of strain hardening, K is valid for logarithmic strain ratio e = 1 and is given in MPa, and

$$e = \ln\left(\frac{h_0}{h_n}\right) \tag{3}$$

where h_0,, h_n is strip thickness before and after cold deformation.

A good validity of relation (2) was also proved in practice for values of normal stress, i.e. for relationships between $R_{p0,2}$ and R_m on one side and e on the other side, namely for the range of values of cold reduction ε = 5 to 65 % which correspond to values of logarithmic strain ratio e = 0.05 to 1.0 according to relation (3).

$$R_{p0,2} = K_{0,2} e^{n_{0,2}} \tag{4}$$

$$R_m = K_m e^{n_m} \tag{5}$$

From equations (4) and (5) it is possible to calculate (at least approximately) mechanical values (flow stress) of strain hardened steels with basic ferritic structure for the selected value of total logarithmic strain ratio e and with known values of variables K and n.

For strain hardened steels with initial austenitic structure these relationships are not accurate any more. In Fig. 4 material constants for equations (4) and (5) for carbon unalloyed steels in the as-rolled unannealed state are determined, which enable approximate determination of mechanical properties of steel strip after cold deformation in the range of 5 - 65 % [3].

5. TECHNOLOGICAL BENDING TESTS

In the field of cold formability of steel testing the conventional tensile test is mostly used in normal practice. Technological testing of rollability of steel on the production technological equipment is also used with cold rolled strip (ε_{FR} in Tab. 1).

Further extension of cold formability testing methods has brought about the introduction of technological bending tests in 1978 [1,3]. This test, performed on a specially designed bending device, enables to test technological cold bendability of steel by application a bending bar with selectable diameter, determination of the limit angle of bending to fracture and of the rate of elastic recovery after bending [1,3].

Examples of interesting relationships of bendability characteristics of cold rolled strain hardened steel strips are shown in Fig. 5. In this figure, maximum acceptable cold reductions ε in dependence on C content are shown for carbon unalloyed steels cold rolled in non-heat treated state. Surpassing of these maximum reductions would lead to non-

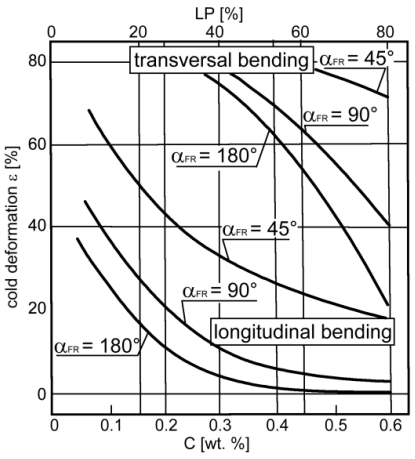

Fig. 5 The effect of strain of unannealed cold rolled strips (ε up to 70 – 80 %) from C-steels on α_{FR} at cold bending - transversal and longitudinal (rB = h). 0.05 to 0.6 % C

achievement of the required bending angle α_{FR}. In the figure the values for ensuring bending angle of 45°, 90°, or 180° are given. Because bendability characteristics are extraordinarilly directionally dependent, the values for the guarantee of bend for longitudinal and transversal direction are considerably different. This direction is in association to orientation of the bending edge in relation to fibers direction.

The Department of Forming Research prepared a comprehensive Atlas of Formability Characteristics of Cold Rolled Steel Strip already in 1978 [1,3]. Preparation of the Atlas, representing work unique in the Czech Republic, enabled subsequent mathematization of relations occurring between steel composition and structure, size of total cold deformation and technological formability, and further determination of cold formability criteria as well as classification of strip steel grades as to their formability.

6. CONCLUSION

The article is a follow-up to the report [1], it adds new information to the report. Currently the universal torsion plastometer SETARAM-MMV was updated, especially control and evaluation of performed experiments. This improved the existing equipment and extended its experimental possibilities. This relates mainly to extended possibilities and specified parameters of physical simulation of forming process, without the troubleshooting influence of external friction [4]. For the purposes of research, mainly of thermal-mechanic processing and optimization of thermal treatment that follows after hot forming, it was necessary to ensure proper cooling for temperatures in the area of phase transformation of austenite to ferrite and/or pearlite and bainite all the way to temperatures close to 400°C. While preparing the plastometer to perform physical simulations in this temperature range, frequent interventions to control software were performed in order to allow gathering data outputs also for these temperature ranges. Currently, using this methodology, it is possible to monitor behavior of Ø 6 mm test bars to temperatures of 400 °C at cooling speed of max. 4°C/s. Presented results of formability of cold rolled steel strips will add a structural analysis in the following period.

7. LITERATURE

[1] Bořuta J. et al.: History and present days of Materials Forming Research in VITKOVICE. In. Plasticity of Metallic Materials, Gliwice : Silesian University of Technology Gliwice, 2004, pp. 95-142. ISBN 83-7335-197-3.

[2] Zrník, J. - Kraus, L. - Prnka, T. - Šperlink, K.: Evropská strategie výrobních procesů (4) - Příprava ultrajemnozrnných a nanokrystalických kovových materiálů extrémní plastickou deformací a jejich vlastnosti, Ostrava : Repronis, 2007, ISBN 978-80-7329-153-2.

[3] Dědek V. - Bořuta J.: The prediction of the cold formability and properties of carbon and low-alloy band steels, In. International symposium on the plasticity and resistance to metal deformation, Herceg Novi, April 1986, pp. 408 -423.

[4] Plášek, B.- Tittel, V.: Lime-based Lubricants improve wire drawing. Wireworld International, Vol. 29, No. 2. 1987, pp. 33-34.

Acknowledgement

This contribution was created within the project **Creation of an international scientific team and incorporation to scientific networks in the area of nanotechnology and unconventional forming material. CZ.1.07/2.3.00/20.0038**, which is financed by the European Social Fund and state budget of the Czech Republic.

european social fund in the czech republic
EUROPEAN UNION
MINISTRY OF EDUCATION, YOUTH AND SPORTS
OP Education for Competitiveness
INVESTMENTS IN EDUCATION DEVELOPMENT

The Rotary Die Equal Channel Angular Pressing System

Tibor DONIČ [a], Ronald BAŠŤOVANSKÝ [a], Silvester POLJAK[a]

[a] *University of Žilina, Faculty of Mechanical Engineering, Department of Machine Buildings and Machine Parts, University street No.1, 010 26 Žilina, Slovak Republic, tibor.donic@gmail.com, ronald.bastovansky@fstroj.uniza.sk, silvester.poljak@fstroj.uniza.sk*

Abstract

For the purpose of creating nanostructures in metallic materials, especially in powder preparations based on aluminium was designed a special experimental system. This system has a very simple way to ensure repeat deformation group procedure that functional part of the system is able to rotate. For this reason, created a computer model of the functional parts of the ECAP, which was then used for deformation group of the design drawings. Blanks for the experimental work was 99,9 % aluminium powder, which was compressed pressure of 600 MPa, then the forward extruded and that the sample was then used in ECAP system. Universal deformation system Rotary Die ECAP was used in the process of static deforming – hydraulic press, but also at higher speeds on Cam plastometer and also for high-speed deformation – HILTI system. Metallographic analysis of products derived from these types of deformation were analyzed in detail. Because the samples before the actual process of ECAP – Rotary Die, were not individual particles and sintered aluminium powder were substantially covered with oxide layer and the operatio of forward extrusion the oxide layer is not perfect destructed and consequently the process sefdiffusion pure aluminium material is very limited. This shortcoming could not be eliminated by the operation nor ECAP Rotary Die as demonstrably proven by metallographic analysis. Upgrade of Rotary Die ECAP with the possibility of heating the functional parts would be a promising procedure for the procedure diffusion activation between aluminium particles which would result in a homogenous ultra fine metal aluminium structure.

Keywords

Aluminium powder, forward extrusion, ultra-fine aluminum microstructure, ECAP, metallographic analysis, cam plastometer, high strain rate.

1. INTRODUCTION

A new ECAP process method called the rotary - die equal channel angular processing (RD – ECAP) method was developed at Japan´s National Institute of Advanced Industrial Science and Technology of Nagoya to form fine – grained bulk materials such as aluminum alloys, aluminum composits, magnesium alloys and titanium. In this paper, the RD – ECAP process is explained and it is use in the processing static and dynamic deformation conditions of aluminum powder of size particals 1 μm. However, in conventional ECAP method, the billet must be removed from the die and reinserted back for the next processing, making the process inefficient. Using the

RD – ECAP method, up to 4 passes of ECAP – style severe plastic deformation is possible without billet removal.

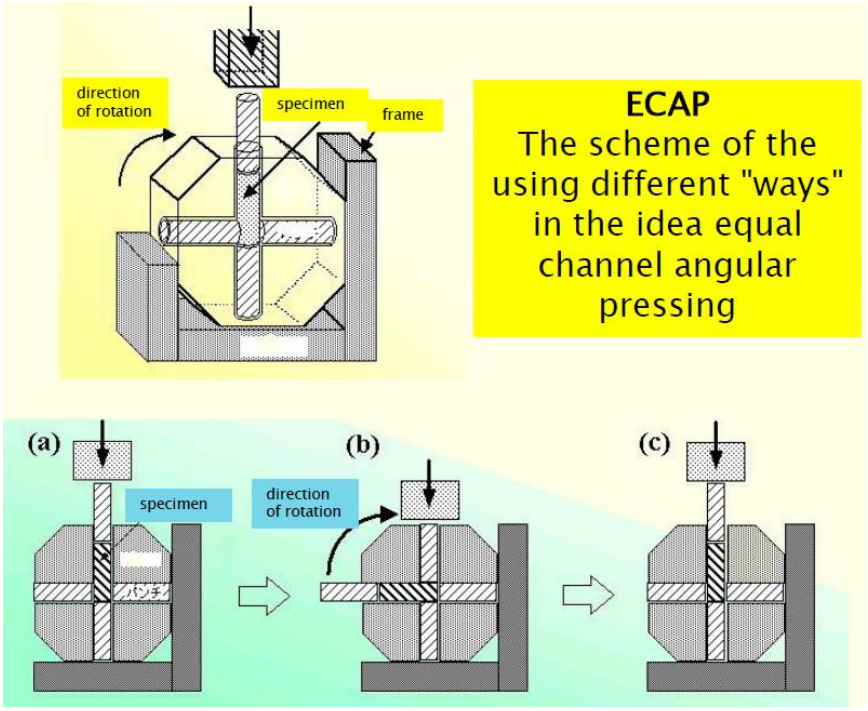

Fig. 1 Schematic diagram of rotary – die equal channel angular processing. Inital state (a), offer the pass (b), after 90º die rotation (c)

Schematic diagrams of the RD – ECAP method are shown in Fig.1. It consists of four cylindrical channels meeting at the center of the rotary die and four punches in the corresponding channels. The sample is set into the center of the hole. Then, the four punches are placed into the holes from the four directions and the die is set on a die holder. The sample is extruded to the left direction because the right punch and the bottom punch are locked in place due to contact with the die holder. After this extrusion, the die is rotated clockwise 90º to the initial configuration with the exposed punch at the top, and a second pressing is performed.

2. MATHEMATICAL MODEL OF NEW RD – ECAP

For construction of deformation system RD – ECAP was necessary to propose mathematical models that respect the basic design requirement.

Mathematical models must comply with desing and technological requirements for the production of this experimental system. The construction must ensure the conditions of universality, that is operative confusion functional parts of the tool. The creation options for the deformation of samples of different diameters to 12 mm in diameter, of course other shapes.

The basic presentation of the mathematical model of RD – ECAP is shown in Fig. 2.

Deformation system RD – ECAP is predominantly loaded by extreme tensile stresses, which spread from the center of plastic deformation, in the centre, where the deformation of the channels cross.

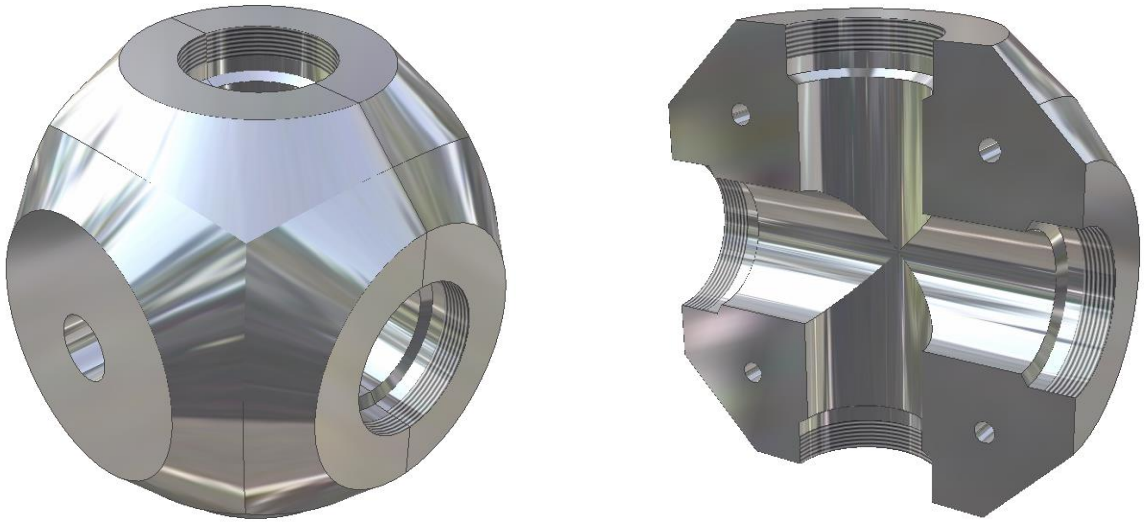

Fig. 2 Principal mathematical model of new RD – ECAP system

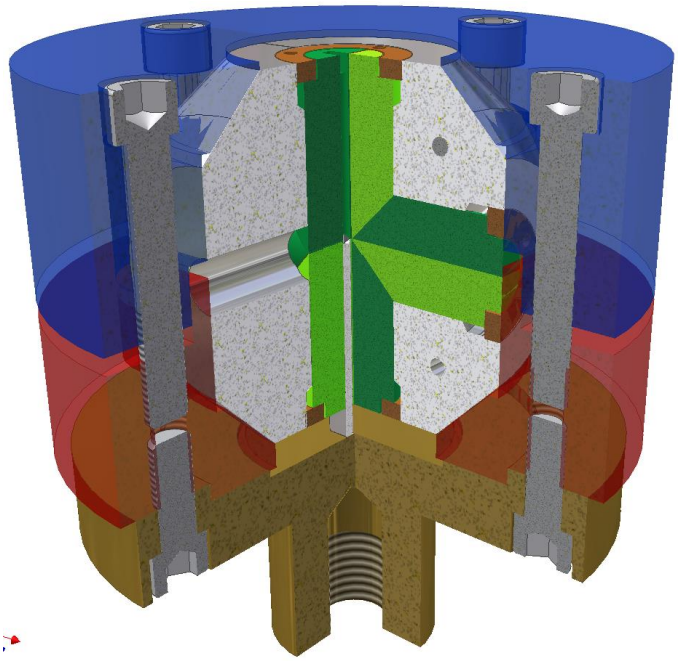

Fig. 3 The core RD – ECAP system located between two blanking elements

Solid fixation of the central zone of deformation in two spherical shaped blanking elements of fortification is very advantageous term provides a great shape and stiffness of RD – ECAP, Fig.3.

The different stages of decomposition of the RD – ECAP are shown in Fig.4.

The experimental material for verifying the functionality of the new RD – ECAP has an aluminium powder with a particle size 1 μm. Verification the RD – ECAP was carried out under static conditions – Heckert system as well as in dynamic conditions of cam plastometer – Fig.5. and explosive devices HILTI – Fig.6. Deformation Speed cam plastometer to be in the range 2 – 10 m/s fo HILTI 800 – 1200 m/s.

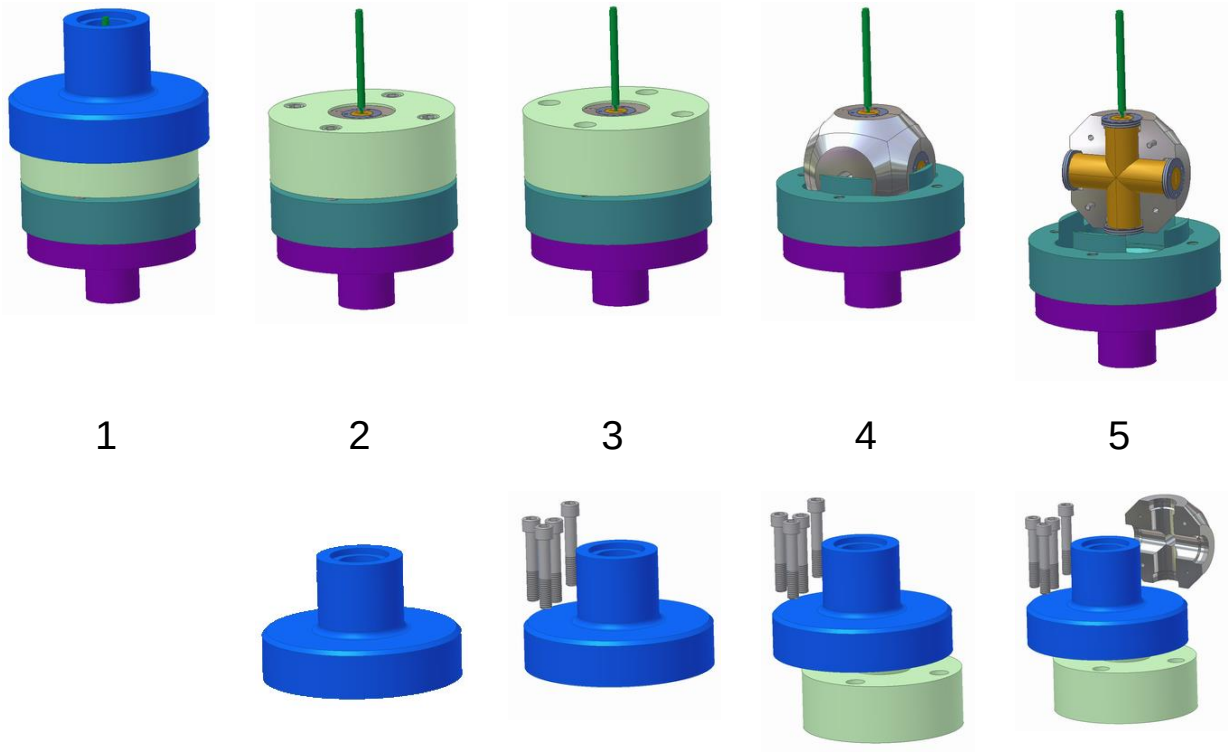

Fig. 4 Different stages of decomposition RD - ECAP

These systems are compact deformation associated with the registration firm Kistler Electric system and recording digital oscilloscope Tektronix TDS 3034. Registration worked very dynamic, crushing forces was smooth. Tightness of the crumple zone was intact, specimens were geometrically perfect.

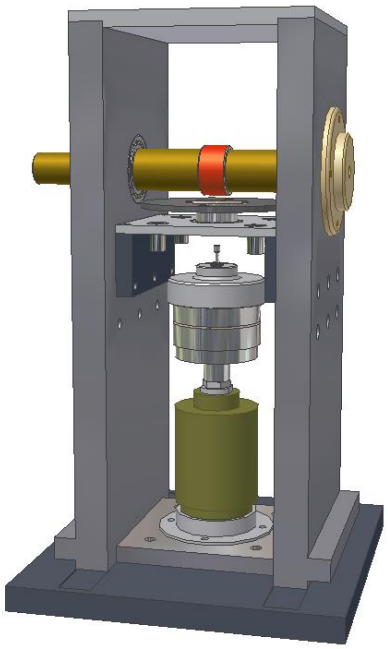

Fig. 5 Experimental dynamic cam plastometer

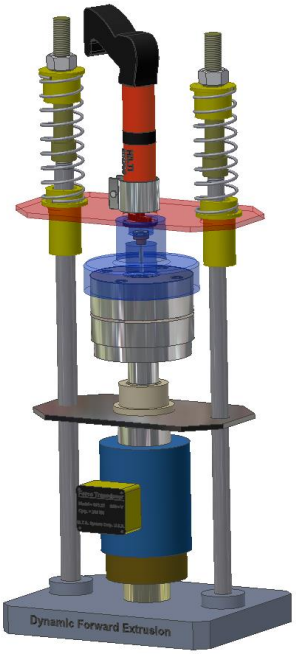

Fig. 6 Experimental high speed system HILTI

3. EXPERIMENTAL VERIFICATION OF THE RD – ECAP

Detail of the dismantling of functional RD – ECAP after deformation is shown in Fig.7 Specimen this case to 3 mm diameter.

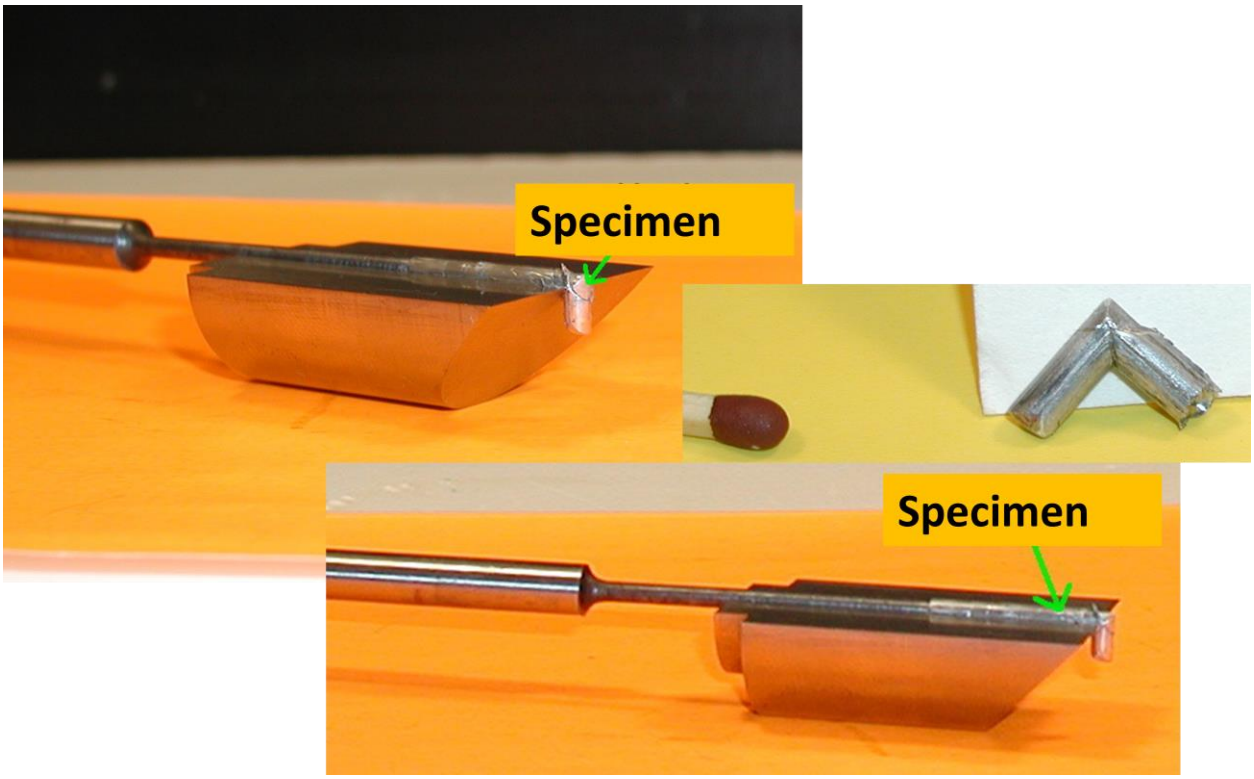

Fig. 7 Decomposition of core RD – ECAP system, specimen 99.99% aluminum powder, partical size 1 μm

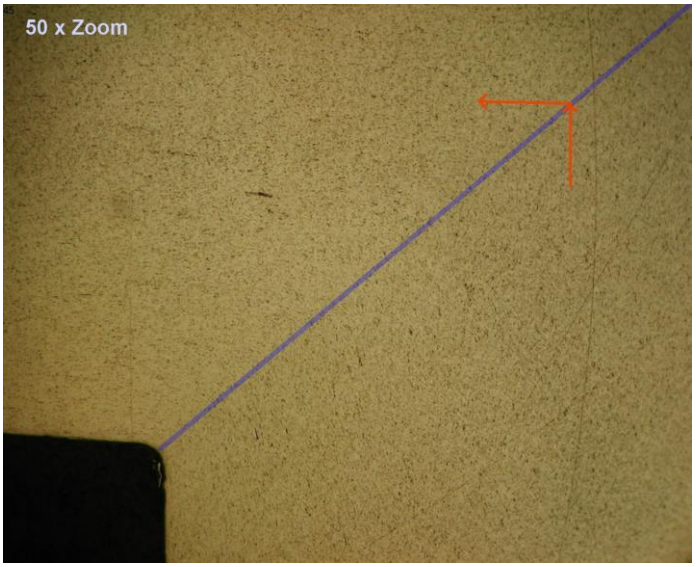

Fig. 8 Microstructure of compaction of aluminum powder in the zone of maximum shear stress of RD - ECAP

Detail of the microstructure of aluminum powder with a particle size of 1μm in the zone of maximum shear deformation is presented in Fig.8.

The zone of deformation identified areas where very likely there was a strong diffusion process of the accumulated strain energy obtained from dynamic shock action. Grain size was below 1μm.

The experimentally obtained load – displacement curves of the plunger for the rotary die equal channel angular pressing is presented in Fig.9. Experimental material is aluminum 99,99% powder, size particles 1 μm.

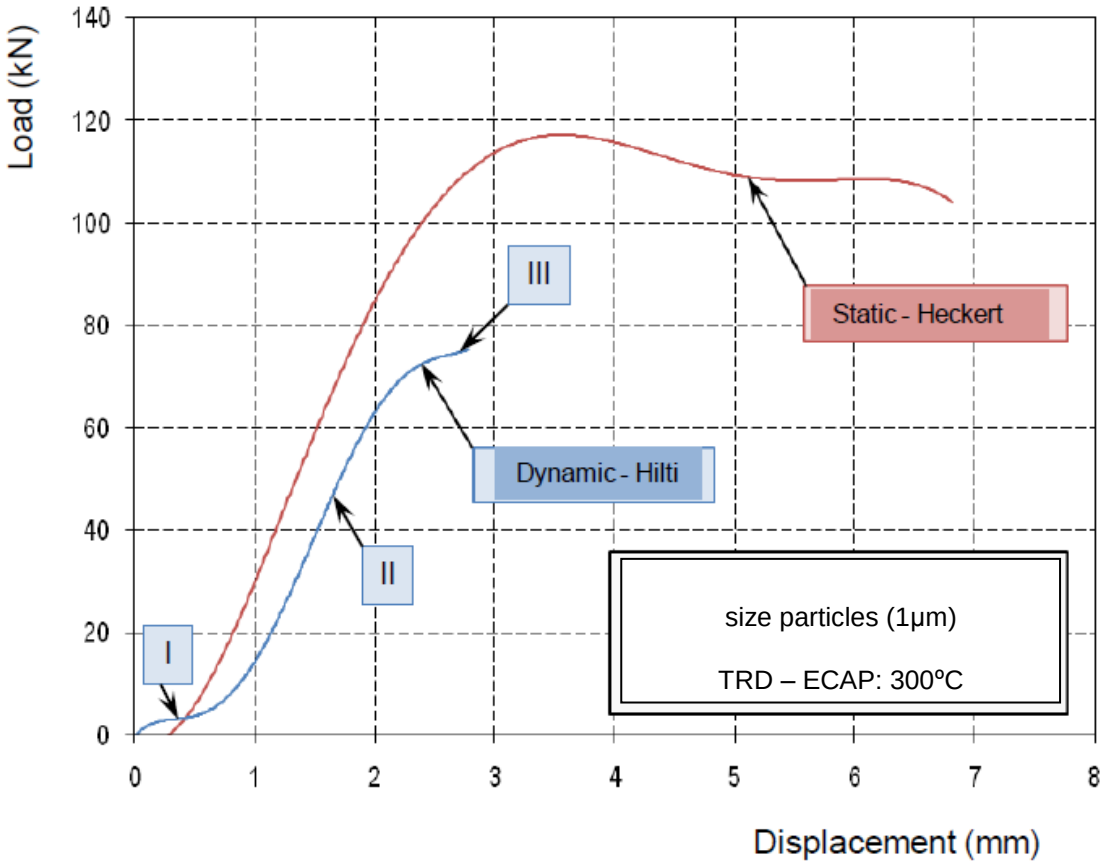

Fig.9 Experimentally obtained load – displacement curves of the plunger for the rotary – die equal channel angular pressing at 300°C, aluminum 99.99% powder, size particals 1μm

The functional dependencies presented in Fig.9. may be made the following conclusions:

- Character, hence the shape of functional dependencies F=f(h) static and dynamic is vastly different
- Incremental increase in dynamic power per unit of time compared to the analogues static change is much more
- Dynamic functional dependency F=f(h) has not monotonous character as the same functional dependence of static
- On functional dependence of the dynamic F=f(h) it is possible to identify at least three distinctive areas, where the first derivate of the path by time i.e. velocity, that rate has different values of acceleration – I, the stable compaction deformation – II and the stead braking – III.

4. CONCLUSION

- ✓ Presented RD ECAP system fulfil extreme requirements on internal and external universality of forming construction - system
- ✓ RD ECAP is possible implemented into three experimental load systems - HECKET, HILTY and CAM Plastometer
- ✓ The heating system module is independent part of system RD ECAP and arrange heating samples up to 700°C
- ✓ RD ECAP system is possible used for circle and square shape of specimens

5. LITERATURE

[1] Donič T., Martikán M., Stoyka v.: Development of Advanced Techniques for Incremental Bulk AlMg3 Nanostructure Alloy Forming. Machine modeling and simulations. Scientific and Technical Society at the University of Žilina, 2009, Horný Vadičov, Slovak Republic, p.215-222, ISBN 978-80-89276-18-9

Acknowledgement

This contribution was created within the project **Creation of an international scientific team and incorporation to scientific networks in the area of nanotechnology and unconventional forming material. CZ.1.07/2.3.00/20.0038**, which is financed by the European Social Fund and state budget of the Czech Republic.

european social fund in the czech republic
EUROPEAN UNION
MINISTRY OF EDUCATION, YOUTH AND SPORTS
OP Education for Competitiveness
INVESTMENTS IN EDUCATION DEVELOPMENT

Aluminum alloy and silver base nanocomposites obtained using powder metallurgy methods

J. Dutkiewicz, W. Maziarz, L. Lityńska-Dobrzyńska

Institute of Metallurgy and Materials Science of the Polish Academy of Sciences Kraków ul. Reymonta 25

1. INTRODUCTION

Recent studies concerning fabrication of Al composite materials using ceramic particles have been reported [1-16]. The most recent research concerning Al matrix composite materials has focused on improving their mechanical properties and the mechanism of sintering of a composite powder [2-13]. The most common used ceramic addition element is Al_2O_3 powder [1-13] of the α allotropic form, however some authors use also ZrO_2 stabilized Y_2O_3 powder addition [14]. There are variety of aluminum alloys used as a matrix for aluminum alloy-ceramic composites, such as 6XXX series [7-15], 2XXX [3, 5, 6], 7XXX [7], or technical purity aluminum [3,16]. The ceramic phase was added to improve elevated temperature behavior [7,10], to improve the abrasive wear characteristics [4,5,14] or simply to obtain higher hardness [2-6,8-11]. In the previous works [1-11] the powder of size of several micrometers was added, however in the more recent works submicron or nanocrystalline powders were added [12-16]. It was reported that mechanical milling allows to obtain uniform distribution of nanocrystalline Al_2O_3 powder. There were also investigations of the matrix grain refinement in 6061/Al_2O_3 composite using Equal Channel Angular Pressing (ECAP) [13]. It was shown that the tensile and fatigue strength of the composite are significantly enhanced by ECAP while the elongation to failure is lower than before ECAP. In [12] the milled 6061 powders with submicrone Al_2O_3 were extruded to obtain bulk samples, while aluminum-nano ZrO_2 composites were prepared by squeeze casting [14]. In other papers [15,16] only milled Al alloy – ceramic powders were investigated without compaction. Therefore, in the present paper nano-composites were prepared from nanocrystalline 6061 or 7XXX alloys milled together with nano size ZrO_2 powder using uniaxial hot pressing in vacuum. The microstructure was studied using TEM technique to resolve structural details in order to explain obtained hardness raise and a compression strength.

Contact materials used in low voltage electric equipment are mainly silver based [17-18]. These are usually well known silver graphite, silver-nickel, and silver-metal oxide materials [17-22]. The metal oxide used is often cadmium oxide (CdO), but because of its considerable toxicity, it should be replaced by other materials [18]. Silver-based refractory contact materials produced by powder metallurgy are used extensively as contact materials due to their high conductivity, good resistance to welding and corrosion properties, high melting temperature and hardness [19-21]. Silver– and domestic circuit-breaker applications where particularly the tungsten refractory materials are used predominantly in industrial products with good weld and erosion resistant properties of these materials are employed. Ag-65 wt.% W composite is the most widely used in air circuit breaker [18-19]. It contains enough silver to be a good conductor. It has less change of welding and greater resistance to arc erosion. Silver–tungsten carbide refractory contact materials are an extension of the silver–tungsten range with similar weld resistance, but

more stable contact resistance throughout the life of the contacts [19-21]. The purpose of this paper is to investigate the microstructure of electrical contact materials based on Ag–W and Ag–amorphous composite based on zirconium easy glass forming alloy [22]. The structure of milled powders within Ag-W system is interesting due to complete immiscibility of tungsten in silver in the solid and liquid state [23] and therefore there is a good electrical conductivity of composites reported in [19]. The stability of the amorphous part during hot pressing as well as the effect of ball milling on the grain refinement and the mechanical properties was also investigated.

2. RESEARCH ON ALUMINUM AND SILVER BASE COMPOSITES AT IMIM PAN

Fig.1 shows a set of optical micrographs taken from immersed in epoxy 40 hours milled powders (a) 6061+10% ZrO_2 and (b) 6061+20% ZrO_2. One can see equiaxial shape of particles of size 5 – 50 μm. The particles are homogeneous and one cannot distinguish coalescence of ZrO_2 additions. In a few places (marked by arrows) one can see cracks due to hardening and fracturing of powder's particles. Their average microhardness measured under load of 1 N is equal to 280 HV for the 40 hours milled powders containing 10% ZrO_2 and 369 HV for the milled powders containing 20% of nano ZrO_2 powder.

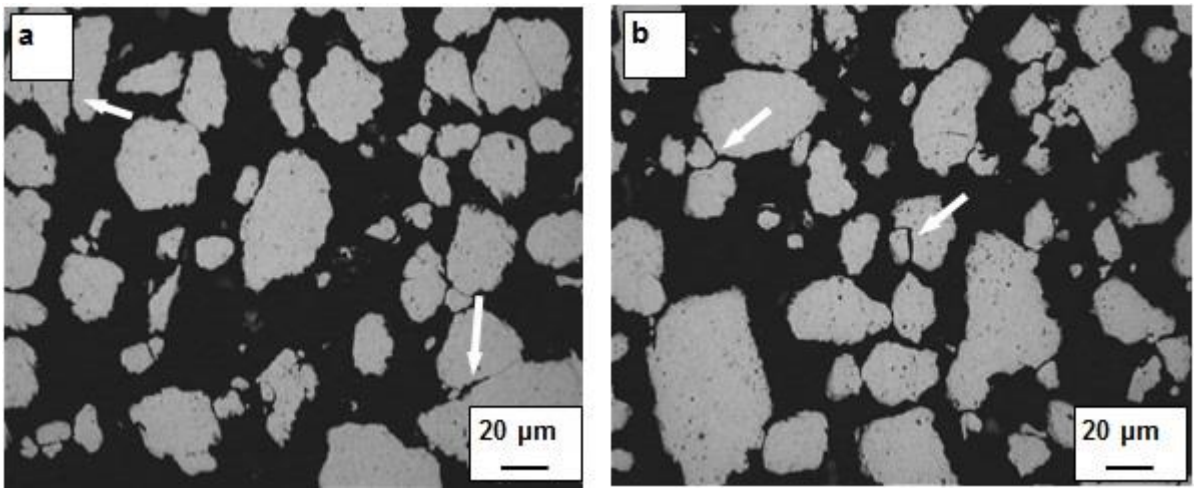

Fig.1 Optical microstructures of (a) 6061+10% ZrO_2 40 hours milled powders and (b) 6061+20% ZrO_2 40 hours milled powders

Fig.2 shows a set of X-ray diffraction pattern taken of 6061 alloy powder mixed initially with 10% and 20 % ZrO_2 taken after various milling times starting from 0, then 5, 10, 20 and 40 hours. One can see broadening of peaks from α(Al) solid solution due to grain size refinement within powder's particles. The amount of the tetragonal ZrO_2 phase seems to decrease after ball milling, however it is difficult to determine the increase of the amount of the monoclinic phase even in the composite containing 20% of zirconia. It can be explained by a small size of ZrO_2 powder which results in formation of extremely fine monoclinic martensite needles formed under deformation during ball milling. It causes formation of diffused peaks from martensite difficult to distinguish from the background.

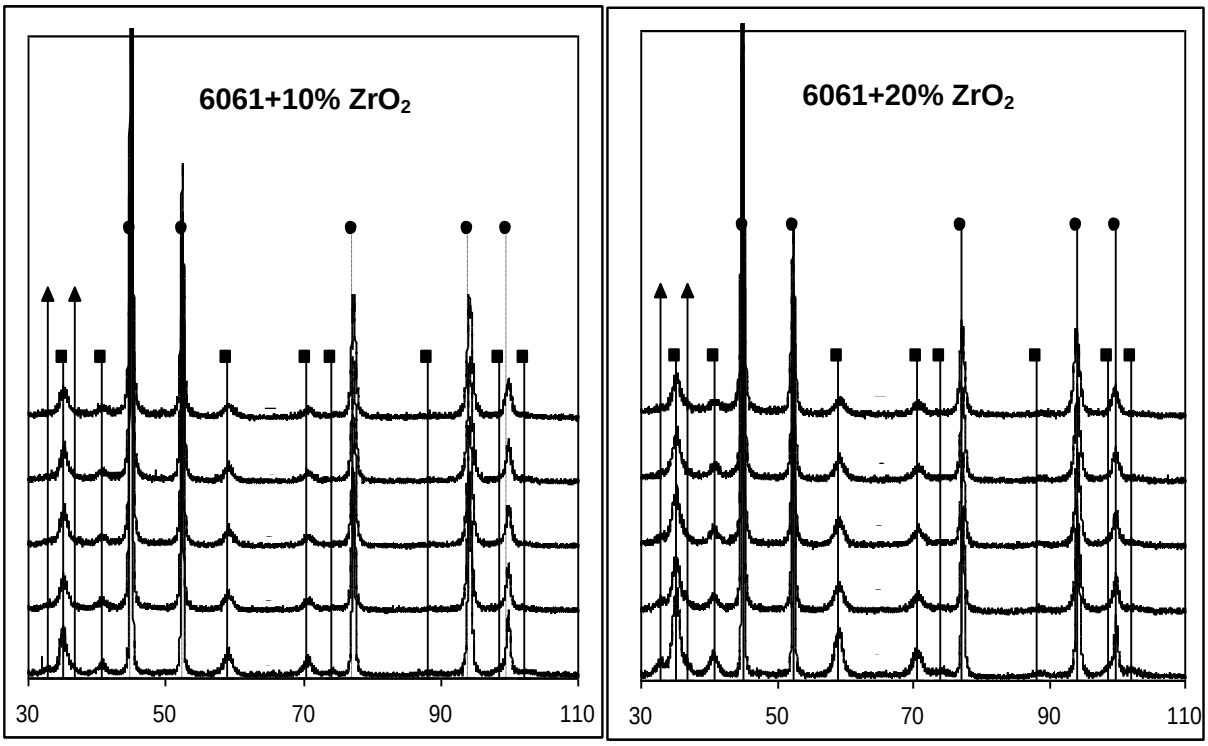

Fig.2 Set of X-ray diffraction curves obtained from 6061+10% ZrO_2 and 6061+20 ZrO_2 powders after various milling times (curve 1 – from initial mixture of powders, curve 2 – 5 hours of milling, curve 3– 10 hours of milling, curve 4 – 20 hours milling, curve 5 – 40 hours milling

Fig.3 shows a set of TEM bright and dark field micrographs and selected area Diffraction Pattern SADP taken from ball milled powders of 40 hours ball milled 6061 alloy powder with 10 % of nano ZrO_2. One can see typical for ball milled powders layered structure resulting from sequence of welding and fracturing of powder's particles. One can distinguish crystals in the reflection positions visible as dark in Fig.3a and one can estimate their average size as 55 nm; similar result one can obtain measuring the size of bright areas in the dark field (Fig.3b). In the SADP one can see ring like reflections, which diameters allow to identify □(Al) solid solution and tetragonal ZrO_2 phase. The small white ring represents the size and position of the objective aperture used to take the dark field micrograph. Similarly like in the X-ray diffraction curves one cannot identify monoclinic phase. Due to extremely small size of ceramic particles it is even difficult to see them in the TEM micrographs, however one can see fine dark in 3a and bright in 3b points, which at higher magnification can be seen as particles giving different contrast as □(Al), which are most probably ZrO_2 particles.

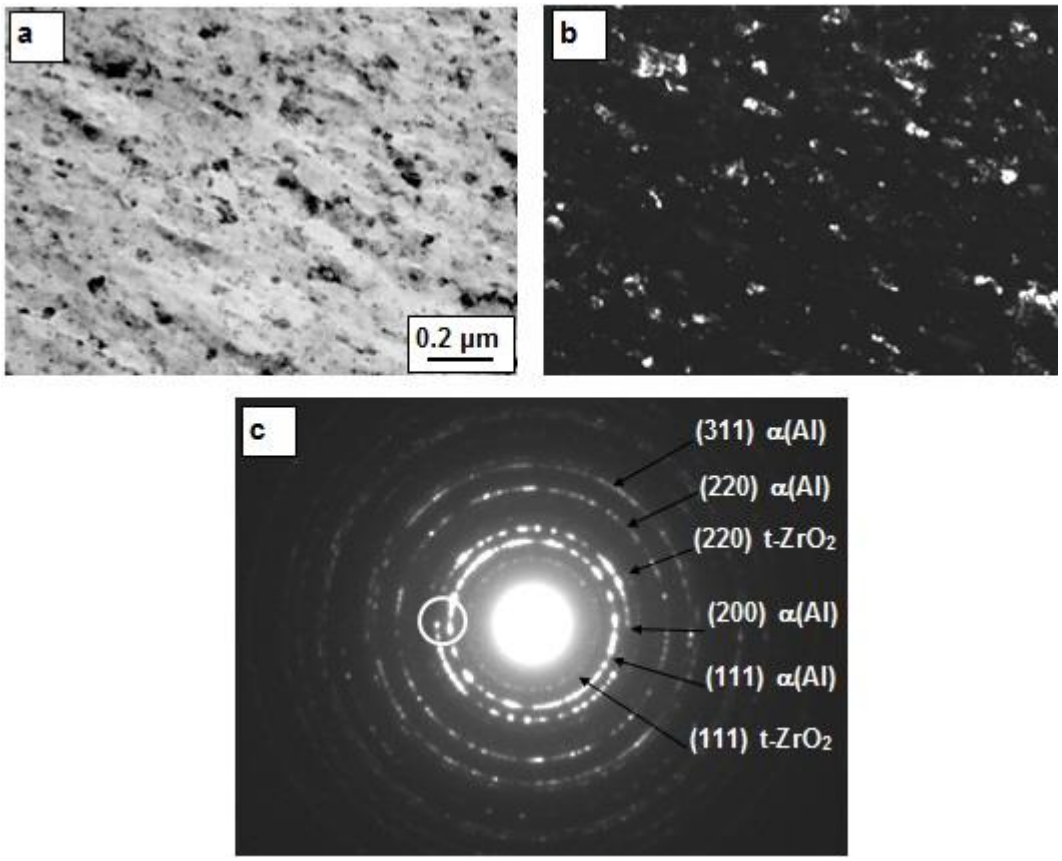

Fig.3 TEM microstructures In the bright (a) and dark field (b) and electron diffraction pat tern (c) from the area in (a) 6061+10% ZrO_2 40 hours milled powder

Figure 1 shows X-ray diffraction curves form the amorphous powder and from 40 hours ball milled composites. Ag + 20% W. One can see a very small grain size of silver and tungsten estimated at 50 nm for silver. Broad halo indicate that most of the amorphous phase is preserved after consolidation at temperatures of 490^{o}C below the crystallization temperature estimated using DSC studies.

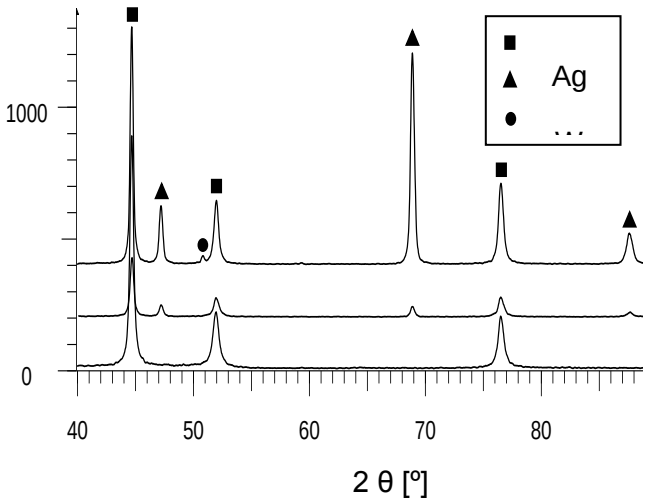

Fig 4. X-ray diffraction curves from compacted ball milled powders of Ag + 20% W and Ag + amorphous ZrCuTiNi

Table I shows hardness of investigated composites. One can see that both types of composites i.e. with the addition of tungsten hardness of the composite increases, however it is lower than that of the composite with the amorphous phase addition which is of the order of 100 HV and at similar conductivity have good perspectives for less erosion than composite with tungsten. In order to see the microstructure of composites SEM structure observations were performed.

Tab. 1 Hardness of composites

Composite	Hardness [HV]
60% Ag + 40% W	87
80% Ag + 20% W	75
80%Ag+20% amorphZr48.5Cu32Ni9Ti10	109

3. LITERATURE

[1] F. V. Beaumont, Int. J. Powder Metall. 36 (2000) 41.

[2] C. Lall, W. Heath, Int. J. Powder Metall. 36 (2000) 45.

[3] Kyung Ho Min, Shin Pil Kang, Dae-Gun Kim, Young Do Kim, J. Alloys Compounds 400 (2005) 150–153

[4] Xian Jia, Xiaomei Ling, Wear 258 (2005) 1342–1347

[5] M. Kők, Composites: Part A 37 (2006) 457–464

[6] L. A. Dobrzański, A. Włodarczyk, M. Adamiak, J. Mater. Proc.Technol., 175 (2006) 186–191

[7] L. Ceschini, G. Minak, A. Morri, Compos. Sci. Technol., 66 (2006) 333–342

[8] Qiang Zhang, Gaohui Wu, Longtao Jiang, Mater. Sci. Eng. A 483–484 (2008) 281–284

[9] G. M. Owolabi, A. G. Odeshi, M. N. K. Singh, M. N. Bassim, Mater. Sci. Eng. A 457 (2007) 114–119

[10] A. M. Klaska, T. Beck, A. Wanner, D. Löhe, Mater. Sci. Eng., A 501 (2009) 6–15

[11] Elisabetta Gariboldi, Antonietta Lo Conte, Compos. Sci Technol., 68 (2008) 260–267

[12] A. M. Al-Qutub, I. M. Allam, T. W. Qureshi, J. Mater. Proces. Technol., 172 (2006) 327–331

[13] L. J. Chen, C. Y. Ma, G. M. Stoica P. K. Liaw, C. Xu, T. G. Langdon, Mater. Sci. Eng., A 410–411 (2005) 472–475

[14] L. Geng, S. Ochiai, H. X. Peng, Lian Gao, Jin Sun, Z. Q. Sun, Scripta Mater., 38 (1998) 551-557

[15] I. Ozdemir, S. Ahrens, S. Műcklich, B. Wielage, J. Mater. Proces. Technol. 205 (2008) 111–118

[16] B. Prabhu, C. Suryanarayana, L. Ana, R. Vaidyanathan, Mater. Sci. Eng. A 425 (2006) 192–200

[17] Keil A.: *Werkstoffe fuer elektrische Kontakte*. Expert Verlag GmbH, Wuertt 1984.

[18] Wojtasik K., Missol W.: Met. Powder Rep. *59*, 34 (2004).

[19] Findik F., Uzun H.: Mater. Des. *24*, 489 (2003).

[20] Slade P. G.: IEEE Trans. Comp. Hybrids Manuf. Technol. *9*, 3 (1986).

[21] Aslanoglu Z., Karakas Y., Ovecoglu M. L.: Int. J. Powder Metal. *36*, 35 (2000).

[22] Ma D., Cao H., Chang Y. A.: Intermetallics *15*, 1122 (2007).

[23] Massalski T. B.: *Binary Alloys Phase Diagrams*, ASM Metals Park, Ohio 1990.

Acknowledgements

This paper was created within the project "**Creation of an international scientific team and incorporation to scientific networks in the area of nanotechnology and unconventional forming material. CZ.1.07/2.3.00/20.0038"**, which is financed by the European Social Fund and state budget of the Czech Republic.

INVESTMENTS IN EDUCATION DEVELOPMENT

Vývoj nových materiálů s požadovanými vlastnostmi: příklad Heuslerovy slitiny

Development of new materials on demand: example on Heusler compounds

Jaroslav HAMRLE [a], Dominik LEGUT [a], Jaromír PIŠTORA [a]

[a] *VŠB – Technická univerzita Ostrava, 17. Listopadu 15, 708 33 Ostrava – Poruba, ČR, jaroslav.hamrle@vsb.cz*

Abstrakt

Vývoj nových materiálů je důležitá oblast dnešní fyziky pevných látek. Mocná technika k vývoji nových materiálů je použití ab-initio výpočtů (tzv. výpočty z prvních principů). Tyto výpočty poskytují elektronovou strukturu systému, ze které se může dále spočítat většina vlastností dané látky, např. transportní (např. vodivost), optické, termodynamické, magnetické vlastnosti, teplotní závislosti, stabilní krystalografické fáze a fázové přechody, vliv krystalogragického neuspořádání atd. Tyto teoreticky navrhnuté a optimalizované materiály jsou pak vyrobeny v objemové formě nebo ve formě tenkých vrstev. Poté prochází sadou krystalografických a spektroskopických testů, aby se otestovala jejich krystalografická a elektronová struktura. Výsledky jsou poté porovnány s ab-initio výpočty. Tato výzkumná posloupnost je v ideálním případě použit iterativně, neboť každý krok (teorie-výroba-charakterizace) poskytuje zpětnou vazbu ostatním krokům.

Klíčová slova

nové materiály, ab-initio výpočty, Heuslerovy slitiny

Abstract

The development of new materials is an important part of today's solid state physics. A powerful way to develop new materials is to include *ab-initio* calculation (called also first principle calculations), calculations providing electronic structure and allowing to calculate most of the material's properties, for example, transport (e.g. conductivity), optical, thermodynamical, magnetic properties, temperature dependences, stable phases and corresponding phase transitions, dependences on crystallographic disorder etc. This theoretically designed and optimized material is then fabricated as a bulk or thin film. Consequently, such a sample is investigated by various crystallographic and spectroscopic tools, in order to probe the crystallographic structure and electronic structure. The results are then compared with *ab-initio* calculations. This investigation chain is ideally employed in an iterative way, as each stage (theory-fabrication-characterization) provides feedback to other stages.

CZ.1.07/2.3.00/20.0038

Keywords

new materials, *ab-initio* calculations, Heusler compounds.

1. INTRODUCTION

Nowadays, there is a large need to developed materials with desired properties. Desired properties may range from special optical, conductive, thermoelectric, magneto-electric etc. properties. Different approaches were established to obtain a given property, such as to develop new bulk materials, or to develop new metamaterials (or composites), a superstructure consisting of already known materials. Here, we discuss on a general way of developing of new materials with a special desired properties, which are bulk and crystalline. As an example, we show development of new materials based on Heusler compounds [1].

2. BULK CRYSTALLINE MATERIALS

The bulk crystalline materials can be described by an infinite number of periodically situated atoms. Then, the electrons inside the material are described by so-called electronic structure, i.e. determining energy, momentum and spin of each electron inside the material. The electronic structure is calculated using *ab-initio* calculations. When the electronic structure is known, most material's properties can be calculated, as material's properties reflect the internal electronic structure of the materials.

3. DEVELOPING AND PREPARATION OF NEW CRYSTALLINE MATERIALS

A way of development of new crystalline materials is sketched in Fig. 1. First, for a given assumed crystallographic structure, electronic structure and required properties are calculated. Using the calculations, structures providing optimal properties. are predicted. Then, such a materials are fabricated, usually first in bulk form, but thin-film fabrication is also possible. In case of Heusler compounds, relatively simple preparation methods such as vacuum melting and consequent vacuum annealing can be used at this stage. The obtained bulk material then passes series of investigations on the crystallographic properties, on the electronic structure and on the desired properties, Then, those results are compared with the *ab-initio* calculations. In ideal case, this procedure goes in an iterative way as each step may require improvement and feedback. Alternative way of material's fabrication is deposition of thin films. In case of preparation of new materials, preferred techniques are those allowing co-deposition of various base materials, such as molecular beam epitaxy (MBE) or pulse laser deposition (PLD).

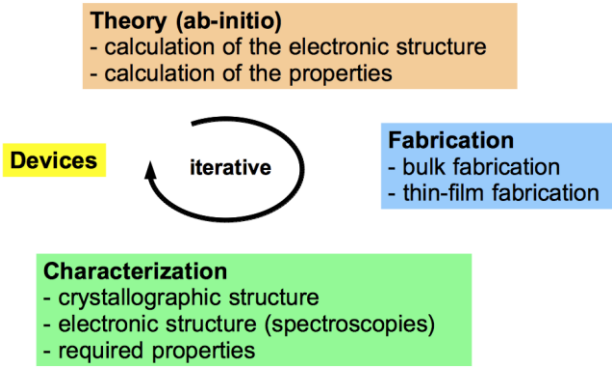

Fig. 1 The sketch of development of new crystallographic material with a required property. The subsequent steps theoretical prediction – material's fabrication – material's characterization are feedbacking each other in an iterative way.

4. CRYSTALLOGRAPHIC PROPERTIES

The first point to be check is usually crystallographic structure of the prepared sample. Many problems may occur during the preparation itself, such as formation of different material phases. Types of crystallographic phases and determination of the inter-atomic distance can be determined by X-ray diffraction (XRD) (see example in Fig. 3). In case of complex systems, such as Heusler compounds, other problem is so-called crystallographic disorder, which means, that not all atoms are in correct atomic positions. In some cases, disorders are problems for desired properties. For example, in case of half-metallic Heusler compounds, for example Co_2FeSi, an ideal ordering is $L2_1$. In case of B2 disorder, i.e. random mixture of Fe and Si atoms, the half-metallicity is preserved. However, in case of DO3 or A2 disorders (when Co atoms are not on a correct position), the half-metallicity disappears. In order to determine amount of each type of disorder, various techniques have been developed. The most simple technique to use is XRD providing long-range disorder level from comparing intensities of the superstructure and fundamental diffraction peaks. However, this does not allow to determine uniquely all types of disorder. Also, for atoms with similar atomic numbers (e.g. Fe and Co), the scattering factor is similar for both atoms and hence difficult to distinguish them by XRD. Therefore, other techniques has been developed, such as determination of short-range disorder using Mossbauer spectroscopy or Nuclear Magnetic Resonance, (NMR) techniques (see Fig. 4). In both techniques, one uses atomic nucleus as a highly local probe of the electronic structure at nucleus position.

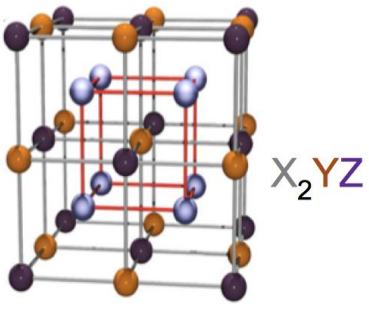

Fig 2 Crystallographic structure of full Heusler compound. In this figure, the structure is fully cryptographically ordered ($L2_1$ order).

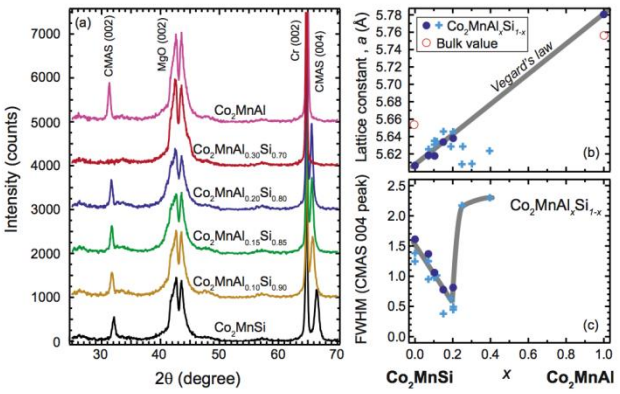

Fig 3 Example of XRD investigation of $Co_2MnAl_xSi_{1-x}$ Heusler compound. Left part of the figure shows theθ-2θ-scan. Right part of the figure shown lattice constant and FWHM (related with the mosaicity), derived from θ-2θ-scan. The ratio of superstructure peak peak intensity (002) and fundamental peak intensity (004) is related with B2 crystallographic disorder (not shown here) [2].

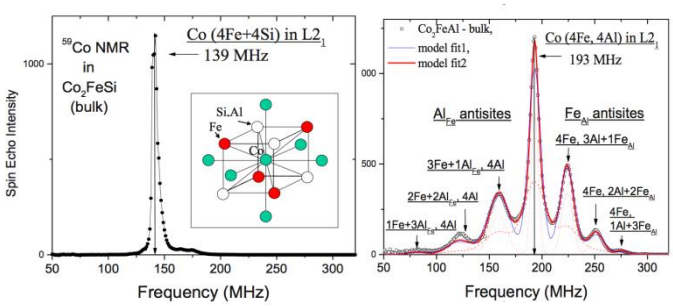

Fig 4 Example on close-range disorder determination using ^{59}Co nuclear magnetic resonance in fully $L2_1$ ordered Co_2FeSi and partly disordered Co_2FeAl. The central peak intensities corresponds to number of Co atoms, which have exactly 4 Fe and 4 Z (Z=Si or Al) atoms. As Co_2FeSi provides only this central peak, it demonstrates that it is fully short-range ordered. On the other hand, in case of Co_2FeAl, satellite peaks shows number of Co atoms having for example having n Fe and m Al atoms (n+m=8), demonstrating at least partial B2 disorder [3].

5. PROBING ELECTRONIC STRUCTURE

There are numerous techniques, which can investigate the electronic structure of the material. Often used technique is photon-photon spectroscopies (basically determining photon absorption in a given spectral range), ranging from infrared-spectroscopy (determination of phonon vibration energies and intraband transitions), optical spectroscopy in visible range (determining intraband transitions, gap-size, gap quality, presence of excitons etc. – see Fig. 5) to X-ray absorption spectroscopy (XAS), determining type of bands, level of oxidization etc. by probing electronic states above the Fermi level. Other spectroscopy technique to probe electronic states are photoemission spectroscopies (photon-in, electron-out), probing electronic states below Fermi level. Powerful variant of this technique is angle-resolved photoemission spectroscopy (ARPES) and inverse-photoemission spectroscopy (IPES, electron-in, photon-out), where the angle of outcoming, incoming electrons is measured and hence allowing to measure dependence of material's electron's energy on electron's momentum. This allows to reconstruct

band structure of the material, i.e. dependence of energy on its momentum, above and below the Fermi level, respectively.

In case of magnetic materials, key information to compare with the *ab-initio* calculations is magnetic moment. In case of spectroscopies, most of above described spectroscopies may have its magneto-optical variant, being sensitive to difference between the part of the band structure corresponding to electrons' spins being parallel and antiparallel with the magnetization direction.

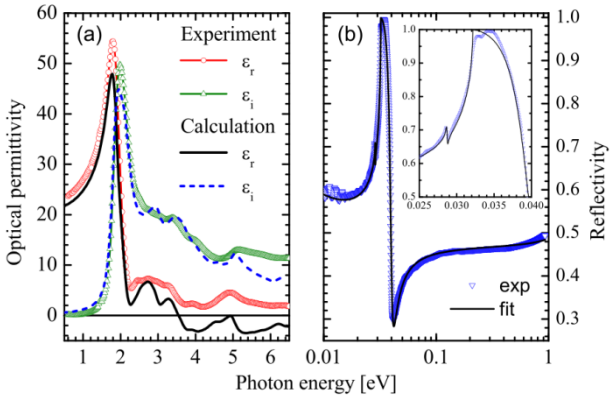

Fig .5 (a) optical permittivity and (b) wide-range infrared reflectivity for thermoelectric semiconducting material CoTiSb. The imaginary part of optical permittivity (i.e. light absorption) clearly demonstrate the presence of gap of width about 2eV, with presence of a strong exciton. The infrared reflection data demonstrates two absorption peaks, originating from light absorption by phonons at those energies [4].

6. CONCLUSION

In conclusion, we did a brief overview, how to design a material with a required properties. The design is based on *ab-initio* calculations predicting a structure of a material with a required properties. Then, such a material is fabricated, usually first in its bulk form. Consequently, its structural characterization is performed, checking present crystallographic phases, interatomic distance, crystallographic disorders etc. Then, the investigations are followed by various spectroscopy investigations, probing the electronic structure of the material. Those investigations run in iterative way, providing feedback between each step.

7. REFERENCES

[1] S. Trudel, O. Gaier, J. Hamrle and B. Hillebrands, J. Phys. D: Appl. Phys. 43, 193001 (2010).

[2] T. Kubota, J. Hamrle, Y. Sakuraba, O. Gaier, M. Oogane, A. Sakuma, B. Hillebrands, K. Takanashi, Y. Ando, J. Appl. Phys. **106,** 113907 (2009).

[3] K. Inomata, M. Wojcik, E. Jedryka, N. Ikeda, N. Tezuka, Phys. Rev. B 77, 214425 (2008).

[4] S. Ouardi et al, to be submitted (2012).

Acknowledgements

The financial support from PIEF-GA-2009-254522 (HEUSPECTRO), CZ.1.05/2.1.00/01.0040 (IT4), and **CZ.1.07/2.3.00/20.0038 is gratefully acknowledged**.

european social fund in the czech republic
EUROPEAN UNION
MINISTRY OF EDUCATION, YOUTH AND SPORTS
OP Education for Competitiveness
INVESTMENTS IN EDUCATION DEVELOPMENT

Processing and characterization of nano-sized metallic powders and fine grained metals.

Yannick Champion [a]

a Institut de Chimie et des Matériaux Paris-Est – CNRS-UPEC,

2 rue Henri Dunant 94320 Thiais, Cedex France.

Abstract

Our group has been involved in nanopowders synthesis since the early 80's with a primary motivation turned to magnetic properties. Great interest in particular for mechanical properties (unusual high strength) focused our research towards fabrication of ultra fine grained metals (UFG) from nanopowder following a powder metallurgy processing. In this short note, we review the main steps on the fondamental aspect of the synthesis of nanopowders and characterization. Then powder processing is detailed for fabrication of bulk UFG. The main output is the investigation on the mechanical behavior of UFG with developement of a modelling able to relate the macroscopic rheology to microscopic paramaters i.e. local structure and chemistry. Objective is to define relevant guideline for designing UFG alloys with improved properties.

Keywords

metal, nanopowder, nanostructure, ultrafined grain, evaporation-condensation, mechanical behavior

1. INTRODUCTION

Metallic nanopowders have been the subject of intensive research since the 80's for their very attractive size effect related properties. Particles with size below 100 nm exhibit high chemical reactivity, unusual magnetic properties (single domain and superparamagnetism), extreme strength. The nanopowders may find interesting use as fillers in composites with various matrices (polymers, metal, ceramic). The nanopowders are also precursors for the preparation with much precise control, of ultrafine grained metals, alloys and dual nanophases materials by compaction and sintering. Study of the synthesis of metallic nanopowders has been intensive in our laboratory since de early 80's (see article by P. Ochin). Objective has been manyfold. First, one aimed at understanding the formation of nanoparticles from the evaporation and condensation of a metallic vapour within a cryogenic medium. Second, the nanopowders were investigated regarding their magnetic properties and their reactivity. Third, the compaction and sintering of the nanopowders leading to the development of a nano-powder metallurgy produced large size ultrafine grained metals for the investigation of the mechanical properties of the new type of materials.

2. NANOPOWDERS OF METALS AND ALLOYS

2.1 Fabrication

Technical details on the fabrication of nanopowders illustrated by the figure 1a, are reported in the paper of P. Ochin and Y. Champion (this meeting). During a decade, many experiments were carried out on various metals (Fe, Cu, Al, Co, Ni, Mg), semi conductors (Si, Ge) and metallic alloys (FeNi, FeCo, CuAg), to understand the mechanism of formation of the nanoparticles [1]. In particular, we empirically approached the control of particles size and agglomeration state (formation of aggregates) by appropriate experimental parameter : cryogenic liquid flow, current and voltage intensities, power supply, r.f. fréquency. Study of metallic alloys consisted in particular in correlating the composition of the master alloy (from which metals are evaporated) to metallic gas (or powder condensed) composition. Such fastidious work consisted in multiple “distillation“ experiments i.e. short time evaporation limiting variation of the master alloy composition and then precise chemical analysis of the nanopowders by inductively coupled plasma optical emission spectroscopy. Fig. 1b is an exemple of results obtained on FeNi alloys which shows that master alloy of Fe30Ni30 (permalloy) gives nanopowders with the same composition. This properties allowed to produce few undreds of grams of this powders studied for their soft magnetic properties [2].

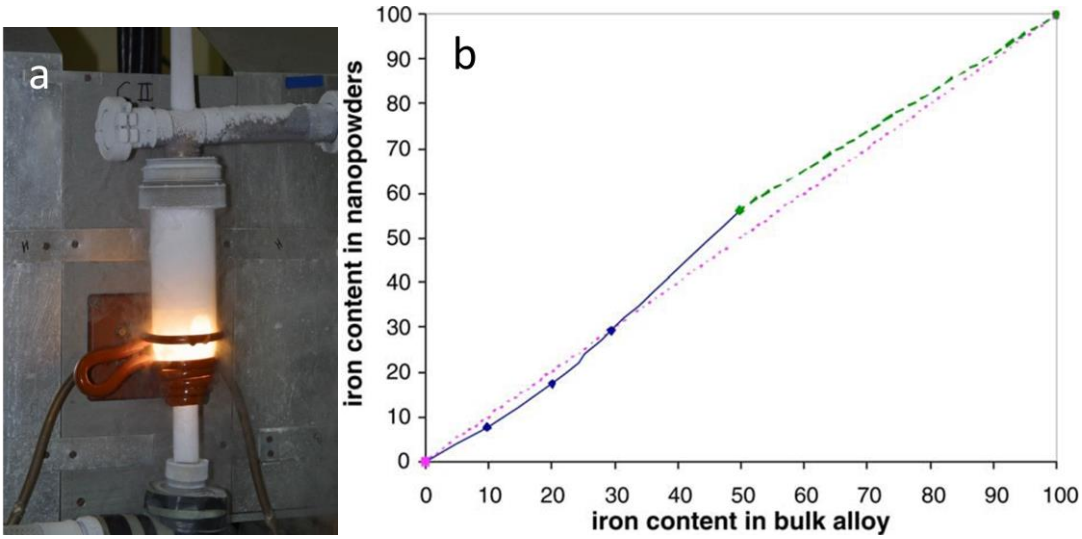

Fig. 1 (a) experimental set up for evaporation and cryo-condensation of metallic nanopowders. (b) Atomic composition (iron content) of evaporated and cryo-condensed nanopowders of Fe-Ni as a function of atomic composition of the master alloy. The curve shows identical composition for permalloy at about 30 at% of Fe.

2.2 Characterization

Motivations for characterization of the nanoparticles were many folds and far beyond the control of the particle size, morphology, specific surface and aggregations, which are of course essential characteristics. Local chemical analysis was developped and performed to analyse the phase distribution, to detecte potential size effect on the thermodynamics of phase equilibrium and eventually effect on physical properties. Much works were concerning chemical analysis using energy loss spectroscopy in the transmission electron microscopy (TEM) image filtering mode. FeNi particles were intensively investigated to evaluate homogenities and composition of the particles‘ oxyde surface (Fig. 2a). These powders were intensively investigated for potential applications as high saturation induction soft magnetic materials under high frequency conditions. Using TEM holography, we showed for the first time that nanoparticles of FeNi

present a vortex structure of their magnetic moment (Fig. 2b) [3]. An other analysis concerned the investigation of distribution of Ag in Cu nanoparticles which was a key parameter for improvement of strength in UFG Cu produced later on by sintering.

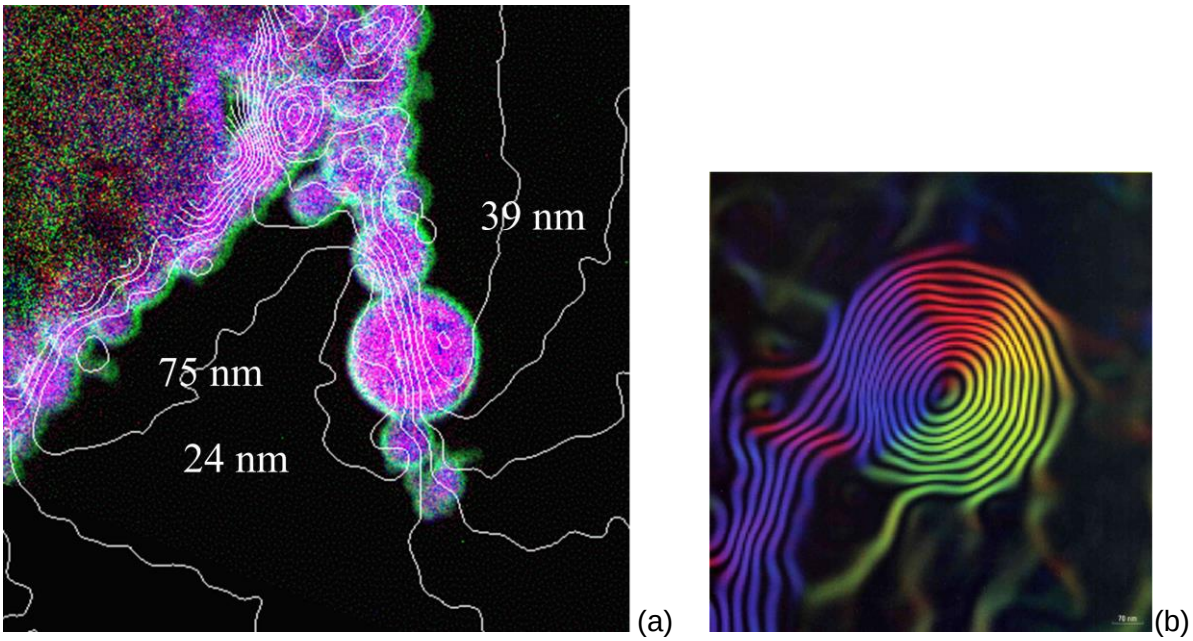

Fig. 2 (a) Chemical mapping by image filtering in energy loss transmission electron microscopy mode (FEI Technai TEM G2 F20 ST) . (b) Vortex structure of the magnetic field observed in TEM holographic mode (CNRS image).

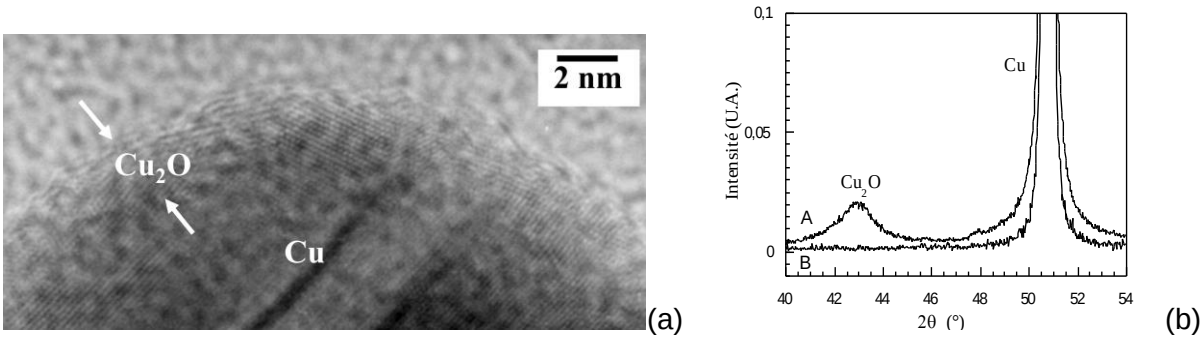

Fig. 3 (a) High resolution TEM micrograph of a copper nanoparticle showing large surface curvature and a 2.5 nm Cu_2O surface layer. (b) Detail of X-rays diffraction patterns on copper nanoparticles showing Cu_2O (A) and after reduction under hydrogen at 100°C (B) with absence of Cu_2O.

A long term research was performed to characterize the structure of the nanoparticles at the atomic scale using high resolution TEM (Fig. 3a) and X-ray diffraction [4]. These works, in particular in situ study of surface oxyde reduction under hydrogen (Fig 3b), were essential to develop the powder metallurgy processing and the fabrication of UFG metals.

3. BULK FINE GRAINED STRUCTURES

3.1 Processing of nanopowders

Investigations on the reduction and reactivity i.e. ability for sintering as function of time and temperature of Cu nanopowders were used to optimize a so-called nanopowder metallurgy processing. These powders are extremely reactive in the sense that reduction under H_2, unsually occurs at 90°C and is followed by sintering starting at 100°C. Dilatometry shows that the nanopowders experience rapid shrinkage up to 150°C when intense grain growth is then occuring.

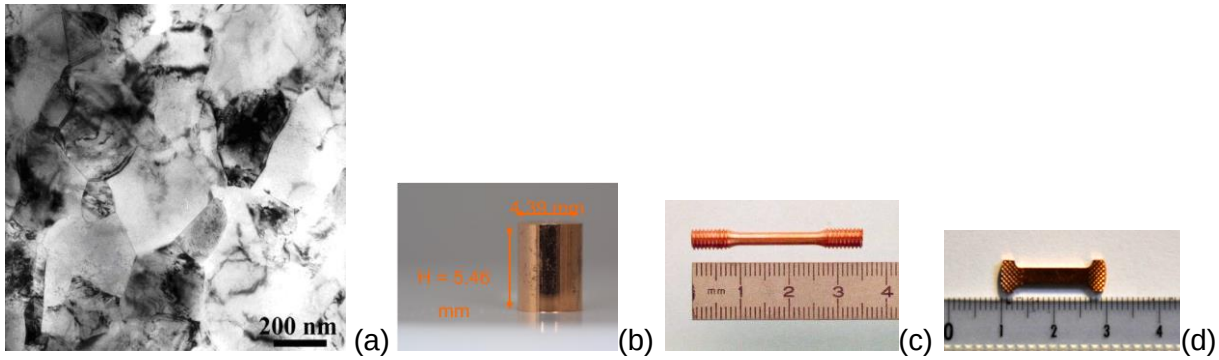

Fig. 4 (a) TEM micrograph of bulk fine grained copper prepared by sintering and extrusion of nanopowders. Samples for mechanical testing (b) in compression (c) in tension. (d) Flat specimen prepared by hydrogen reduction and spark plasma (SPS) flash sintering.

This reactive thermal treatment allows to obtain pure fine grained Cu but with about 6% residual porosity not removable exept if grain growth is allowed at temparature larger than 150°C or for longer time. To keep the fine grained structure, differential hydrostatic extrusion i.e. extrusion under hydrostatic pressure where sample is extruded within a back pressure zone, was used [5]. This processing produces near fully dense UFG with grain size in the range of 100 nm (Fig.4a) in the form of cylindrical bar (50 mm length and 8 mm diameter), from which one cuts compression (Fig. 4b) and tensile test specimens (Fig. 4c). Recently and alternative processing was developped using the spark plasma sintering technique (SPS). Nanopowders are previously reduced under hydrogen and then pressed and sintered by current induced heating. Plate-like disk, 20 mm diameter and 1 mm thickness are obtained from which flat tensile test specimens are cut.

Alternatively, we approach the formation of fine grained structure by equal channel angular pressing on aluminum alloys [6-7].

3.2 Properties

The fabrication of UFG (Fig. 4) was the starting point for works on the mechanical properties, rheology and approach of the mechanism of deformation. Near perfect elasto-plastic deformation was observed for the first time on this UFG Cu in tension (Fig. 5a red curve) [8]. It was subsequently shown that the plasticity at constant stress (in contradiction to the Considère criterion) was ascribed to an unusual high strain rate sensitivity thus following the Hart's criterion predicting delay in necking. Strain rate sensitivity was reported by various authors as decreasing with strain rate, which lead to deacrease and eventually absence of elongation though concomitant to increase in strength (see blue curve in Fig. 5a). Jump tests at various strain rates and temperature as well as different testing such as nanoindentation and relaxation

tests were perfomed to analyse the rheology and identify parameters controlling the deformation.

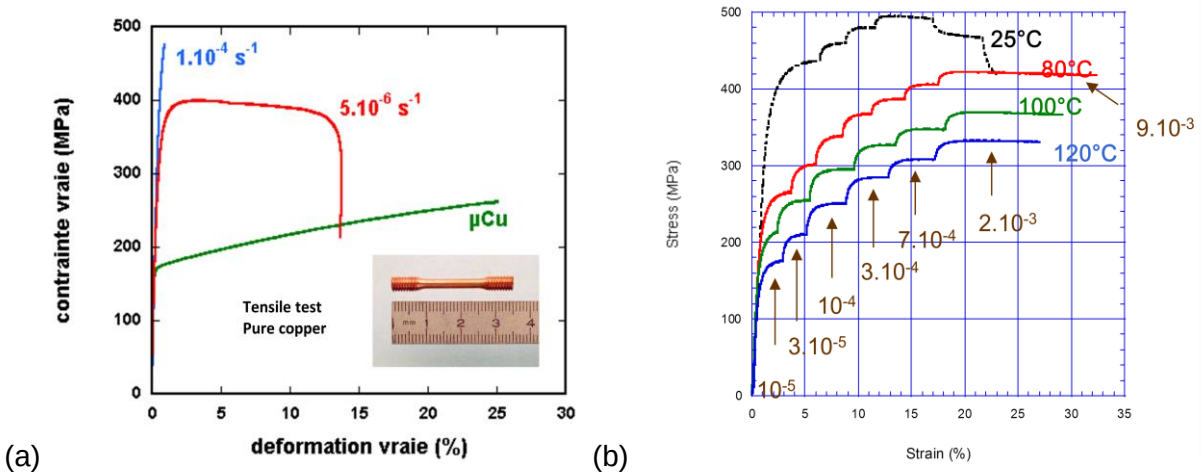

Fig. 5 (a) Tesile tests on bulk fine grained copper at room temperature (blue at 10^{-4} s^{-1}), (red at 5.10^{-6} s^{-1}), (green at 10^{-4} s^{-1}, on a copper with large grains, 50 micrometers for comparison). Fine grained specimen does not exhibit work-hardening. It shows strain rate sensitivity and absence of elongation at larger strain rates. (b) Jump tests on specimens like in Fig. 4(b) showing strain rate sensitivity.

From strain rate sensitivity we derived a model describing the micromechanism of deformation emphasizing in particular the events controlling the deformation (i.e. thermally activated) [9]. The relation between macroscopic rheology (strain rate sensitivity, m) and the local microscopic events is rendered by and with v the activation volume, k the Boltzman constant, T the absolute temperature, τ the shear stress and $\dot{\gamma}$ the shear rate:

$$v = \frac{kT\partial \ln \dot{\gamma}}{\partial \tau} = \frac{kT}{m\tau} \tag{1}$$

Which led to a law of behavior of the form:

$$\dot{\gamma} \approx \dot{\gamma}_0 \left(\frac{B}{C\tau_0^*} \right)^{1/2B} \exp\left(\frac{v^*}{kT}(\tau - \tau_0) \right) \times (\tau - \tau_0)^{1/B} \approx \gamma_0^{\#} \tau^{1/m} \tag{2}$$

Most interesting is the parameter B, connected to the strain rate sensitivity and then to the level of ductility. The work shows that this parameter is related to the properties of the grain boundaries with respect to interactions with dislocations. It suggests relevant guideline for designing grain boundary (in terms of structure and chemistry i.e. for exemple twin, segregation, fine precipitation) which would be much favourable for combination of strength and ductility in UFG.

4. CONCLUDING REMARK AND OBJECTIVES

Experience and expertise concern the fabrication of UFG metal and metallic alloys to study their behavior in deformation and develop strategy for designing UFG with improved properties. From our own experience and according to literature, UFG metals should most likely show propention for strength and plastic elongation when they exhibit complex microstructure in the sense that

dislocations source is needed for plasticity as well as strong barrier to limit their propagation and local softening.

5. REFERENCES

[1] Y. Champion, Gas phase synthesis of nanopowders in Nanomaterials and nanochemistry. (Ed. C. Bréchignac, Ph Houdy, M. Lahmani) Springer berlin (2007) 396-426.

[2] C. Duhamel, Y. Champion, M. Tencé and M. Walls, Synthesis of controlled-chemistry ultrfine FexNi(1-x) ferromagnetic powders J. Alloys and Coumpounds 393/1-2 (2005) 204-210

[3] M. J. Hÿtch, R.E. Dunin-Borkowski, M.R. Scheinfein, J. Moulin, C. Duhamel F. Mazaleyrat and Y. Champion, Vortex flux channeling in magnetic nanoparticles chains. Physical Review Letters, 91 (25) (2003) 257207.

[4] Y. Champion, F. Bernard, N. Guigue-Millot et P. Perriat, Sintering of copper nanopowders under hydrogen: an in situ X-ray diffraction. Materials Science and Engineering, A360 (2003) 258-263.

[5] C. Langlois, M.J. Hÿtch, P. Langlois S. Lartigue-Korinek and Y. Champion, Syntesis and microstructure of bulk nanocrystalline copper. Metal. Mater. Trans. A 36A (2005) 3451-3460.

[6] A. Korchef, N. Njah, Y. Champion, S. Guérin, C. Leroux, J. Masmoudi and A. Kolsi Materials Flow during equal channel angular pressing of aluminium containing Al8Fe2Si precipitates. Advanced Engineering Materials, 6 (2004) 222-228.

[7] A. Korchef, N. Njah, J. Masmoudi, A. Kolsi, Y. Champion, S. Guérin and C Leroux.Evolution of the mechanical properties of aluminium containing Al8Fe2Si precipitates during equal angular pressing Advanced Engineering Materials, 6 (2004) 639-643.

[8] Y. Champion, C. Langlois, S. Guérin-Mailly, P. Langlois, J-L Bonnentien and M. J. Hytch, Near-perfect elasto-plasticity in pure nanocrystalline copper. Science 300 (2003) 310-311.

[9] C. Duhamel, Y. Bréchet and Y. Champion, Activation volume and deviation from Cottrell-Stokes law at small grain size. International Journal of Plasticity, 26 (2010) 747-757.

Acknowledgement

This contribution was created within the project **Creation of an international scientific team and incorporation to scientific networks in the area of nanotechnology and unconventional forming material. CZ.1.07/2.3.00/20.0038**, which is financed by the European Social Fund and state budget of the Czech Republic.

european social fund in the czech republic
EUROPEAN UNION
MINISTRY OF EDUCATION, YOUTH AND SPORTS
OP Education for Competitiveness
INVESTMENTS IN EDUCATION DEVELOPMENT

New trends of materials in the automotive industries

Marcel KLOS[a]

a VSB – Technical university of Ostrava, 17. listopadu 15, 708 33 Ostrava – Poruba, CZ, E - mail: mklos@visteon.com

1. INTRODUCTION

Development automotive industry and global depression doing of new requirements on cost saving in the time.

In terms of development companies economies and prediction of loss on the global market is necessary of search for alternative market on the basic economical prediction.

Firstly for growth of company and positive economical develop is implementation of innovation production programs and alternatives material to serial production. Necessary is use of currently capacity of industrial production.

Suppliers to automotive industry search cost saving in products portfolio and search new opportunities of companies marketing. The supplier's primary generated of cost saving in investment.

Obviously these aspects have of implementation of new materials to serial productions, which it has in the reason of high investment in modernization of production process and increasing of product quality.

Strategically is necessary be on the look for new industries for exercise of nanomaterials, that are not dependent of economies stagnation.

2. ACTUAL STATUS IN AUTOMOTIVE INDUSTRIAL

Actual status of automotive industry is a joint venture between same economical subjects and creation of individual companies. Creation of a multinational corporation with minimal market share 8%. Join venture effect is a mineralization of loss located on the global market.

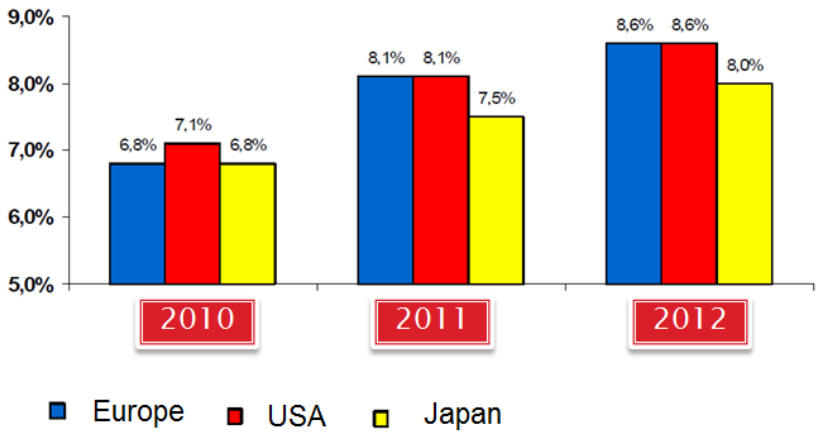

Chart. 1 Develop of automotive industrial [2,8,10]

3. POTENTIAL USAGE OF NANOMATERIALS

Many university and private companies have developed processes for the manufacture of nanomaterials. The global nanotechnology industry has strong R&D backup from universities and related institutions at EU and USA.

While several companies are including nanomaterials in their products, only a few (e.g. manufacturers of paints, the breake systems of the care, combinations materials in care body, polymer composites) are using nanoparticles as significant elements in vehicles.

3.1 The Break system

New concept of a brake system - Lightweight construction with aluminum alloy parts. Break discs from carbon – ceramic composites. The composite break disc has approximately quarter weight compared to a classic steel break disk.

Fig. 1 The break system [16]

3.2 New concept of a car body

The body constructions use new types of technology and material combinations. Combinations have their rigidity increased by approximately 20%. New types of cowlings and fenders give to modification of deformation zones.

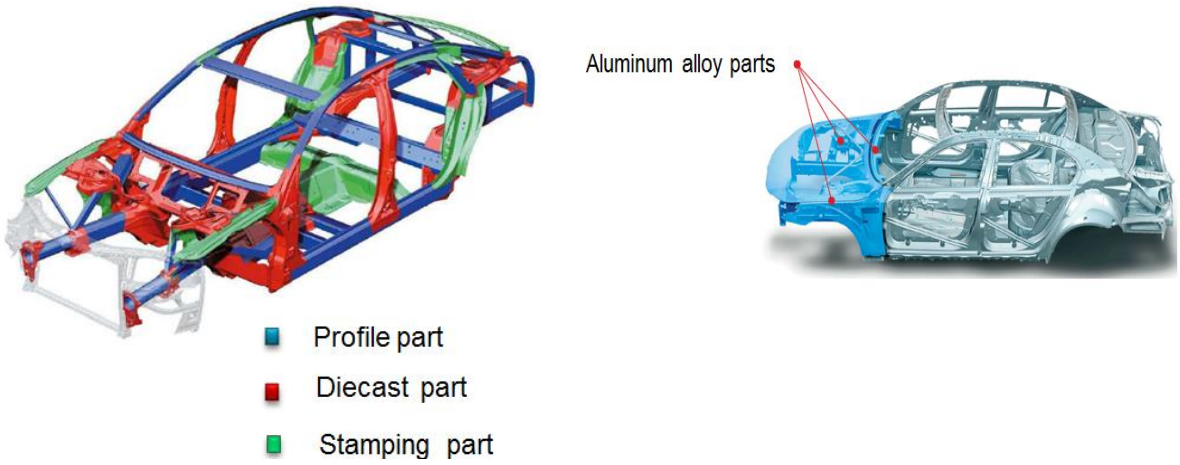

Fig. 2 New concept of a car body [9,13]

3.3 Nano plastic material – composite

Nano plastic materials have two characteristic properties:

Deformation up to 100 %

Faster return to its original dimensions after end of deformation

Change of properties to those of plastic materials at the lower temperature (Tg- Glass transition temperature). Elastic behavior is defined by maximal structural parameters: „material amorphous“ – entropy.

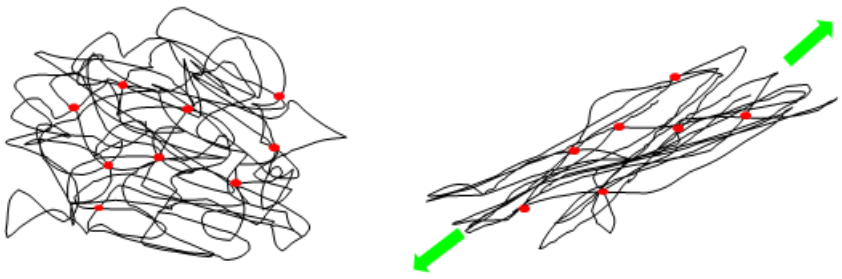

Fig. 3 Nano plastic material – composite

3.4 Air conditioning system

Refrigerant hose assemblies are the refrigerant conduit connecting the compressor, condenser, and the evaporator/accumulator. Because the suction hose assembly and discharge hose

assembly are attached to the A/C compressor, which in turn is attached to the engine, some amount of flexible refrigerant hose is required in these assemblies to compensate for engine relative motion and provide isolation from compressor/engine vibration and pulsations.

Liquid hose assemblies typically contain a section of flexible refrigerant hose for routing purposes or to facilitate hose installation, but all metal liquid tube assemblies are permitted, provided they meet the same requirements of a flexible liquid.

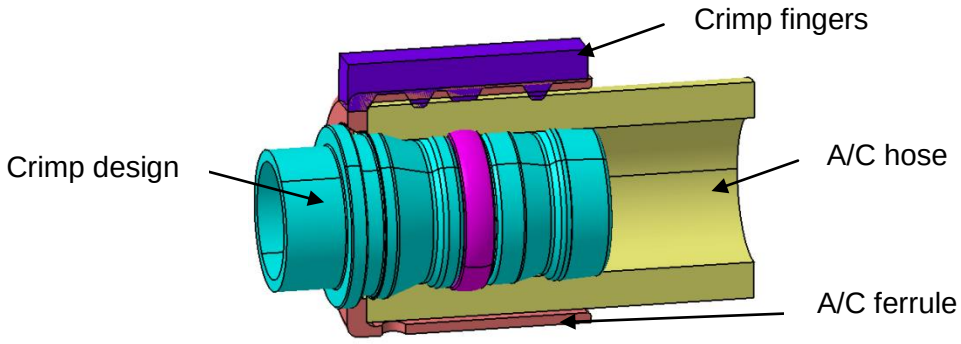

Fig.4 Crimp fitting assembly

4. CONCLUSION

- Nanomaterials usage in automotive industry is around 2% (nano-plastic materials, nano-lacquers, nano-textile)
- Implementation of new materials stands for 0,07% of total portfolio values.

5. LITERATURE

[1] ABUŠINOV, Alexandr. Lehčené kovové struktury. *MM Průmyslové spektrum*. 2003, č. 1, s. 62.

[2] *Audi Deutschland* [.online]. 2009 [.cit. 2009-05-26]. Dostupný z WWW: <http://www.audi.de>.

[3] *Automotive Aluminum* [.online]. c2006 [.cit. 2008-05-20]. Dostupný z WWW: http://www.autoaluminum.org>.

[4] *BMW Group PressClub* [.online]. 2000-2009 [.cit. 2009-02-05]. Dostupný z WWW: <http://www.press.bmwgroup.com>.

[5] *BMW X5 Fender : Case Study*. [.s.l.] : [.s.n.], c2007. Dostupný z WWW: <http://www.borealisgroup.com/pdf/literature/borealis/casestudy/

[6] K_CAST048_GB_AA_2007_10_B.pdf>. s. 1-2.

[7] BOUCNÍK, P., ČECH, J., JUŘIČKA, I.: Použití hořčíkových slitin ve slévárenství. 5. Medzinárodna vedecká konferencia CO-MAT-TECH, Trnava,14.10. - 15. 10.1997.

[8] DAWSON, Steve. *Compacted Graphite Iron: Mechanical and Physical Properties for Engine Design*. Dresden, 1999. 22 s. Oborová práce. Dostupný z WWW: <http://www.sintercast.com/data/content/DOCUMENTS/200431723285110vdi_paper.pdf>.

[9] *GermanCarFans.com* [.online]. c2009 [.cit. 2009-05-23]. Dostupný z WWW: <http://www.germancarfans.com>.

[10] GREGER, Miroslav, et al. Využití hořčíkových slitin v automobilovém průmyslu. In *METAL 2008*. Hradec nad Moravicí : [.s.n.], 2008. s. 1-12.

[11] HERMAN, Aleš, STUNOVÁ, Barbora. Výhody použití Mg slitin v porovnání s ostatními konstrukčními materiály. *MM Průmyslové spektrum*. 2005, č. 10, s. 92.

[12] HIRSCH, J.. *Automotive Trends in Aluminum, The European Perspective*

[13] [.online]. Bonn : c2009 [.cit. 2009-05-25]. Dostupný z WWW:

<http://www.keytometals.com/Article135.htm>.

[14] HLUCHÝ, Miroslav, KOLOUCH, Jan. *Strojírenská technologie : Nauka o materiálu*. Praha : Scientia, 2002. 266 s.

[15] JANČÁŘ, Josef. *Úvod do materiálového inženýrství kompozitů*. Brno : [.s.n.], 1999. 39 s.

[16] Modern Casting.: *Magazine for Foundries and Diecasters : Iron Alloys* [.online]. c2009 [.cit. 2009-05-21]. Dostupný z WWW: <http://www.moderncasting.com/content/view/629/183/>.

[17] Plasty stále žádanější při stavbě automobilů. *Technický týdeník : Plasty*. 2007, č. 16, s. 5. 28

[18] PODRÁBSKÝ, Tomáš, NĚMEC, Karel, JULIŠ, Martin. *Neželezné kovy a jejich slitiny : doplnění a rozšíření přednášky "Strojírenské materiály" z předmětu BUM*. [.s.l.] : [.s.n.], 2008. 40 s.

Acknowledgement

This contribution was created within the project **Creation of an international scientific team and incorporation to scientific networks in the area of nanotechnology and unconventional forming material. CZ.1.07/2.3.00/20.0038**, which is financed by the European Social Fund and state budget of the Czech Republic.

european social fund in the czech republic
EUROPEAN UNION
MINISTRY OF EDUCATION, YOUTH AND SPORTS
OP Education for Competitiveness
INVESTMENTS IN EDUCATION DEVELOPMENT

Characterization of magnesium nanocomposites

Pavel LUKÁČ, Zuzanka TROJANOVÁ

Charles University, Faculty of Mathematics and Physics, Ke Karlovu 5, 121 16 Praha 2, CZ,

lukac@met.mff.cuni.cz; ztrojan@met.mff.cuni.cz

Abstract

Aluminium and magnesium alloys reinforced with ceramic particles are used in different applications. The reinforcement of magnesium (magnesium alloys) with ceramic nanosize particles has given rise a new class of composite materials – nanocomposites. The addition of nanosize particles increases the strength (yield strength, ultimate tensile strength, maximum flow stress), stiffness and hardness. The shape of reinforcements plays an important role in the mechanical properties. The type and amount (volume fraction) of reinforcements influence the yield strength. Recently, some studies have shown that the addition of nanosize particles can also increase ductility of composites at room temperature. The authors investigated the deformation behavior of magnesium reinforced with Al_2O_3 and ZrO_2 at different temperatures between room temperature and 300 °C. It was shown that the test temperature significantly influences the deformation behavior of composites including the yield strength.

The results obtained show that the deformation behavior characterized by a high strength at room temperature and low strain hardening at elevated temperatures may be explained both by the interaction of moving dislocations with nanosize particles and by the effect of the matrix and particles properties as well as the interfaces between the matrix and the particles. The effect of the microstructural factors is discussed.

Keywords

Particle reinforced magnesium, yield strength, volume fraction of reinforcement

1. INTRODUCTION

There are different methods how to increase the strength of a metallic material. Refinement of grains and reinforcement are very often used in order to achieve considerable improvement (an increase) of the mechanical properties of magnesium and its alloys too. Other method is preparation of a composite. Composites are materials containing two (or more) different materials as a certain combination. Metal matrix composites (MMCs) – usually prepared by the addition of ceramics fibres and/or particles to metallic matrix – exhibit higher yield stresses and higher tensile strengths than the matrix [1]. It is important to mention that the composite properties can be tailored, even if it is not easy because the properties ate influenced by many factors as

for instance: type, volume fraction, size, morphology of reinforcing phase and of course properties of the matrix.

Magnesium alloys are used in many applications because of their special properties. They are lightweight, have relative high strength and hence high specific strength and specific stiffness. Magnesium based alloys are attractive for applications where weight must be reduced. Their disadvantages are their mechanical properties at elevated temperatures. It is expected that both refining grains in the matrix and fabrication of composites with particles will be most effective means to attain both a higher strength and higher ductility. Considerable improvement of the mechanical properties of composites, as well as their thermal stability can be achieved.

The aim of the present paper is to give the deformation behavior and mechanical properties of commercial pure microcrystalline magnesium reinforced with alumina and zirconia nanosize particulates (hereafter called also nanoparticles).

2. EXPERIMENTAL PROCEDURE

Microcrystalline magnesium was used as a matrix material. The microscaled Mg powder having a particle diameter of about 20 μm was prepared by gas atomization of a magnesium melt with argon atmosphere containing 1% oxygen for powder passivation. Both Al_2O_3 (alumina) and ZrO_2 (zirconia) powder with a mean particle size of 14 nm were prepared by evaporation with the pulsed radiation of a 1000 W Nd:YAG laser and subsequent condensation of the laser-induced vapor in a controlled aggregation gas. A detailed description of the preparation method of the nanoparticles is given elsewhere [2, 3]. The nanoparticles were mixed and milled together with microcrystalline Mg in an asymmetrically moved mixer for 1 h. Mixture was pre-compressed followed by hot extrusion at a temperature of 400 °C and a pressure of 150 MPa. The original more or less equiaxial grains changed into elliptical ones with the long axis parallel to the extrusion direction. The grain size was in the extrusion direction tens μm and in the cross-section about 3 μm. The majority of ceramic nanoparticles was situated near to the grain boundaries; only a few nanoparticles were inside the grains.

Specimens for testing of mechanical properties were machined from the extruded bars in cylindrical form with their symmetrical axis parallel to the extrusion direction. The cylindrical specimens were deformed in an Instron testing machine at temperatures between 20 and 300 °C at a constant crosshead speed giving an initial strain rate of 6.2×10^{-5} s^{-1}.

3. RESULTS AND DISCUSSION

Figure 1 shows the true stress–true strain curves for microcrystalline magnesium reinforced with 3 vol.% of Al_2O_3 nanoparticles a) and 3 vol.% ZrO_2 nanoparticles b) obtained for various temperatures.

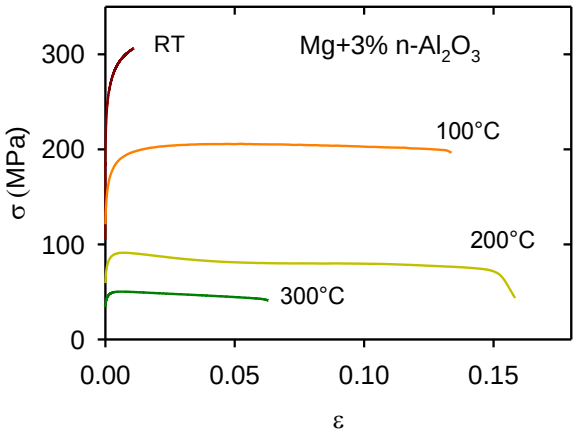

Fig. 1a True stress-true strain curves of microcrystalline Mg with alumina nanoparticles obtained for various temperatures

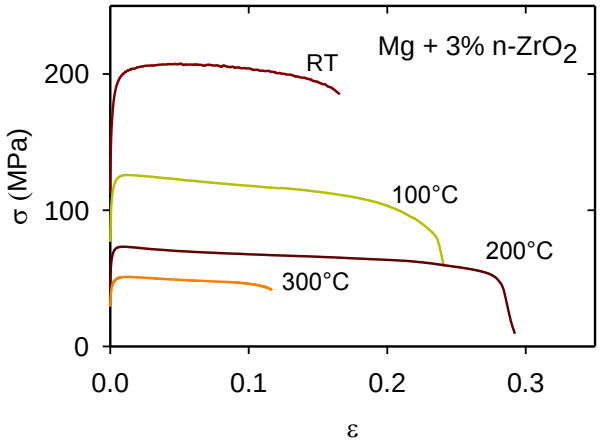

Fig. 1b True stress-true strain curves of microcrystalline Mg with zirconia nanoparticles obtained for various temperatures

It can be seen that the flow stress decreases very rapidly with increasing temperature. At elevated temperatures, the strain hardening is very close to zero. It means that hardening and softening are in a dynamic balance. The values of the flow stress (below 300 °C) for Mg + 3% n-Al_2O_3 are higher than those for Mg + 3% n-ZrO_2.

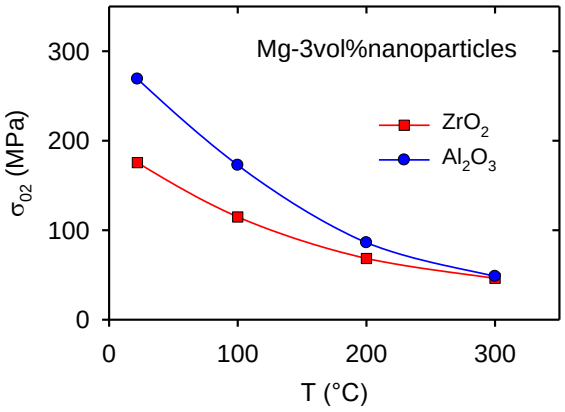

Fig. 2 Temperature dependence of the yield stress for nanocomposites with alumina and zirconia nanoparticles.

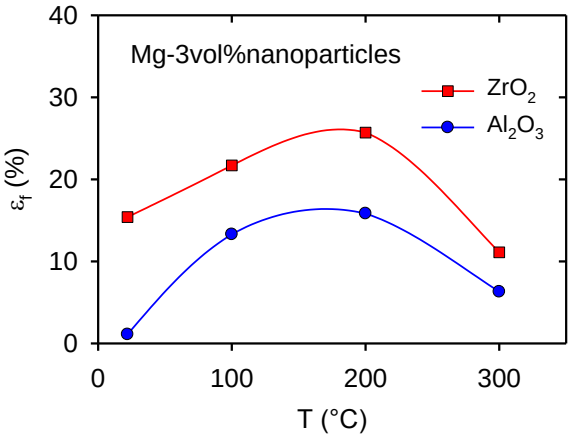

Fig. 3 Temperature dependence of the ductility for nanocomposites with alumina and zirconia nanoparticles.

The difference in the flow stresses is clearly apparent from the temperature dependence of the yield stresses for both types of the nanocomposites investigated. The temperature dependence of the yield stress is given in Fig. 2. The difference in the yield stress for both nanocomposites deformed at room temperature is about 100 MPa. The elongation to failure for nanocomposites with zirconia nanoparticles is substantially higher than that for composites with alumina nanoparticles. The temperature variations of the fracture strain exhibit a maximum at a temperature of 200 °C, shown in Fig. 3. The results show a significant influence on the deformation of magnesium matrix reinforced with nanoparticles. Annihilation of dislocations and grain boundary sliding should be taken into consideration. It is obvious that the test temperature influences both processes.

The interface between the matrix and the reinforcement plays an important role in the deformation behavior of the composite. The interfacial bond, as one characteristic of the interface may significantly influence the crack resistance and therefore the strain to failure [4]. It is clear that the physical and mechanical properties of the matrix are different from those of the particles. Both the elastic modulus mismatch and difference

in the coefficients of thermal expansion (CTE) may cause an increase in the density of dislocations. The density of the newly created dislocations due to the coefficient of thermal expansion mismatch is proportional to the temperature change and to the difference between the coefficients of thermal expansion. The dislocation density is inversely proportional to the radius of particles [5]. In our case, the coefficients of thermal expansion of Mg, Al_2O_3 and ZrO_2 have the following values: $26.1x10^{-6}$, $7.9x10^{-6}$ and $12.1x10^{-6}$ $°C^{-1}$. It can be seen that the difference between CTEs of magnesium and Al_2O_3 is higher than that of magnesium and ZrO_2. This can contribute to the yield stress values – the yield stress of the nanocomposites with alumina should be higher than that of nanocomposites with zirconia, which is observed. Trojanová et al. [6] using internal friction measurements were able to show how cooling and annealing influence changes in the dislocation density in magnesium reinforced by 1 vol.% of nanoscaled alumina.

The title of the table will be placed above the table – **Table 1**. Table along with the caption is aligned to the left edge.

4. CONCLUSIONS

This paper presents the main characteristics of the deformation behavior of magnesium reinforced with alumina and zirconia nanoparticles: the true stress-true strain curves, yield stress and elongation to failure. Type of the reinforcing phase and the test temperature are the key factors influencing the mechanical properties of the investigated nanocomposites.

The following particular topics important for educational and professional needs should be described:

1. Processing of ultrafine-grained metallic materials and nanomaterials (severe plastic deformation, milling, rapid solidification).

2. Conditions for superplastic deformation.

3. Characteristics of superplasticity.

4. Factors affecting superplastic deformation.

5. Superplastic forming.

6. Applications of superplasticity.

5. LITERATURE

[1] CLYNE, T.W., WITHERS, P.J. An Introduction to Metal Matrix Composites. Cambridge: Cambridge Univ. Press, 1993. (ISNB: 0 521 41808 9).

[2] FERKEL, H., RIEHEMANN, W. Bonding of alumina ceramics with nanoscaled alumina powders. Nanostructured Materials, November 1996, vol. 7, no. 8, p. 835-845. Elsevier, (ISSN: 1359-6459).

[3] NASER, J., FERKEL, H., RIEHEMANN, W. Grain stabilisation of copper with nanoscaled Al2O3-powder. Materials Science and Engineering, August 1997, vol. A234-236, p. 470-473. Elsevier, (ISSN: 0921-5093).

[4] MORTENSEN, A., JIN, I. Solidification processing of metal matrix composites. International Materials Reviews, 1992, vol. 37, p. 101-128. Maney Publishing, (ISSN: 0950-6608).

[5] ARSENAULT, R.J., SHI, N. Dislocations generation due to differences between coefficients of thermal expansion. Materials Science and Engineering, August 1986, vol. 81, p. 175-187. Elsevier, (ISSN: 0921-5093).

[6] TROJANOVÁ, Z., LUKÁČ, P., FERKEL, H., MORDIKE, B.L., RIEHEMANN, W. Stability of microstructure in magnesium reinforced with nanoscaled alumina particles. Materials Science and Engineering, August 1997, vol. A234-236, p. 798-801. Elsevier, (ISSN: 0921-5093).

Acknowledgement

This contribution was created within the project Creation of an international scientific team and incorporation to scientific networks in the area of nanotechnology and unconventional forming material. CZ.1.07/2.3.00/20.0038, which is financed by the European Social Fund and state budget of the Czech Republic.

european social fund in the czech republic
EUROPEAN UNION
MINISTRY OF EDUCATION, YOUTH AND SPORTS
OP Education for Competitiveness
INVESTMENTS IN EDUCATION DEVELOPMENT

Experience with the project proposal evaluation of European Community programmes for research and technological development

Karel Malaník

VÚHŽ a.s., 739 51 Dobrá 240, CZ, malanik@vuhz.cz

Abstract

The presentation deals with the project proposal evaluation of the European Community R&D programmes. The experience with procedures of evaluation is performed within the programme Research Fund for Coal and Steel.

There are mentioned particular steps of proposal evaluation for research, pilot and demonstration projects – evaluation (justification of marking, resubmitted proposals, outcome of the individual evaluation, thresholds), consensus (consensus meeting, marking, outcome of the consensus meeting), ranking list.

The main attention is dedicated to the individual evaluation process of proposals, especially to the evaluation criteria - that means scientific and technical approach, innovative content, consistency of resources and quality of partnership, industrial interest and scientific / technical prospects, added value for the European Union and contribution to EU policies.

Keywords

EU funds, R&D projects, proposal, evaluation process, evaluation criteria

1. EVALUATION OF PROPOSALS

The preparation and processing of the EU R&D projects is difficult. To increase the probability of success in selection procedure, the detailed knowledge of the evaluation process is necessary. In this term the entry gives the information about the rules for processing of the proposals in the R&D programme RF Coal and Steel.

The proposals are processed according to the Information Package, which is addressed to all applicants and provides any necessary information on the preparation and submission modalities of proposals. After administrative eligibility check follows the stage of evaluation.

The Commission invites independent experts to the Commission's premises in order to carry out the evaluation of proposals. A minimum of three evaluators examine each eligible proposal submitted to the Commission before the deadline.

Initially, each evaluator works independently. Expert gives marks and comments for each criterion. Evaluators must substantiate their marks with comments in a form suitable for

providing feedback to the proposers. Comments serve as input to the consensus meeting and related consensus report.

Proposal that has been evaluated in one or several prior call(s) for proposals and was not retained for funding may be resubmitted (special conditions). These proposals are evaluated independently from their scoring obtained in previous evaluations. The evaluation report is available for applicants.

1.1 Evaluation criteria

The following criteria will be applied for the examination of the quality and relevance of research, pilot and demonstration project proposals.

It is suitable to hold the sequence of the criteria in the technical description of the project proposal (facilitation of evaluation).

Criterion 1 Scientific and technical approach *(there is an eliminating threshold for this criterion)*

a) Does the proposal address the scientific and technological issues of the Programme objectives?
b) To what extent do the applicants demonstrate their knowledge of the international state-of-the-art of related work (adequate documentary evidence, including results of current or completed RTD projects)? Failure to provide the reference of previous projects of major relevance to the objectives of the proposal may result in the rejection of the proposal.
c) Is the feasibility of the proposed work convincingly addressed?
d) Are the proposed methods and techniques clearly described and well explained? Is the overall approach suitable for achieving the project objectives?

Criterion 2 Innovative content (there is an eliminating threshold for this criterion, *if < 3, proposal is eliminated)*

a) Please summarise the innovative aspects of the proposal.
b) Does the proposal have an appropriate level of innovative value / originality? i.e. does it indicate how the intended results could lead to progress beyond the state-of-the-art, be it of incremental or breakthrough nature, through
   - the development of new or improved products, processes or technologies
   - a significant progress in the existing knowledge or technologies?
c) Does the proposal clearly describe its innovative aspects?
d) Please assess the span of the expected findings: Do these offer the perspective of a wider and general use or are their innovative value of restricted use for a specific application and/or product?

Criterion 3 Consistency of resources and quality of the partnership

(failure to provide a realistic estimate of the budget deemed necessary may result in the rejection of the proposal)

a) Is the work plan adequate? Is it clearly described & well defined? Are the scheduled tasks responding to the set objectives? To what extent are the manpower, technical and financial resources appropriate for the tasks described in the different Work Packages?
b) Do the partners fulfil complementary tasks without duplication of work?
c) Is the partnership appropriate to achieve the expected results? To what extent are the profiles and the skills of the partners complementary

d) Do bar charts clearly show partner/task inter-dependencies? Is the project scheduling realistic and adequate?

e) If applicable: Is the need to organise a workshop within the proposed research work clearly identified? Is the estimated cost realistic?

Criterion 4 Industrial interest and scientific / technical prospects

a) What are the industrial benefits for the related sector? Are the main project deliverables in terms of industrial interest, scientific/technical prospect and strategic relevance clearly identified?

b) What impact will the expected project results have on the competitiveness of the related sector? Is this clearly explained?

c) Are issues on the use and/or implementation of the results addressed and credible? Do these include modelling, simulation and/or field testing?

d) Does the proposal include relevant industrial participation?

Criterion 5 Added value for the European Union and contribution to EU Policies

a) Is there a clear need and clear benefit to carry out the project at European level instead of at national or private level?

b) Does the proposal show strategic importance to the related sector? Will the expected results be transferable throughout the European *coal* or *steel* industry?

c) Will the expected project results have a positive impact on occupational health and safety in and around the workplace?

d) How might the project impact the preservation of natural resources, energy and the environment?

Criterion mark: 0 to 5, if the proposal addresses an annual priority, 1 point is added, total score - maximum 26

The European Union financial contribution is limited to a maximum of 60 % of the allowable costs for R&D projects.

1.2 Proposal marking and thresholds

Each evaluation criterion is marked by the expert evaluators on a six-point scale from 0 to 5. In this scale, the scores indicate the following with respect to the criterion under examination:

0 - The proposal fails to address the issue under examination or cannot be judged against the criterion due to missing or incomplete information; 1 – Poor; 2 – Fair; 3 – Good (does not mean average !); 4 - Very good; 5 - Excellent

Criteria 1 and 2 have a threshold of 3. Every proposal failing to pass the threshold for one of the two above-mentioned criteria is considered to be ineligible for funding regardless of the total scoring. Therefore, they will be rejected.

2. OUTCOME OF THE INDIVIDUAL EVALUATION

The submission of the individual evaluation form signed by an evaluator completes his individual reading and assessment.

2.1 Consensus

The objective of the consensus meeting (experts + Commission moderator) is to reach a fair consensus and generate a full consistent final evaluation, the comprehensive, concise and clear summary of the comments made in line with the scores. Comments may include, clear and detailed recommendations, where appropriate.

The evaluators attempt to agree on a consensus mark for each criterion. Any change in individual marks decided as a result of discussion shall be reported in the consensus report grid. The scores must be in line with the comments in the consensus report. If the evaluators cannot reach a consensus on a particular aspect of the proposal, the Commission services in charge of the evaluation may ask additional evaluators to examine the proposal.

2.2 Outcome of the consensus meeting

Consensus report includes a final score, as an average of the total scores after consensus and a set of comments for each criterion, which justify the scores given. It has to be ensured, that the consensus report faithfully reflects the consensus reached.

3. RANKING LIST

Following the individual evaluation and the consensus for all proposals, the Commission services prepare a draft ranking list which reflects the outcome of the evaluations. Final score for the proposal is calculated as the average consensus marks of all the evaluators involved in the evaluation of the proposal. Proposals of similar merit shall be ranked according to a predefined cascade mechanism. Any proposal failing to achieve the set thresholds will not be proposed for discussion in the plenary meeting of the Advisory Group. The applied thresholds depend on the different type of funded actions (Research, pilot and demonstration proposals - threshold of 3 for the first two evaluation criteria namely "*Technical and scientific approach*" and "*Innovative content*").

4. CONCLUSIONS

Good knowledge of the evaluated criteria and evaluation procedures is very useful and essential for high-quality preparing, processing and management of project proposals and so the presented information should help to improve the probability of the support obtaining from the EU funds.

Acknowledgements

This paper was created within the project "**Creation of an international scientific team and incorporation to scientific networks in the area of nanotechnology and unconventional forming material. CZ.1.07/2.3.00/20.0038"**, which is financed by the European Social Fund and state budget of the Czech Republic.

evropský sociální fond v ČR
EVROPSKÁ UNIE
MINISTERSTVO ŠKOLSTVÍ, MLÁDEŽE A TĚLOVÝCHOVY
OP Vzdělávání pro konkurenceschopnost
INVESTICE DO ROZVOJE VZDĚLÁVÁNÍ

Effect of grain refinement in magnetocaloric Heusler alloys

Wojciech MAZIARZ

Institute of Metallurgy and Materials Scienc,e Polish Academy of Sciences, Reymonta Str. 25, 30-059 Kraków, Poland

E - mail address w.maziarz@imim.pl

Abstract

The effect of rapid solidification and vacuum hot pressing on the transformation behavior, microstructure and mechanical properties of Ni-Mn-Sn Heusler alloy has been studied by X-ray diffraction, scanning and transmission electron microscopy, differential scanning calorimetry and compression test. The rapid solidification process allowed to obtain the flaky form ribbons with the two phase structure L21 and modulated martensite. The modulations depend on chemical composition of martensite determined by TEM investigations. The ribbons were mechanically fragile and very brittle what limits their applications. The ball milling process conducted in argon atmosphere was applied for pulverizations of ribbons and then vacuum hot pressing of powders at 650°C under 350MPa allowed to obtain compacts with densification of about 98% of theoretical density. The average grain size of compacts was about of 500 nm. One step martensitic transformation in the vicinity of room temperature has been detected both in the ribbons as well as in the hot pressed compacts. The significant improve of plasticity was observed in the hot pressed samples. This effect was confirmed in the compression tests performed for hot pressed as well as hot pressed and solution treated samples. The selected magnetic properties of melt spun ribbons also are presented.

Keywords

Magneto-caloric effect, Heusler alloys, rapid solidification, vacuum hot pressing, martensitic transformation, microstructure, mechanical properties

1. INTRODUCTION

The interest in magnetic refrigeration as a new solid state cooling technology competitive with the conventional vapor compression approach has grown considerably over the past 10 years coinciding with rising international concerns about global warming due to an ever increasing energy consumption. As pointed out by Coulomb [1] in his introductory talk at the Second International Conference on Magnetic Refrigeration at Room Temperature (Thermag II), 15% of the total worldwide energy consumption involves the use of refrigeration (air conditioning, refrigeration, freezing, chilling, etc.). In addition, he noted that the International Institute of Refrigeration is taking an active role in helping to develop magnetic refrigeration which has the potential to lower energy consumption by 20–30% over conventional vapor compression technology. Compounds with a strong coupling between crystallographic structure and magnetism usually exhibit a magnetic field dependence of the structural transitions. A typical

example is the $Gd_5(Si_xGe_{1-x})_4$ alloys ($0.24 \leq x \leq 0.5$), where a transformation from the paramagnetic monoclinic phase to the ferromagnetic orthorhombic phase can be induced either by cooling or by the application of a magnetic field [2]. This feature brings about a giant magnetocaloric effect (MCE), making Gd–Si–Ge alloys one of the most promising magnetic refrigeration materials. Recently, a magnetically induced austenite (MIA) was reported in Ni–Mn–X systems (X = In, Sn, Sb) and their Co-doped alloys [3-5]. In contrast with Gd–Si–Ge, these Heusler-type alloys exhibit a structural transformation from the paramagnetic/antiferromagnetic martensite phase to the ferromagnetic austenite phase upon heating or the application of a magnetic field. As a result, a so-called inverse MCE (sample cools upon magnetization) was reported [6]. The melt-spinning technique has proven to be very useful for synthesizing various functional magnetic materials with a homogeneous chemical composition and a refined microstructure [7–9]. The morphology and magnetic state of precipitates present in the ribbons and their influence on MIA and MCE are also studied. It will be shown that an adequate annealing decreases both H_h and H_{cr}, and increases the degree of atomic order. Therefore, the ribbons and particles are a suitable precursor for MSM–polymer composites or as a staring material for powder production. The development of an MSM–polymer composite and grain refinement powder metallurgy produced materials is a feasible solution to overcome the brittleness of MSM alloys [10]. Furthermore, the blocking stress originated from the magnetostructural transformation in the Ni–Mn–In–Co alloys is expected to be large enough to drive the polymer matrix and lead to a large MFIS.

2. EXPERMENTAL PROCEDURE

The alloy with the chemical composition as follow $Ni_{50}Mn_{37,5}Sn_{12,5}$ was cast by induction melting of elements with purity better then 99.9%. Then ingot were homogenized at 1000°C for 6 hours in a vacuum. The rapid solidification trough the melt spinning onto copper wheel rotating at a surface speed of 25 m s^{-1} was used for production of ribbons. Pulverization of melt spun ribbons was performed by ball milling in the Fritsch P5/4 mill in the argon atmosphere. The densification of powders into dense compact was made by vacuum hot pressing at 650°C under 320 MPa for 10 min. The investigations of microstructure were performed by light (LM), scanning (SEM) and transmission electron microscopy (TEM). The crystallographic structure of samples were examined by X-ray diffraction (XRD) and characteristic temperature of martensitic transformation by differential scanning calorimetry. Mechanical properties were determined by compression test.

3. RESULTS AND DISSCUSION

Fig. 1a and b presents the results of microstructure investigations of melt spun ribbons performed by SEM and LM microscopy.

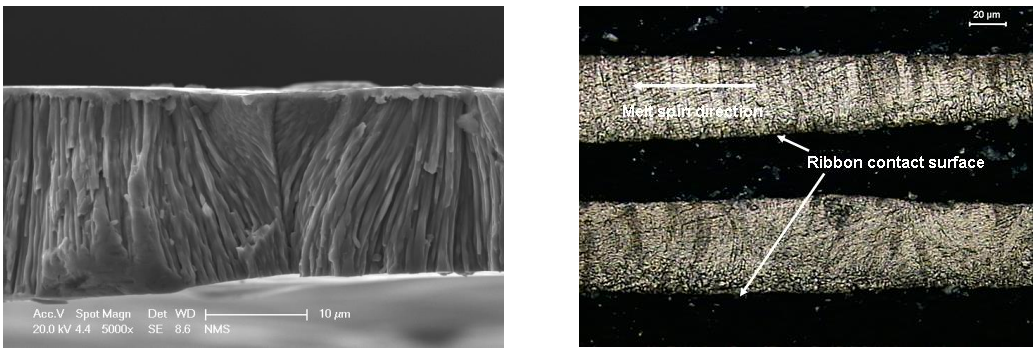

Fig. 1. Microstructure of melt spun ribbons performed by a) SEM and b) LM microscopy.

Fig. 1a shows SEM micrograph of fracture surface from the $Ni_{50}Mn_{37,5}Sn_{12,5}$ ribbon. There are a dendrites microstructure caused by solidification shrinkage in a 20-µm-thick ribbon. Fig. 1b presents the LM micrograph of cross section of $Ni_{50}Mn_{37,5}Sn_{12,5}$ ribbon. There are columnar grains characteristic for melt spinning process due to direction of heat transfer during crystallization. The crystallographic structure analyze of melt spun ribbons showed that two phase structure consisting of $L2_1$ austenite and modulated orthorhombic martensite can be well indexed.

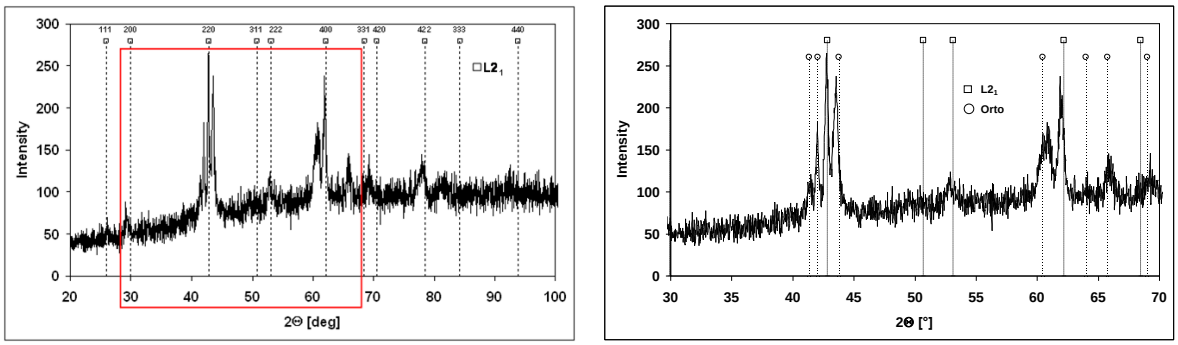

Fig. 2. X-ray diffraction patterns of ribbon presented in the two 2 theta range for better visibility of the martensite structure.

Detailed studies of microstructure of two phase ribbons were performed by the TEM investigations. Fig. 3 presents bright field (BF) image and corresponding STEM-HAADF showing Z-contrast image of ribbon.

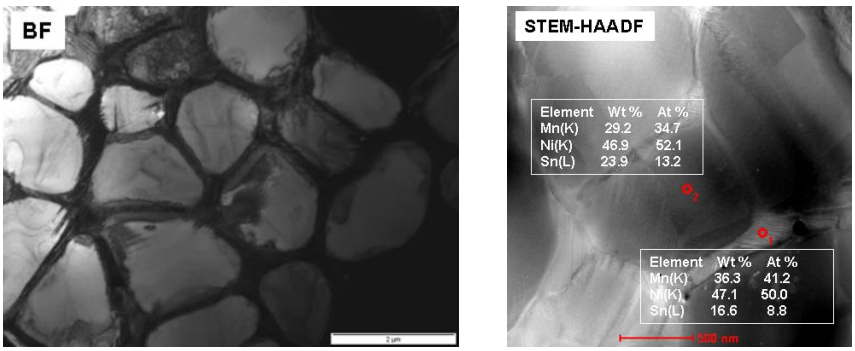

Fig. 3. Bright field (BF) image and corresponding STEM-HAADF showing Z-contrast image of ribbon.

The typical cellular microstructure is observed with the cells of size of about 1,3 μm ±0,3 and intercellular area with the mean area of about 0,3 μm ±0,1. The point EDS chemical analysis performed in these two areas shows differences in chemical composition, especially it concerns a manganese and tin. This causes the different valence electron concentration e/a calculated as e/a=8.167 for cellular grain and e/a= e/a=8.236 for intercellular area, respectively. So, we can see that rapid solidification process introduces some chemical heterogeneity (segregation of particular elements) on the grain boundaries forming the cellular microstructure. In order to determine a crystallographic structure of these two areas, electron diffraction investigations (SADP) were performed. Fig. 4 shows BF images and corresponding SADPs for cellular grain and intercellular area respectively. It can be seen that in case of cellular grain the diffraction pattern can be well indexed based on $L2_1$ Heusler structure with the [110] zone axis, whereas intercellular area has a lower symmetry four layered martensite with the orthorhombic structure and [010] zone axis. This result is in good agreement with the X-ray investigations. Due to a bigger e/a ratio in the intercellular area the martensitic transformation start temperature M_s is shifted into higher temperature range and we can observe a martensite phase in the room temperature. So it can be assumed that during cooling of ribbons the preferentially martensitic transformation occurs at the grain boundaries of austenite $L2_1$ phase.

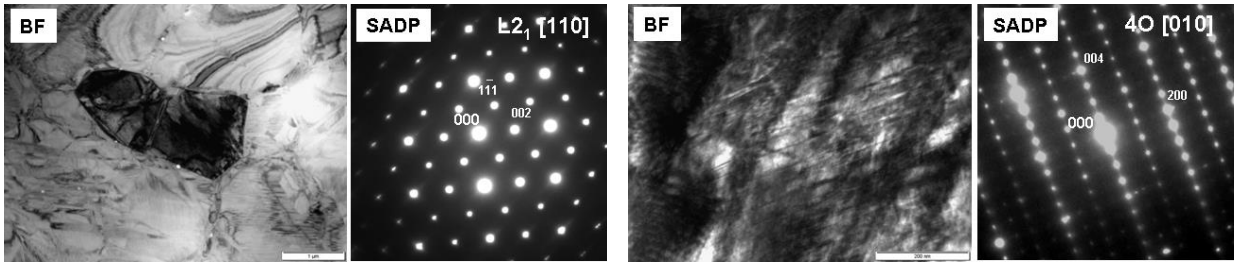

Fig. 4. Bright field (BF) image and corresponding STEM-HAADF showing Z-contrast image of ribbon.

In order to obtain the dense sample from the ribbons their were pulverized then compacted by the vacuum hot pressed at 650°C under 350MPa. Fig. 5 presents LM images of hot pressed compact taken at two magnifications. The compact density was about of 98% of theoretical density. Well sintered powder particles without the additional phases on the boundaries were observed.

Fig. 5. LM images of hot pressed compact taken at two magnifications a), b) and SETM-HAADF image c).

The structure hot pressed sample was similar like in case of ribbons consisted of austenite and martensite phases, however the shape of grains was changed. The homogenous equi-axed

grains of size of about 500 nm were observed both of marteniste and austenite phase, what is illustrated in Fig. 4c. It means that vacuum hot pressing of pulverized ribbons leads to the chemical homogenization by diffusion processes. These processes are accelerated by introduction of high amount of dislocation through applying an external pressure. Additional solution treatment at 900°C for 1 h and water quenching caused an increase of volume fraction of martensite phase and decreasing a dislocation density (Fig. 6).

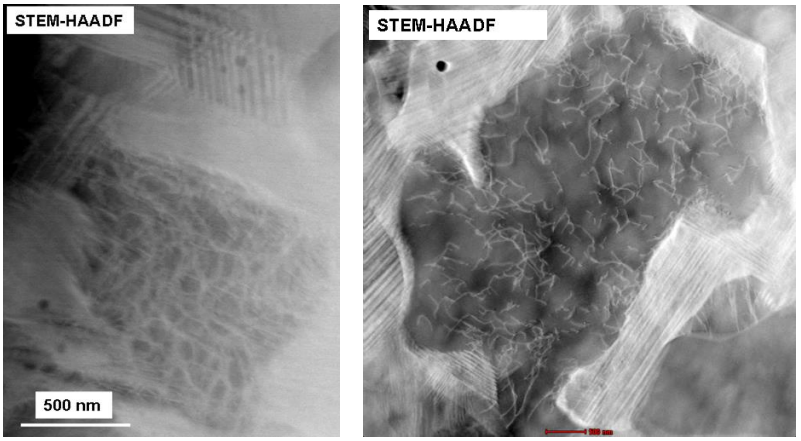

Fig. 6. STEM - HHADF images of as compacted (left) and as compacted and solution treated (right) sample

The same martensite type 4O like in a ribbon was observed in the solution treated sample. So we can conclude that compaction and solution treatment doesn't change of the structure, but changing a chemical homogeneity, grain size and their shape, dislocation density and volume fraction of constituent phases. These factors influence on mechanical properties of alloy. While ribbons are very small and brittle the determination of their mechanical properties is almost impossible, the compact has an enough size for preparation of sample for compression test. Fig. 7 shows the compression test result of as compacted and as compacted and solution treatment sample. One can see that as compacted and as compacted and solution treated samples shows a high compression strength of compacts 1920 MPa and 1410 MPa respectively, and plastic deformation of about 7,6 and 9,4% respectively. Especially the improve of plasticity is a big advantage because the Heusler alloys both as conventionally cast an heat treated as well as rapid quenched into the ribbon form do not have practically plasticity.

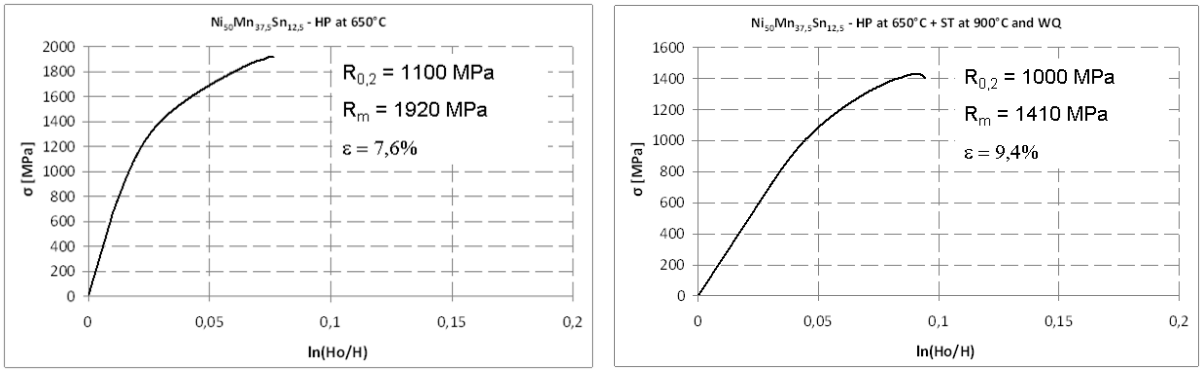

Fig. 7. Result of compression tests for as compacted (left) and as compacted and solution treatment sample (right).

The martensitic and reverse transformations of samples after different processing were analyzed by use DSC method. Fig. 8 presents collective result of DSC measurements during

cooling and heating cycles of samples after tree different treatment i.e. ribbons, as compacted and as compacted and solution treated.

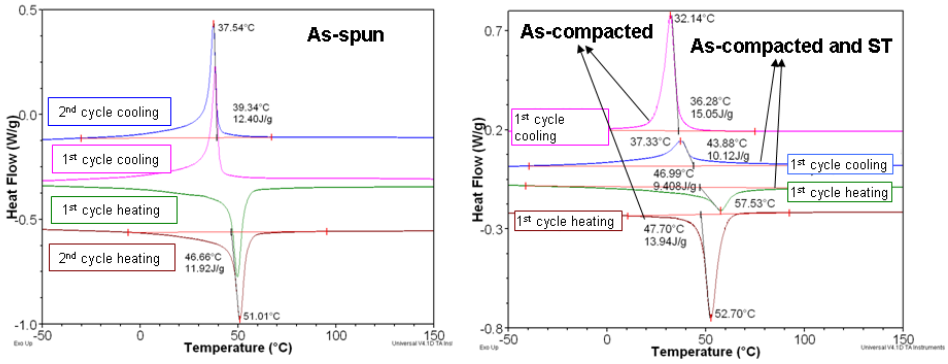

Fig. 6. Result of compression tests for as compacted (left) and as compacted and solution treatment sample (right).

The martensitic and reverse transformations were observed both in as-spun and as-compacted samples in vicinity of room temperature. This is good phenomena in terms of magnetocaloric application. The transformation with the highest heat of about 14 J/g realized close to room temperature was found in as-compacted and solution treated sample. Combining this effect with beneficial plasticity makes this material very promising for future applications.

4. CONCLUSIONS

1. Selected fabrication processes consisting of rapid solidification and powder metallurgy allowed to obtain the dense compacts of size 20 mm of diameter and 5 mm of thickness of $Ni_{50}Mn_{37,5}Sn_{12,5}$ alloy.
2. The cellular type of microstructure was formed in very brittle melt-spun ribbons as result of micro-segregation of elements with different melting points. The $L2_1$ parent phase and 4O martensite were identified in cells and intercellular area respectively, as result of differences of their chemical composition and e/a ratio.
3. The cellular microstructure was observed in as-compacted samples. High density of dislocation introduced by high stresses during hot pressing process were observed in cells of $L2_1$ phase. The solution treatment of compacts caused reduction of dislocations density in $L2_1$ phase an slightly increase of grain size.
4. The compression tests of as-compacted and as-compacted and solution treated samples showed a high compression strength of compacts 1920 MPa and 1410 MPa respectively, and plastic deformation of about 7,6 and 9,4%.
5. The martensitic transformation were observed both in as-spun and as-compacted samples in vicinity of room temperature. The transformation with the highest heat of about 14 J/g realized close to room temperature was found in as-compacted and solution treated sample.

5. LITERATURE

[1] Coulomb, D. The IIR and environmental challenges facing the refrigeration sector. In: Poredos, A., Sarlah, A. (Eds.), Proceedings of the Second International Conference on Magnetic Refrigeration at Room Temperature, 2007 April 11–13, Portoroz, Slovenia. International Institute of Refrigeration, Paris, pp. 3–5.

[2] Gschneidner Jr KA, Pecharsky VK, Tsokol AO. Rep Prog Phys 2005;68:1479.

[3] Kainuma R, Imano Y, Ito W, Sutou Y, Morito H, Okamoto S, et al. Nature (London) 2006;439:957.

[4] Krenke T, Acet M, Wassermann EF, Moya X, Manosa L, Planes A. Phys Rev B 2005;72:014412.

[5] Yu SY, Ma L, Liu GD, Liu ZH, Chen JL, Cao ZX, et al. Appl Phys Lett 2007;90:24250

[6] Krenke T, Duman E, Acet M, Wassermann EF, Moya X, Manosa L, et al. Nat Mater 2005;4:450.

[7] Liu J, Scheerbaum N, Hinz D, Gutfleisch O. Appl Phys Lett 2008;92:162509.

[8] Gutfleisch O, Yan A, Mu¨ ller KH. J Appl Phys 2005;97:10M305.

[9] Yan A, Gutfleisch O, Gemming T, Mu¨ ller KH. Appl Phys Lett 2003;83:2208.

[10] Scheerbaum N, Hinz D, Gutfleisch O, Mu¨ ller KH, Schultz L. Acta Mater 2007;55:2707.

Acknowledgements

This paper was created within the project "**Creation of an international scientific team and incorporation to scientific networks in the area of nanotechnology and unconventional forming material. CZ.1.07/2.3.00/20.0038"**, which is financed by the European Social Fund and state budget of the Czech Republic.

european social fund in the czech republic
EUROPEAN UNION
MINISTRY OF EDUCATION, YOUTH AND SPORTS
OP Education for Competitiveness
INVESTMENTS IN EDUCATION DEVELOPMENT

EXPERIMENTAL POSSIBILITIES OF SPD INVESTIGATION IN ALUMINIUM ALLOYS

Vladivoj OČENÁŠEK

SVÚM a.s., Podnikatelská 565,190 11 Praha 9- Běchovice, CZ, ocenasek@svum.cz

Abstract

Aluminium and its alloys belong to materials in which the SPD (Severe Plastic Deformation) effect on the microstructure and properties is often studied. The most usual deformation methods are ECAP (Equal Channel Angular Pressing), HPT (High Pressure Torsion), ARB (Accumulative Roll Bonding); a special equipment Conform can be also used in some cases. These methods are relatively difficult from the experimental point of view and, consequently, only smaller deformations are reached in bulk materials or in greater volumes what is insufficient for the industrial applications. At the present time, ECAP and Conform methods seem to be the most suitable. Further, the aim of deformation experiment influences substantially its performance. It is important for the choice of alloy and its state, whether the plastically deformed material is used for different investigations (e.g. creep resistance, superplasticity, structural stability) or the resulting material state is considered as the final one. In aluminium alloys, the heat-treatable or non het-treatable alloy type influences also the way of deformation experiments. For SPD investigation, the both alloy types are used. In the present paper, the attention is paid particularly to the choice of deformation parameters in the dependence on the alloy type and initial structural state. Typical examples of alloys deformed mostly by ECAP method are shown.

Keywords

Aluminium alloys, severe plastic deformation, heat-treatable alloys, non heat-treatable alloys

1. INTRODUCTION

Severe plastic deformation leads to a fine-grained microstructure characterized by the sub-micron grain size. The present paper deals above all with the choice of deformation parameters in the dependence on Al alloy type and on the initial structure namely from the point of view of possible applications and contemporary production technologies as well. The results of SPD experiments on typical heat-treatable and non heat-treatable Al alloys are mentioned. Owing to simplicity and some specific features of different SPD methods, the following considerations are aimed at the most utilized SPD method, i.e. ECAP method. Alloys produced by powder metallurgy (PM) as well as metal matrix composites are not dealt with in this paper.

SPD method has been widely applied on a considerable amount of Al alloys and initial structural states. There are many reasons for investigation of SPD effect. For example, the aim can be

both the study of the influence of severe plastic deformation on the refinement of structure in the model material and the research of the material use for particular applications. Then, various material tests follow – e.g. thermal stability tests (creep, superplasticity) or corrosion resistance and fatigue tests. Experimental material is of various origin and history and that is why the following heat treatment resulting in the defined initial structural state is carried out before the start of experiment. However, the material of unknown origin and undefined initial structural state is sometimes used for experiments and this fact can influence unfavourably both the interpretation of the results and possible applicability. Thus, a particular attention is paid to the initial structural state of the material and to its effect on the choice of SPD parameters as well as on the use of the results in practice.

As it was mentioned above, materials of various origin are used for the study of SPD effect on their structure and properties. The initial structure influences markedly both the deformation conditions of experiments and the final properties resulting from the SPD performance. The lack of information on the material origin (i.e. its processing history) can decrease the value of the results, make their reproducibility impossible or complicate their interpretation. The scheme of common technological procedure used in production of Al and its alloys is shown in Fig. 1. It consists of casting, high temperature annealing (homogenization), hot deformation, cold deformation, interannealing and final heat treatment. Some operation can be omitted in the dependence on alloy- and product type. SPD experiments can be performed after each operation. Experimental material is delivered mostly in the wrought state (rolled, extruded) or heat treated to obtain a defined temper (e.g. T4, T5, T6, T7X). Thus, we usually have not enough information on the material origin and, consequently, we cannot influence some structural parameters. On the other hand, the above mentioned problems following from the ignorance of technology can be eliminated if the material is prepared systematically for experiments and all processing data are available.

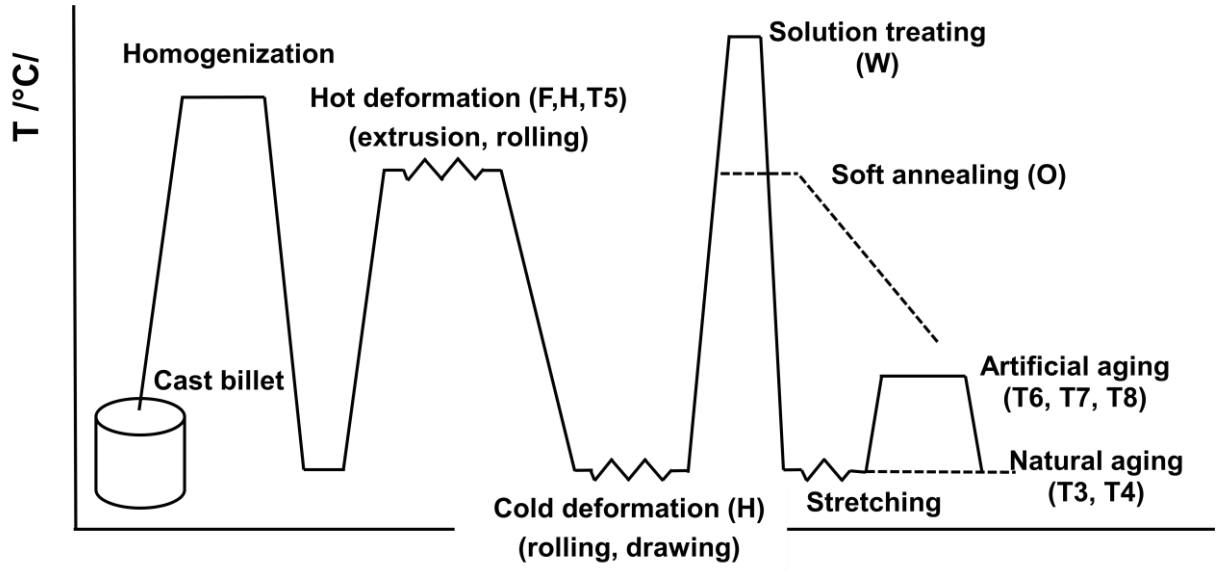

Fig. 1 Scheme of common technological procedure by preparing aluminium products

2. EXPERIMENTAL MATERIALS USED FOR SPD STUDIES

From the point of view of material preparation and its final properties, Al alloys can be divided in usual way into two groups, i.e. into the heat-treatable and non heat-treatable ones. In this paper, the third group - Al alloys containing Sc and Zr which can be considered as the members of the both groups – are also dealt with.

Typical non heat-treatable materials used in SPD experiments are pure Al and Al-Mg alloys. Considered from the point of view of SPD study, pure Al is the classical model material. However, owing to its low mechanical properties and low temperature stability, it has no practical use in a highly deformed state and therefore the attention will not paid to it in this paper. Alloys of 5XXX type (Al-Mg) are frequently used. Furthermore, 6XXX type alloys containing Mg and Si as well as 7XXX type alloys containing Zn, Mg and Cu are also often studied by SPD method (e.g. 6061, 6082 and 7075 alloys). In the dependence on the contents of alloying elements and technological parameters of the material preparation, the composition of intermetallic phases, hardening phases, workability and, consequently, final material properties after SPD are changed. Considering the large scope of SPD experiments carried out, only some chosen aspects of these experiments will be further discussed.

3. INITIAL STRUCTURE AND CHOICE OF PARAMETERS FOR DEFORMATION EXPERIMENTS

Some technological parameters which can substantially influence the programme, course and results of the experiments will be dealt with.

3.1 As cast structure and structure after high temperature annealing

As the structural stability after SPD is strongly influenced by size and distribution of primary and precipitating phases, the casting- and high temperature annealing (homogenization) conditions are very important. We aim at obtaining a fine grained structure during casting that contains smaller and uniformly distributed particles of intermetallic phases. When the as cast material is coarse grained, the particles of intermetallic phases are also coarse which results in deterioration of the final properties. The following high temperature annealing and its parameters (temperature, cooling rate from the annealing temperature) determinate the change of the shape and composition of dispersed particles as well as the conditions for precipitation of hardening phases in heat-treatable alloys. After homogenization, the shape and composition of dispersed particles remain substantially unchanged in the course of the following operations. In the case of material that is not homogenized, deformability decreases and intermetallic phases change in the dependence on the following processing steps. Therefore, the parameters of the casting process as well as those of high temperature annealing would be also taken in consideration during the preparation of experimental material for SPD tests [1].

3.2 Structure in the dependence on the alloy type

The initial structure is quite substantial for the course of deformation experiments as it determines the strategy of the experiment and vice versa; for particular strategy it is necessary to choose a suitable initial structure. Both the material state (soft or hardened) and the presence of intermetallic phases and/or precipitates are quite substantial. Furthermore, it is necessary to assess the possible changes in the structure during the relatively long-term tests. In addition to the alloy type (heat-treatable, non heat-treatable), the demands on the final structure (thermal

stability, superplastic behaviour, high strength at ambient temperature together with sufficient plasticity) play an important role. Typical combinations of initial states of structure and deformation parameters are as follows:

a) Non heat-treatable alloys

The initial state for deformation experiments in these alloys is – similarly to pure Al- the recrystallized structure. The tests are performed mostly at room temperature with the exception of high alloyed Al-Mg alloys, where elevated temperatures are indispensable owing to a lower deformability. Non heat-treatable alloys are not often used for the investigation of SPD effect on structure and properties. Their properties become more important under extreme SPD conditions, e.g. when HPT method is applied or in the case of alloying by other elements (Sc, Zr).

b) Non heat-treatable alloys containing Sc and Zr

Non heat-treatable alloys Al-Mn and Al-Mg containing several tenths percent of Sc and Zr have very interesting properties that are caused by Al_3(Sc,Zr) phase precipitation. This dispersoid originates as early as during cooling from the casting temperature and its size reaches some nanometers. The phase is coherent up to a relative high temperature, uniformly dispersed, inhibits recrystallization and, in addition to it, contributes to hardening. Al-Mn and Al-Mg alloys containing Sc and Zr have an outstanding resistance against recrystallization. In the case of heat treatment, e.g. during the homogenization annealing, a metastable or stable dispersoid is formed; it cannot be dissolved under usual conditions as it dissolves at temperatures close to the solidus temperature. When the high temperature annealing is not carried out, a relatively sufficient amount of Sc and Zr will remain in the solid solution. This situation can be utilized for a marked hardening that results from the annealing between 300 and 350°C. Therefore, there are substantially two possible performances of deformation experiments. The first one utilizes the initial structure in which the precipitation of Al_3(Sc,Zr) phase is completed. The following heat treatment (e.g. inter annealing) after cold working at about 400°C) changes dispersiods structure no longer. The second possibility is very interesting and utilizes as cast structure. Deformations at successive passes are carried out at 300 – 350°C when the resistance to deformation is lower and, at the same time, the precipitation of Al_3(Sc,Zr) dispersoid occurs. The resulting wrought microstructure is fine grained and work hardened not only by dislocations but also by Al_3(Sc,Zr) particles. In the case of AlMg3 alloy, it can be supposed that the hardening leads to the strength value of approximately 450 MPa which is the level typical for high strength heat-treatable alloys.

c) Heat-treatable alloys

In the case of heat-treatable alloys, the situation is more complex owing to the necessity of carrying out the solution heat treatment at temperatures between 475°C (7075 alloy) and 530°C (6XXX alloys). If SPD were performed before the solution heat treatment, the stored deformation energy would lead during the solution treatment to recrystallization and completely lost of the intended fine grained structure. It is practically impossible to obtain the submicron grain size in this way. If the experiment aims at obtaining the grain size of several hundred nanometers and, at the same time, at reaching high strength values corresponding with the investigated alloy, it will be necessary to perform the deformation after solution heat treatment. On the other hand, when the deformation is not performed immediately after cooling from the

ageing temperature, it must be considered that the alloys will age naturally and the hardening will occur. The increment of hardening caused by natural ageing can be equal to 50 – 100 % hardening effect obtained by artificial ageing. During the deformation caused by successive passes, deformation hardening as well as precipitation hardening (which become faster owing to deformation) will occur in the material. Thus, there is a fundamental restriction for high strength heat-treatable alloys as it is very difficult to carry out the multipassed deformation at room temperature after solution heat treating [2]. To utilize effectively the precipitation potential of the investigated alloy, the deformation temperature would not exceed the temperature of the artificial ageing [3]. In this case, the deformation temperatures will be mostly under 200 °C. Maximum strength values depend on the total time during which the alloy is held on the deformation temperature (including the heating up period). As the time of artificial ageing depends on the alloy type and on the ageing temperature and reaches 4 – 12 hours, the multipassed deformation (e.g. ECAP method) can be usually performed within this time interval. It follows from above that the investigation of SPD effects in heat-treatable alloys without solution heat treatment has practically no sense. SPD hardening is lower than precipitation hardening and the material prepared in this way would be utilized in practice only in the case if a fine grain were – from some reason – the determining parameter (superplasticity).

The investigation of SPD in 7075 alloy from the point of view of its use for high strain rate superplasticity (HSR SP) is carried out frequently. In this case, the initial structure is a soft state obtained by the slow cooling from temperatures about 400°C, cooling rate being lower than 50 °C/h. Heat treatment connected with the hardening to reach the optimum mechanical properties would be applied after the superplastic forming. In this case, SPD aims at obtaining the fine grained structure that enables to gain improved parameters of superplastic forming as compared with the common way of preparation of the fine grained structure with grain size 5 – 10 μm. To reach this initial grain size, a special four step thermo mechanical processing treatment is usually applied before the superplastic forming of 7075 sheets is carried out [4,5,6].

Quite extraordinary mechanical properties have been reached recently by HPT method. It can be seen from Fig. 2 that the strength of about 1000 MPa and ductility of 9 % was obtained for 7075 alloy [7]. This is obviously connected with extreme deformation conditions of HPT method; they cannot be assured during the experiments performed by other methods (ECAP, ARB, Conform).

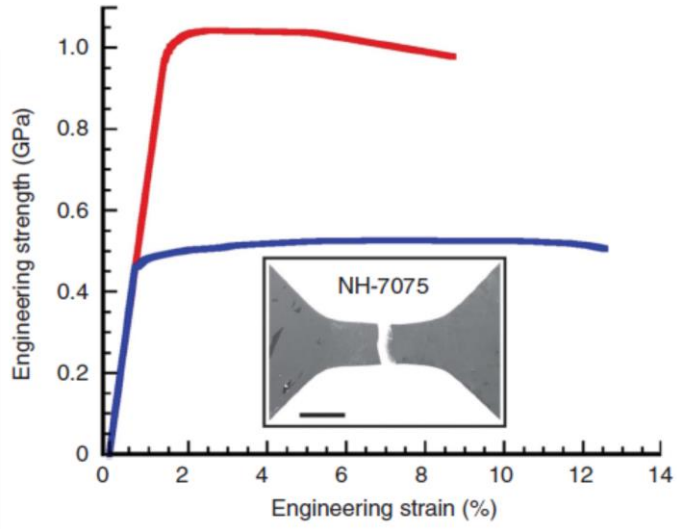

Fig. 2 Mechanical properties after HPT of 7075 alloy [7] Commercially treated (blue line) Special heat treatment before HPT (red line)

4. CONCLUSION

The paper aimed at calling attention to some connections between the preparation technology of experimental material and the conditions for SPD investigation in Al alloys. Considering the demands on the properties of fine grained structures, it is necessary to know not only the initial structure for experiments but also the history of preceding technological operations (casting, heat treatment of as cast structure). The performance of deformation experiments depends on the alloy type and on demands that are laid down for the deformed material.

5. LITERATURE

[1] L. Lodgaard.: Precipitation of dispersoids containing Mn and/or Cr in Al-Mg-Si-alloys, Thesis, (2000), NTNU Trondheim

[2] Y. Zhao at al.: Microstructures and mechanical properties of ultrafine grained 7075 Al alloy processed by ECAP and their evolutions during annealing, Acta Materialia 52 (2004) 4589-4599

[3] X. Sauvage, M. Yu. Murashkin, R. Z. Valiev.: Atomic scale investigation of dynamic precipitation and grain boundary segregation in a 6061 aluminium alloy nanostructured by ECAP, Kovove Mater. 49 (2011) 11-15

[4] J. A. Wert, N. E. Paton, C. H. Hamilton, and M. W. Mahoney.: Metall. Trans.,12A (1981) 1267

[5] V.Ocenasek at al.: Effect of heat treatment on the structure of the aluminium alloy aa7075 subjected to intensive plastic deformation by ecap, Conf. Metal 2008, CD ROM

[6] K. Turba, P. Malek, E. F. Rauch, and M. Cieslar.: The optimization of ECAP conditions to achieve high strain-rate superplasticity in a Zr- and Sc-modified AA 7075 aluminum alloy, Int. J. Mater. Res. (Zeitschrift für Metallkunde) 100, 2009, 851 – 857.

[7] P. V. Liddicoat at al.: DOI:10.1038/ncomms1062 (2010)

Acknowledgement

This contribution was created within the project Creation of an international scientific team and incorporation to scientific networks in the area of nanotechnology and unconventional forming material. CZ.1.07/2.3.00/20.0038, which is financed by the European Social Fund and state budget of the Czech Republic.

european social fund in the czech republic
EUROPEAN UNION
MINISTRY OF EDUCATION, YOUTH AND SPORTS
OP Education for Competitiveness
INVESTMENTS IN EDUCATION DEVELOPMENT

Production of nanosized metallic powders

Patrick OCHIN [a], Yannick CHAMPION [a]

[a] *ICMPE Institut de Chimie et des Matériaux Paris Est, CNRS-Université Paris Est UMR 7182, 2-8 rue Henri Dunant, 94320 Thiais France, ochin@icmpe.cnrs.fr*

Abstract

Nanometric metallic powders have been synthesized based on the evaporation-condensation principle since the middle of 70's. Another process, cryomelting also based on the gas condensation technique, has been developed since 1983 at CECM-CNRS (*today ICMPE*). It consists in overheating a molten metal in contact with a cryogenic fluid (nitrogen or argon). Fusion by induction in electromagnetic levitation avoids any potential chemical reaction with a container and permits the overheating of the melt and a subsequent improved evaporation rate. Nanocrystalline powders of pure metals (Fe, Co, Cu, Cr, Al) and magnetic alloys (Fe-Ni, Co-Ni) have been produced. A moderate rate of production (less than 50g per hour) is obtained which allows to produce macroscopic compacts (through pressing and subsequent sintering).

We present in this article, after a brief survey of different methods, a detailed description of this process and its limits. We focused on a summary of our results on iron, copper (using liquid nitrogen) and aluminium (using liquid argon). Different conceptual models have been proposed to explain the formation of each of the two kinds nanocrystalline metal particles.

Keywords

Induction melting in levitation, cryomelting, evaporation-condensation, nanosized powders, induction coupled plasma.

1. INTRODUCTION

Synthesis of Ultrafine powders, in the range of a few to a hundred nanometers, began as early as the beginning of the 20th century. Kohlschutter et al (1912) produced sub-micronic particles of Zn, Cd, As by slow distillation under vacuum or different gas (H_2, N_2, CO_2), others authors using colloidal suspensions (gold), and after in the 30's by evaporation of metals with a high vapour pressure (such as zinc) [1]. We have to wait the beginning of the 70's to see an extend of research and production scale of UFP's (Ultra-Fine Particles), due mainly by the interest for the production of high quality magnetic recording tapes, with works of Granqvist et al [2], Gleiter et al in the 80's [3].

UFP's can be obtained by physical or chemical methods [4]. The choice of the method depends on the required compound, taking into account its physical and chemical properties, the cost and production rate.

Mechanical alloying is today among the most utilized methods. Commercial instruments (mainly planetary ball milling) have been developed which allow to obtain compounds with varied structural and microstructural states including nanocrystalline (agglomerates a few tens of nanometers) [5]. Devitrification after adjusted heat treatments of metallic glasses can lead to nanostructured alloys with ultra-fine grains as thin as 10 nm [6].

The principle of evaporation of a bulk compound, metal or inorganic/ceramic compositions, followed by nucleation (homogeneous or heterogeneous), followed by condensation into individual particles or onto a substrate, has also been largely used. Different techniques depending on the heating sources (resistant heating direct or indirect [7], electron beam, laser, electric arc or plasma [9]) and the gaseous atmosphere (vacuum, low pressure inert gas) have been developed. N. Wada for instance used a reactor with a tungsten crucible for melting and a rotating copper cooled disk to gather the fine particles [8], and studied the effects of the nature of gas partial pressure and temperature of the melt on particles morphology and size.

Many chemical methods have demonstrated good results mostly for ceramics and precious metals [4], and are commonly based on reduction in situ (generally oxides), thermal decomposition of an organometallic precursor or spray pyrolisis, which is a related technique at higher temperatures. In this latter method solutions of pure or mixed metal salts are converted to aerosols, which pass through a high temperature furnace or a plasma torch.

We present in this short review some results we obtained in our laboratory by using the cryogenic melting technique to produce Fe, Cu, Al and Fe-Ni nanosized powders.

2. PRODUCTION OF NANOSIZED METALLIC POWDERS AND NANOSTRUCTURED ALLOYS AT ICMPE.

We present on Fig.1. a synoptic of ultrafine metallic powders in our Institute. One route starts from the molten state and leads to rapidly solidified nanostructured products the second one by using the cryomelting technique to form nanosized particles. Another route from the solid state leads, by ball milling, to ultrafine agglomerates (nano to micrometer grain size) of elementary or alloyed particles. We will focus only on the method based on evaporation – condensation principle which has been developed at ICMPE (former CECM Vitry) by using induction melting in levitation, as a heating source, in a cryogenic fluid [10].

Granqvist in [2] proposed a versatile method by evaporation from a temperature regulated crucible, as a vapour source, in a chamber under a reduced inert atmosphere (Fig.2b). Different elemental (resistive) ultrafine particles smaller than 20 nm, almost spherical of oxidized Al, Mg, Zn, Cr, Fe, Ni, Cu and Ga have been produced. The logarithm of the particle diameter has a Gaussian distribution for the smallest sizes whereas bigger ones deviate from this behaviour. The metal vapour is cooled in the gas. The efficient cooling produces locally a high supersaturation of metal vapour, which leads to a homogeneous nucleation. For most materials nucleation and growth takes place only in a region above the molten metal surface whose thickness depends the vapour pressure and temperature. Coalescence is supposed to be the dominant growth mechanism. In the rest of the vessel the crystalline particles are carried by convective gas flow. Larger particles size have been found to be favoured by higher atomic weight of the gas.

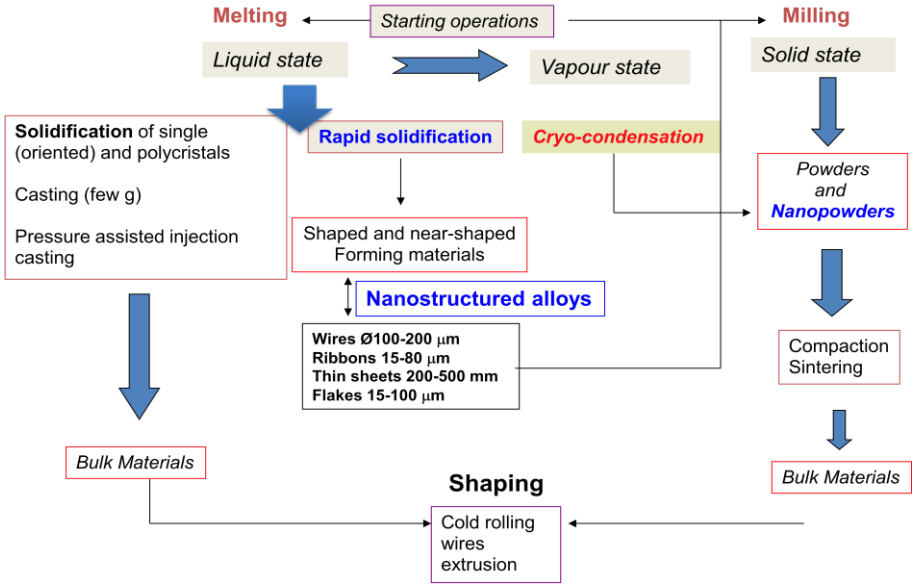

Fig. 1 Synoptic of nanostructured alloys and nanosized metallic powders preparation at the materials production facilities of the institute ICMPE-CNRS Thiais.

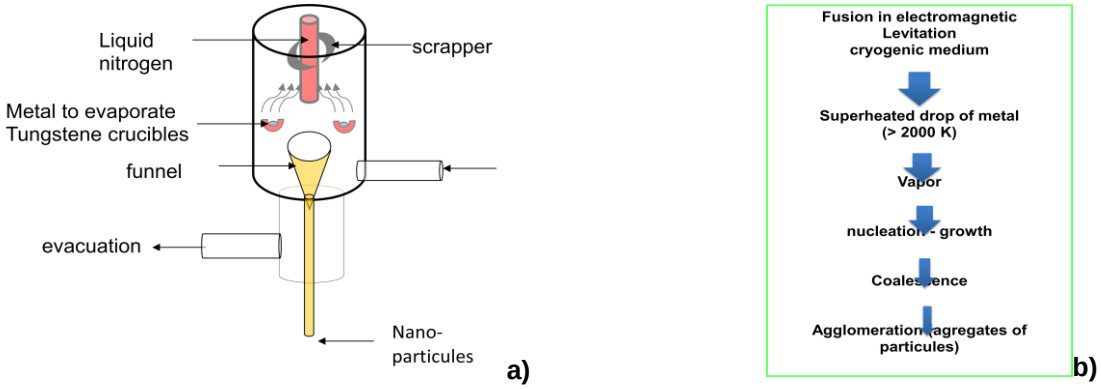

Fig. 2 Scheme of the evaporation-condensation method for the production of nanocrystalline particles: a) C.G. Granqvist apparatus sketch [2], particles are trapped on a liquid nitrogen cooled finger. b) synopsis of the cryomelting method for the production of nanosized metallic particles.

The use of refractory crucibles becomes incompatible with high melting point and/or more chemically reactive metals, thus electromagnetic levitation has been used [10]. This process enables these metals to be brought up to around 2000°C and to obtain a powder production of several grams per minute. Fig.2b presents a synoptic of the process. When a metal is heated in a cryogenic liquid such nitrogen or argon, a turbulent calefaction forms isolating the surface of the molten metal from the cryogenic liquid. In this layer the metallic vapour condenses into fine nanometric particles that are carried away by the gaseous phase produced and collected by filtration. To obtain powders from metals such as iron, nickel or cobalt one must reach very high tempertures, greater than 2000°C in order to get a sufficient vapour pressure. The sketch of the device is reported on Fig.3.

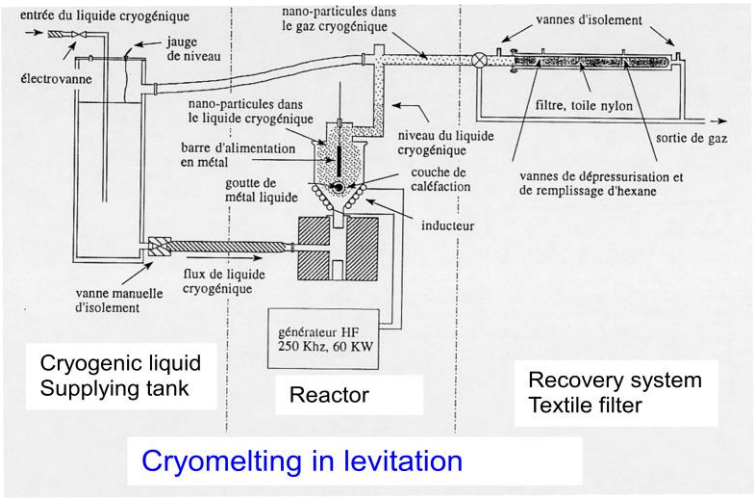

Fig. 3 Experimental apparatus for producing nanocrystalline powders.

The cryogenic liquid supply system enables to maintain a constant level in the reactor. The reactor with the levitation coil is placed in a transparent silica vessel where the molten metal and the cryogenic liquid are in contact (Fig.4 right). A metal rod is lowered in regular intervals to feed the drop of metal. The recovery system for powders collecting is made of a nylon sieve of defined porosity. The HF generator is an aperiodic generator 150 kW (Five-Celes) with a frequency close to 150 kHz.

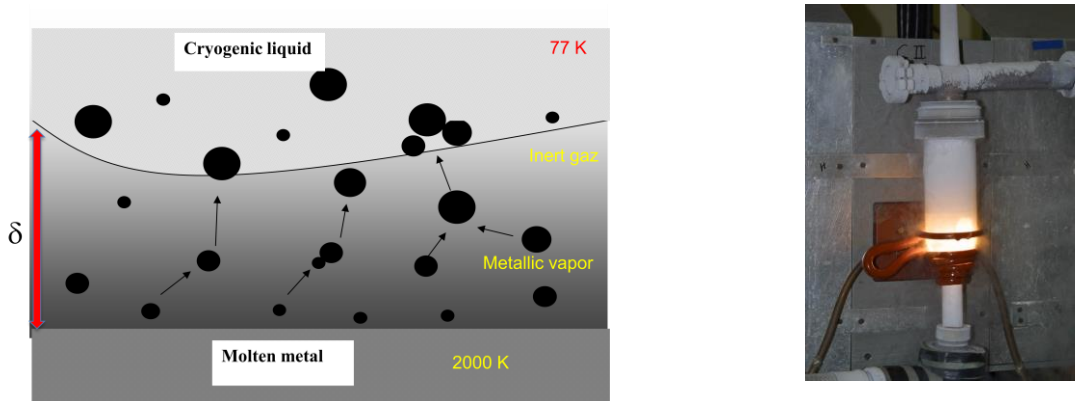

Fig. 4 On the left: a conceptual model of cryomelting-evaporation and condensation of ultrafine powders. On the right: photograph of electromagnetic levitation in a cryogenic liquid experiment.

The Fig. 4 left. shows the conceptual model of the method. A turbulent calefaction layer, consisting of gas vapours from the cryogenic liquid and supersaturated metal vapour, forms between the molten surface (about 2000K) and the cryogenic liquid (her N2 L 77K). A strong temperature gradient is created on this short distance δ thick. Three stages succeed, from the molten drop surface to the cryogenic liquid, first nucleation and growth mechanism located at the lower part of the zone, coalescence and coagulation of nanosized particles, finally particles quenching step.

Production of nanocrystalline powders depends critically on the vapour pressure of the overheated metal (Table 1.). The powder production rate depends on the vapour pressure, therefore on the temperature and on the evaporation surface. The morphology of individual particle is generally spherical and the structure monocrystalline.

Table 1 Vapour pressure of some experienced metals and production rate

Metals	Cu	Fe	Ni	Co	Al	Mg	Cr	Si	Sn	Ti	Zr	W
Vapour pressure at 1700K (torrs)	0,1	0,01	0,001	0,001	0,1	10^3 at 1400 K	10^{-2}	10^{-3}	10^{-1}	10^{-4}	10^{-8}	$<10^{-11}$
ProductionYield (g/minute)	1	1	1	1	0.1	Few 100 mg	Few mg	nm	nm	0	0	-

For instance we obtained for iron 1.52 g/mn for a 4 cm^3 levitated drop and 2.38 g/mn for 6 cm^3. Chromium, due to the high melting point and reactivity, is difficult to produce with this method, for Ti, Zr and W, due to their low vapour pressure, it was impossible to obtain particles with the limited temperature we can reach by induction melting in levitation.

The cryogenic liquid must not react with the melt, thus for metal like iron, cobalt or copper liquid nitrogen was used and liquid argon for aluminium and chromium. The cryogenic liquid level has an influence on powders: powders produced with the level close to the molten drop have an average diameter of one micrometer, then size diminishes when the level of liquid increases until 50 cm high. In normal conditions for iron their average diameter is 30 nm.

Fig. 5 shows TEM micrographes of iron and copper produced powders with their respective size distribution. Production rate for Cu reached only 1g/mn for a distribution log-normal 25 nm. One can observe a Cu2O external layer 3 nm thick, which is strained to accommodate the surface curvature (Fig. 6) [11]. Aluminium powders have been produced in liquid argon to avoid nitride formation. The production is limited to 0.15 g/mn, four times lower than for Fe and Cu in spite of a similar vapour pressure. It is suspected that the spontaneous formation of oxide (external layer of 3 nm) substantially lowers the evaporation rate. Another experimental scheme had to be adopted where Al powders where particles are formed in the argon gaseous zone.

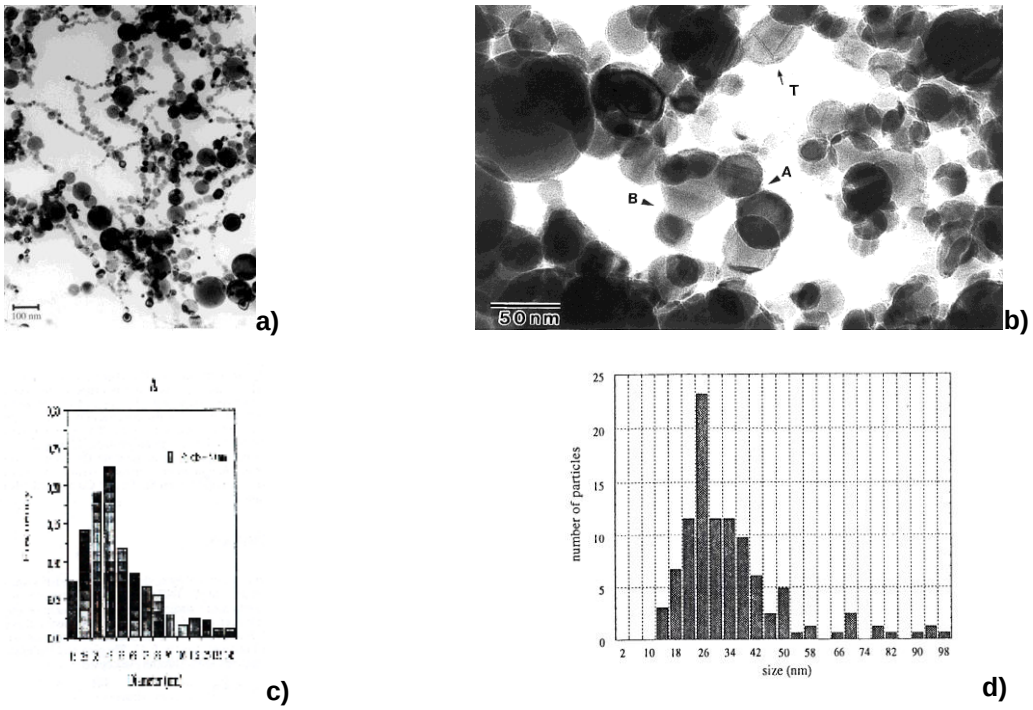

Fig. 5 a) iron UFP mean Ø 50nm and size distribution frequency vs diameter on **Fig. 5c – b** copper powders mean Ø 25 nm with size distribution on **Fig. 5d**.

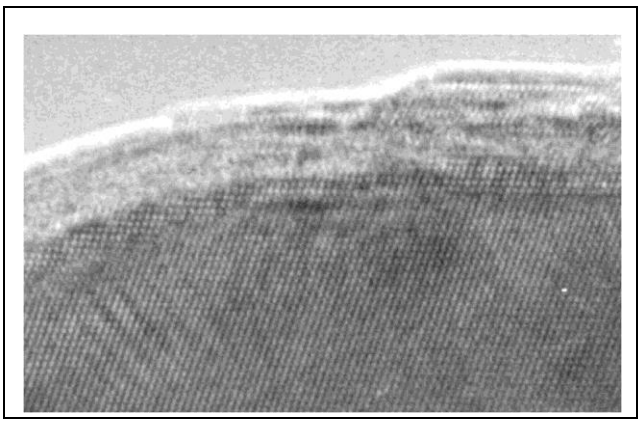

Fig. 6 HRTEM picture of the surface of an Al particle with a 3nm thick Cu_20 layer, mean Ø100 nm with 60% of grain having a size below 70 nm.

3. CONCLUSION

Fe, Ni, Co, Cr, Cu, Al Fe-Ni and Co-Ni nanosized powders have been prepared by cryomelting in levitation in a range 25-100 nm diameter. The size, morphology and yield rate of particles are strongly dependent on the stability of the evaporation and metal vapour condensation rates. Overheating of the molten drop is limited to about 2000°C by the technique which does not permit Ti, Ta or Nb UFP's synthesis. Electromagnetic levitation heating will be replaced in a new project by an inductive couple plasma torch which is a more versatile technique and allows to reach much higher temperatures for refractory compounds not only metallic.

4. REFERENCES

[1] A. H. Pfund, J. Opt. Soc. Am., 23 (1933) 375

[2] C. G. Granqvist, R. A Buhrman, J. Appl. Phys., 47, N°5 (1976) 2200-2219

[3] H. Gleiter, Nanostructured Materials, 1 (1992) 1-19

[4] S. J. Savage, O. Grinder, Advances in Powder Metallurgy and Particulate Materials, 7 (1992) 1-17 Structural Applications of Mechanical Alloying, F.H. Froes and J.J. de Barbadillo (edts) ASM Int. 1990

[5] M. Muller, N. Mattern, L. Illgen, Z. Metallkde., 82 (1991) 895-901.

[6] N. Wada, Jap. J. of Appl. Phys. 7, N°38 (1977) C2-219

[7] M. Uda, Trans. National Research Institute for Metals, 24, N°4 (1982) 36

[8] J. Bigot, A. G. Goursat, G. Vernet, J.F. Rimbert, J. Foulard, T. Sarle, French Patent n° Z8307414 (1983)

[9] J. Bigot, Ann. Chim. Fr., 18 (1993) 369-378

[10] Y. Champion, J. Bigot, Scripta Mater. 35,N°4 (1996) 517-522

[11] Y. Champion, J. Bigot, Nanostructured Materials, 10, N°7 (1998) 1097-1110

Acknowledgement.

This contribution was created within the project **Creation of an international scientific team and incorporation to scientific networks in the area of nanotechnology and unconventional forming material. CZ.1.07/2.3.00/20.0038**, which is financed by the European Social Fund and state budget of the Czech Republic.

evropský sociální fond v ČR
EVROPSKÁ UNIE
MINISTERSTVO ŠKOLSTVÍ, MLÁDEŽE A TĚLOVÝCHOVY
OP Vzdělávání pro konkurenceschopnost
INVESTICE DO ROZVOJE VZDĚLÁVÁNÍ

Technologie spojování UFG materiálů
Joining Technology for UFG Materials

Vladislav OCHODEK

VSB – Technical university of Ostrava, 17. Listopadu 15, 708 33 Ostrava – Poruba, Czech Republic, vladislav.ochodek@vsb.cz

Abstrakt

Materiály se zjemněnou strukturou (UFG-ultra fine grain sized material) mají díky speciálním výrobním postupům využívající extrémní plastickou deformaci (SPD- Severe Plastic Deformation) výrazně vyšší mechanické vlastnosti než materiály s obdobným legováním vyrobené klasickými postupy. V případě, že není možné danou technologii vyrobit přímo finální výrobek je nutné uvažovat o volbě následné výrobní technologie a jejím vlivu na vlastnosti materiálu resp. finálního výrobku. V příspěvku je proveden přehled a charakteristika možných vhodných technologii spojování daných materiálů se zaměřením na svařování, pájení a lepení. Dosažení požadovaných vlastností finálního výrobku je možné pouze za předpokladu optimální volby materiálu, technologie spojování a vlastního konstrukčního návrhu.

Klíčová slova

ultra jemné materiály, svařování, pájení, lepení

Abstract

The ultrafine grain sized material (UFG- ultra fine grain sized material) have due to special manufacturing processes using extreme plastic deformation (SPD-Severe Plastic Deformation) significantly higher mechanical properties them materials with similar alloying produced by conventional methods. In the event that the technology can not directly produce the final product should be considered on the choice of subsequent production technology and its influence on the material and final product properties respectively. The paper presents the review and characterization suitable joining technology with a focus on the welding, brazing and adhesive bonding. For attainment required properties of the final product is necessary optimal choice of materials, joining technology and structural design.

Keywords

UFG materials, welding, brazing, adhesive bonding

1. ÚVOD

UFG materiály patří mezi velmi perspektivní materiály pro aplikace v řadě průmyslových odvětví. Jemná struktura byla docílena řadou variant SPD technologii [1,2]. Jen ale ve velmi málo případech je možné primární technologii vyrobit finální tvar součásti. Z tohoto důvodu je nutné věnovat pozornost vlivu dalších výrobních technologii na kvalitu těchto materiálů zejména pak povrchu ať je to soustružení, frézování nebo broušení. Širší použití daných materiálů ve strojírenství je rovněž podmíněno vhodnou volbou technologie spojování s minimalizací negativních účinků. S ohledem na požadavek minimálního ovlivnění struktury materiálu patří mezi perspektivní technologie spojování vybrané technologie svařování, pájení a lepení. Pro úspěšný návrh spoje požadovaných vlastností je nutný soulad mezi materiálem, technologii a konstrukcí viz obr.1. V případě svařování je nutné pečlivě volit množství tepla vhodnou volbou

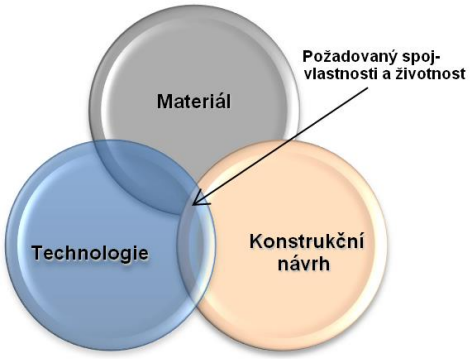

Obr. 1 Návrh obecného spoje

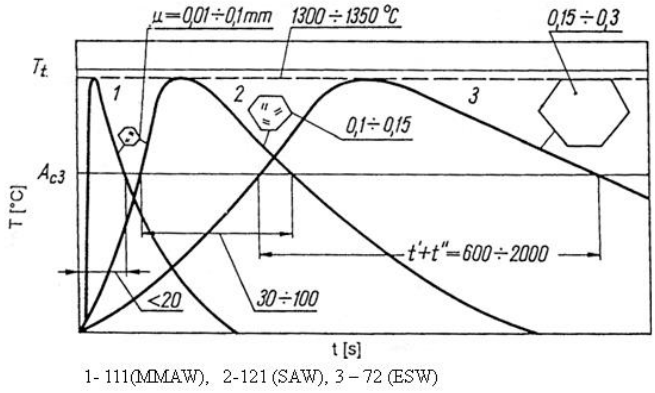

Obr. 2 Teplotní cykly běžných technologii svařování

technologie svařování. Důležité jsou základní charakteristiky teplotních cyklů svařování jako rychlost ohřevu v_h , maximální teploty cyklu T_{max}, rychlost ochlazování v_c ,čas výdrže nad rekrystalizační teplotou t_{Ac3} , čas ochlazování $\Delta t_{8/5}$. S ohledem na minimální degradaci jemnozrnné struktury musí být teplotní cyklus vybrané technologie velmi úzký a musí minimálně ovlivňovat zhubnutí jemnozrnné struktury. Tuto podmínku nesplňují tradiční technologie svařování jejichž teplotní cykly jsou na obr. 2. Zvyšování energie v dopadové stopě může ale vést u některých materiálů k tvorbě nežádoucích struktur (skel) na spojované ploše viz obr. 3.

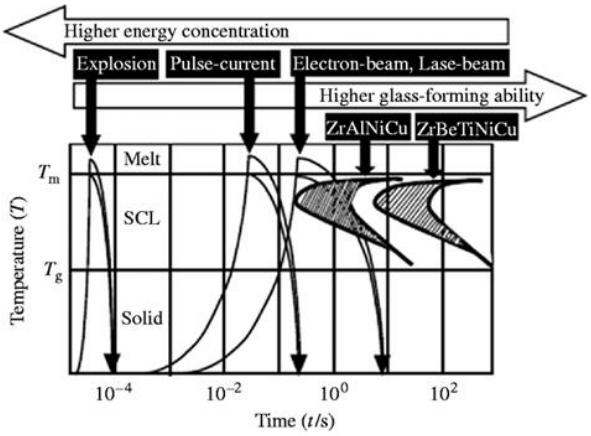

Obr. 3 Porovnání rychlosti ochlazování pro různé technologie svařování [3]

2. TECHNOLOGIE SVAŘOVÁNÍ

Podmínce na úzký teplotní cyklus lze pro svařování UFG materiálu uvažovat s technologiemi o vysoké koncentraci energie na jednotku plochy a to svařování laserem, elektronovým paprskem případně mikroplazmou [3,4]. V případě požadavků svařování materiálů s vysokou afinitou ke kyslíku je vhodná technologie svařování elektronovým paprskem viz obr. 4, kdy svařování probíhá ve vakuu. Nevýhodou jsou konstrukční omezení spoje. I přes minimální rozměry svarového spoje a TOO dochází v průběhu natavení k

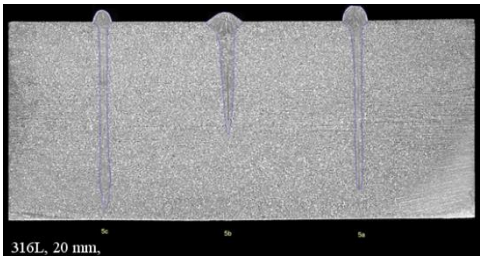

Obr. 4 EB spoj, ocel 316L, 20mm

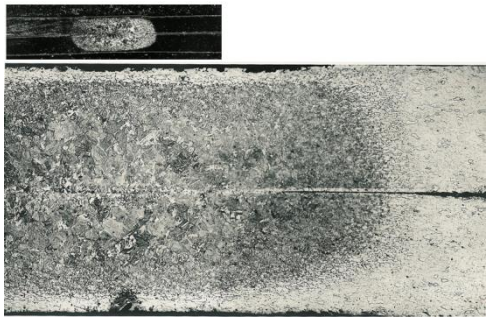

Obr. 5 Mikrostruktura bodového spoje-ocel 2mm

zrušení původní jemné mikrostruktury byť v malé oblasti. Daleko perspektivnější skupinou technologii svařování vhodnou pro spojování UFG materiálu jsou tlakové technologie svařování, kde díky tlakové složce můžeme významně snížit množství dodávaného tepla a tím minimalizovat zpětné zhrubnutí zjemněných zrn. Z tlakových technologii lze uvažovat o odporovém svařování (obr. 5) zejména je vhodný tvrdý režim svařování (krátké svařovací časy a vysoké hodnoty svařovacího proudu) a různé varianty svařování třením, které je vhodné jak pro oceli tak i neželezné kovy příp. heterogenní spoje. Zvláštní pozornost zasluhuje varianta FSW (friction stear welding), kdy rotující trn vytváří třením třecí teplo a zároveň promíchává spojované materiály [5] .Technologie je vhodná jak pro oceli ale i neželezné kovy jako hliník, titan. První výsledky svarových spojů na SPD materiálech slitiny Al–Cu–Mg–Ag jsou uvedeny v lit. [6,7,8] a čistého hliníku AA1050 a AA6016 v [10,11,12]. Dílčí výsledky ukazují, že technologie svařování může částečně vylepšit plastické vlastnosti materiálů, ale nejlepších výsledků lze dosáhnout ještě použitím následného tepelného zpracování. Zlepšení lze dosáhnout i aplikaci druhého teplotního (třecího) cyklu [13]. Další perspektivní možností může být svařování tlakem za studena příp. difuzní svařování [14].

3. TECHNOLOGIE PÁJENÍ

Pájení patří mez tradiční technologie spojování materiálů. Základním rozdílem od svařování je, že nedochází k natavení spojovaných ploch pouze k jejich smáčení viz obr. 6. Teplotní ovlivnění základního materiálu závisí od typu použité pájky (Cu, Al, Ag) a reakčního času na rozhraní pájka-spojovaný materiál. Krátký reakční čas a poměrně nízká teplota tavení pájek zaručuje minimální ovlivnění materiálu a případné zhrubnutí zrna. Pro dosažení pevnostních vlastností spoje je ale nutné respektovat odlišný design spoje než jak je tomu u svařování viz obr. 7. S ohledem na použití ve strojírenství příp. automobilovém průmyslů jako vhodné pájky pro spojování ocelí se jeví pájky na bázi Ag, pro slitiny hliníků na bázi Al.

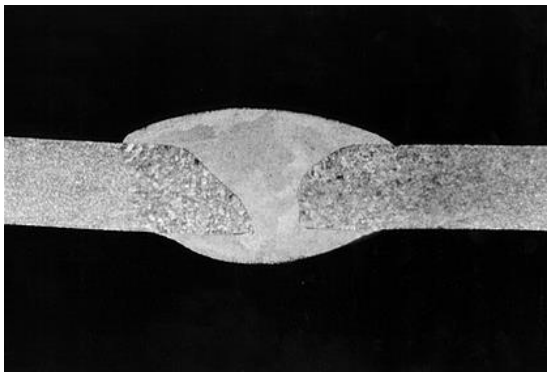

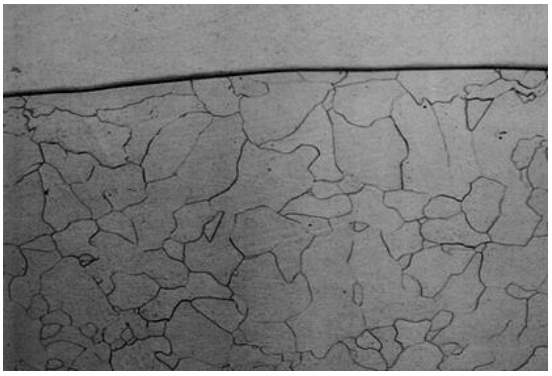

Obr. 6 Makrostruktura pájeného spoje [15] **Obr. 7** Mikrostruktura pájeného spoje-rozhraní [15]

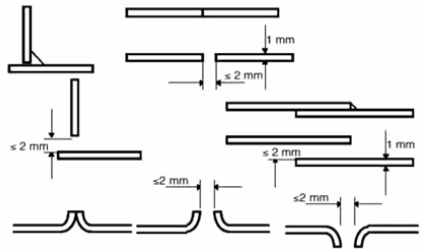

Obr. 8 Základní typy pájených spojů

4. TECHNOLOGIE LEPENÍ

Lepení patří mezi tradiční technologie spojování materiálů. V posledních letech byla vyvinuta řada lepidel, které umožňují vytvářet široké spektrum spojů kovových materiálů používaných ve strojírenství [16,17,18]. Hlavní předností lepení je minimální příp. žádné ovlivnění spojovaných materiálů, nevýhodou je výrazné teplotní omezení lepených spojů. Nutnou podmínkou úspěšné realizace lepeného spoje je jeho vhodný konstrukční návrh (viz. obr.10), dostatečná plocha lepených povrchu (nutná pro uplatnění adheze) a minimalizace namáhání ve směru odlupování („peel“) viz. obr.9.

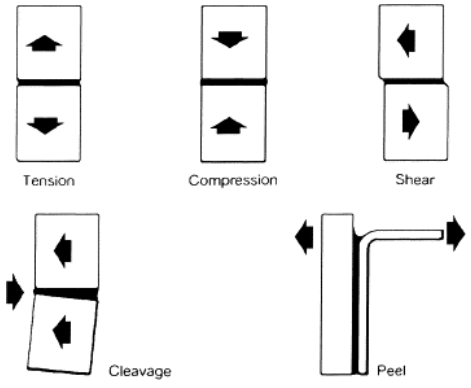

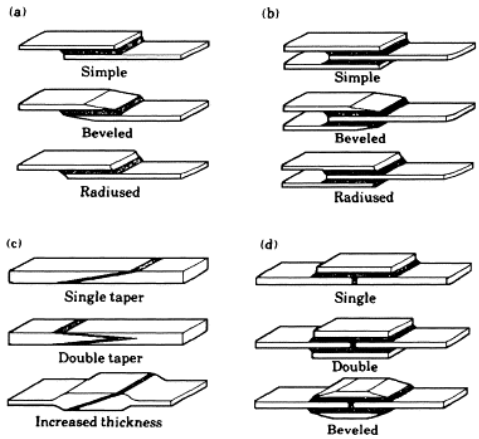

Obr. 9 Základní typy namáhání lepeného spoje [16] **Obr. 10** Základní typy lepených spojů [17]

5. ZÁVĚR

V příspěvku je proveden základní rozbor možných technologii spojování ultra jemných materiálů (UFG) získaných SPD technologiemi. Pro širší aplikaci daných materiálů v průmyslu je nutné danou problematiku řešit souběžně s vývojem nových materiálů a primárních výrobních technologii. Je si nutné si uvědomit, že většina technologii spojování jak svařování, pájení, lepení v menší nebo větší míře negativně ovlivňuje výsledné vlastnosti spoje a docílení požadovaných vlastností je možné pouze při optimálním nastavení vzájemných relací materiál-technologie-konstrukce. Pro návrh optimální technologie spojování daných materiálu je nezbytné znát detailně vlastnosti daných materiálů a to nejenom strukturní a pevnostní ale i např. rozložení zbytkových napětí, které výrazně ovlivňují možnost aplikovat danou technologii spojování [18].

6. LITERATURA

[1] ZRNÍK, J., KRAUS, L., PRNKA, T. A ŠPERLINK, K. *Příprava ultrajemnozrnných a nanokrystalických materiálů extrémní plastickou deformací a jejich vlastnosti*, IV. Řada, Evropská strategie výrobních procesů, ČSNMT, 2007, ISBN 978-80-7329-153-2

[2] VALIEV, R. Z. *Some Trends in SPD Processing for Fabrication of Bulk Nanostructured Materials*, Mat. Sci. Forum, 503–504, 2006

[3] KAWAMURA, Y. *Liquid phase and supercooled liquid phase welding of bulk metallic glasses*. Mater. Sci. Eng. A, 375/377 (2004), pp. 112–119

[4] MING, G., XIAOYAN ZENG, QIANWU HU, JUN YAN. *LASER-TIG hybrid welding of ultra-fine grained steel*. In. *Journal of Materials Processing Technology* 209 (2 0 0 9),p. 785–791

[5] FUJII,H, UEJI,R., TAKADA,Y.,KITAHARA,H.,TSUJI,N.,NAKATA,K.,NOGI,K. Mater. Trans.47 (2006) 239–242.

[6] NIKULIN, I., MALOPHEYEV, S., KIPELOVA, A., KAIBYSHEV, R. *Effect of SPD and friction stir welding on microstructure and mechanical properties of Al–Cu–Mg–Ag sheets.*In. Materials Letters 66 (2012),p 311–313.

[7] HOSSEINI,H., DANESH, MANESH,H. *Immersed friction stir welding of ultrafine grained accumulative roll bonded Al alloy*. In*. Materials and Design* ,31 (2010), p. 4786–4791.

[8] SATO, Y.S., KURIHARA, Y., PARK, S., KOKAWA, H., TSUJI, N. *Friction stir welding of ultrafine grained Al alloy 1100 produced by accumulative roll-bonding*. *Scripta Mater* 2004;50:57–60.

[9] TOPIC, I., HOPPEL, H.W., GOKEN, M. *Friction stir welding of accumulative rollbonded commercial-purity aluminium AA1050 and aluminium alloy AA6016. Mater Sci Eng* A 2009;503:163–6.

[10] SATO, Y.S., URATA, M., KOKAWA, H., IKEDA, K., ENOMOTO, M. *Retention of fine grained microstructure of equal channel angular pressed aluminium alloy 1050 by friction stir welding. Scripta Mater* 2001;45:109–14.

[11] HOFMANN, D.C., VECCHIO, K.S. *Submerged friction stir processing (SFSP): an improved method for creating ultra-fine-grained bulk materials*. *Mater. Sci. Eng.* A 2005;402:234–41.

[12] HOFMANN, D.C., VECCHIO, K.S. *Thermal history analysis of friction stir processed and submerged friction stir processed aluminum. Mater. Sci. Eng.* A 2007;465:165–75.

[13] EL-RAYES,M., EL-DANAF, E.A.The influence of multi-pass friction stir processing on the microstructural and mechanical properties of Aluminum Alloy 6082. *Journal of Materials Processing Technology,* xxx (2012), xxx– xxx.

[14] LILLEBY,A, GRONG, R., HEMMER, H. *Cold pressure welding of severely plastically deformed aluminium by divergent extrusion*. *Materials Science and Engineering*, A 527 (2010) 1351–1360

[15] SCHWARZ B., PLIHAL A., MARTINEC J.,ŠVEIDLER Z.,SCHLIXBIER M. *Metoda GMA určena pro svařování pozinkovaných plechů*. XXV Dny svařovací techniky, Vamberk 2002.

[16] ADDERLEY, C. *Adhesive Bonding Materials and Design*, 9 (5) (1988), pp. 287–293

[17] KALPAKJIAN,S. *Manufacturing Engineering and Technology*, ch. 30, 2nd ed. Addison-Wesley, New York, 1992.

[18] BARNES, T., PASHBY, I. *Joining techniques for aluminium spaceframes used in automobiles Part II D - adhesive bonding and mechanical fasteners*. Journal of Materials Processing Technology 99 (2000)

[19] OCHODEK, Vl. *Analýza zbytkových napětí po aplikaci technologie DRECE-ověření metodiky.* Nepublikované výsledky. VŠB TU Ostrava, prosinec 2011.

Poděkování

Tento příspěvek byl vytvořen v rámci projektu **Tvorba mezinárodního vědeckého týmu a zapojování do vědeckých sítí v oblasti nanotechnologií a nekonvenčního tváření materiálu CZ.1.07/2.3.00/20.0038**, který je spolufinancován z Evropského sociálního fondu a státního rozpočtu České republiky.

INVESTMENTS IN EDUCATION DEVELOPMENT

Vliv velikosti částic jílu na vlastnosti sklovitého smaltového povlaku

Influence of Clay Particles Size on Properties of Vitreous Enamel Coating

Jitka PODJUKLOVÁ, Vratislav BÁRTEK, Tomáš LANÍK, Petr ŠRUBAŘ, Kateřina SUCHÁNKOVÁ, Sylvie KOPAŃÁKOVÁ

VŠB – Technical University of Ostrava,17.listopadu 15,708 33 Ostrava – Poruba,, CZ

jitka.podjuklova@vsb.cz, vratislav.bartek@vsb.cz, tomas.lanik@vsb.cz, petr.srubar@vsb.cz, katerina.suchankova@vsb.cz, sylvie.kopanakova@vsb.cz

Abstrakt

Korozní proces znehodnocuje kovové výrobky, které jsou v kontaktu s korozním prostředím. Sklovitý smaltový povlak je povrchová úprava, která zajišťuje nejen perfektní ochranu materiálu proti korozi, ale také dává povrchu základního materiálu vyjímečné vlastnosti. Sklovité smalty jsou skelné povlaky vytvářené na kovovém podkladu vypalováním při teplotě nad 800 °C. Tento povlak můžeme využít v různých oborech strojírenství. Vytvoření celistvého smaltového povlaku (bez vad a trhlin, které pronikají až k podkladovému kovu) je základním předpokladem pro využití jeho funkčních vlastností. Vlastnosti povlaku jsou závislé na jeho struktuře, textuře a chemickém složení. Nejdůležitějšími anorganickými komponenty při výrobě tohoto povlaku jsou jíl a sklovitá frita. Užití různých velikostí těchto komponent má vliv na finální kvalitu povlaku. Hlavním cílem je porovnání vlastností sklovitých smaltových povlaků vytvořených užitím anorganických částic v běžné velikosti a anorganických částic o velikosti nanorozměrů. Příspěvek rovněž studuje vliv jílové složky jako vstupní suroviny, vložené do povlaku v různé časové posloupnosti na mechanické vlastnosti sklovitých smaltových povlaků.

Klíčová slova

sklovitý smaltový povlak, koroze, jíl, nanorozměr, vlastnosti

Abstract

Corrosive process depreciate of the products which are in contact with corrosive environment. Vitreous enamel coating is surface treatment, which ensure not only perfect protection of materials against corrosion, but also give for surface of basic material the exceptional properties. Vitreous enamels are glazes formed on a metallic undercoat by burning at temperature exceeding 800 °C. This coating can be used in various fields of engineering. Forming of a compact enamel coating (with no defects or cracks penetrating up to ground metal) is a fundamental prerequisite for utilization of its functional features. Properties of the coating are dependent on its structure, texture and chemical composition. The most important inorganic components during production of this coating are clay and fritted glass. Usage of

various sizes of these components influences final quality of the coating. The main goal of this thesis is to compare properties of vitreous enamel coatings made by using commonly-dimensioned inorganic particles and of inorganic particles in nano-dimensions. Contribution also studies effect of clay component like input raw material which is add in different time sequence on mechanical properties of vitreous enamel coatings.

Keywords

vitreous enamel coating, corrosion, clay, nanodimension, properties

1. INTRODUCTION

Glass-ceramic coatings are used in various technical areas, e.g. in mechanical engineering, civil engineering, restoration work, in the food industry. Vitreous enamel coatings have various positive properties, such as good resistance to aggressive, corrosive environments, surface abrasion, long-lasting service life and chemical stability. The size of clay components in the nano-scale have affects on the mechanical properties. Positively affect brittle-fracture properties and especially in nano -scale clay are proof.

2. EXPERIMENTAL MATERIAL

As background material for experiments vitreous enamel coating steel plate was used KOSMALT E300T. On specimens were used two types vitreous enamel mush with clay component sizes smaller than 5 μm with a 1D size of 400 nm (base and cover), milling of clay was carried out on a jet mill vertical Sturtevant. The samples were being degreased in water and Simple green spa for 5 minutes. Rinse was being carried out by immersion into a water spa for 1 minute. Then enamel slurry was applied in a common way and with the respective amount of micro-sized clay and nano-sized fine milled clay in size 20 to 200 nm. The samples were being dried at a temperature of 100 °C for 5 minutes. Burning was carried out in an oven at temperatures of 820 to 840 °C for a period of 8 to 12 minutes, accompanied by formation of enamel coating with subsequent cooling in the air.

Kinds of clay compounds used in the enamel suspension:

- ✓ MIC fine milled clay
- ✓ MIC classic clay

3. EXPERIMENTAL WORKS

METHODS OF EXPERIMENTAL WORK:

- ✓ SEM analysis
- ✓ Measuring of kinematic viscosity and determination of dynamic viscosity of enamel slurry
- ✓ Measuring of the roughness on selected glass-ceramic coating
- ✓ A test of enamel resistance to mechanical impacts in compliance with

  ČSN ISO 4532 (945050)

- ✓ Microhardness tests according to Vickers and according to Knoop in compliance with ČSN EN ISO 4516
- ✓ Determination fracture toughness of vitreous enamel coating

3.1 SEM ANALYSIS

The main difference between grain size for coarse and fine clay is visible on the **Fig. 1**. Micro-sized clay component sizes smaller than 5 μm with a 1D size of 400 nm and nano-sized fine milled clay in size 20 to 200 nm. Fine milled clay shows more uniform structure and the fraction.

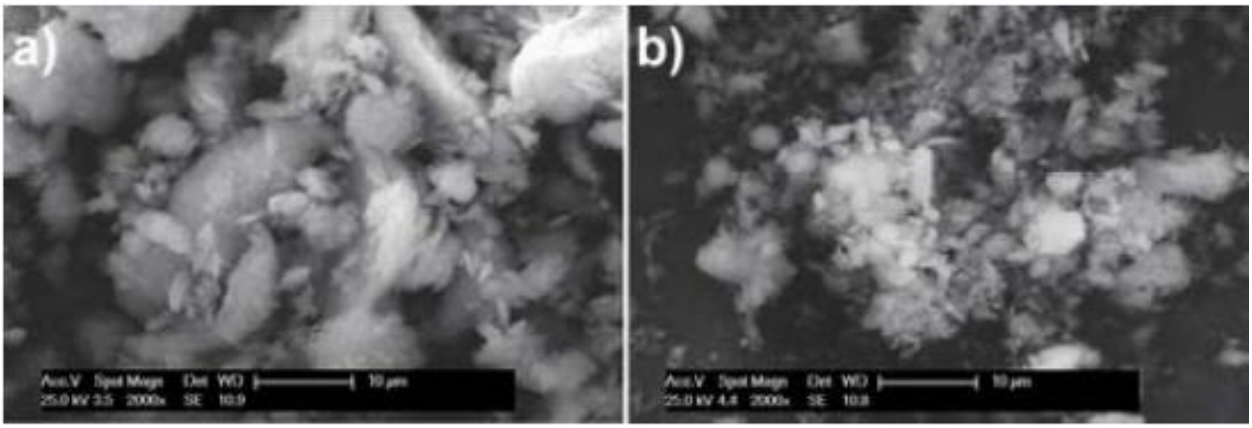

Fig. 1 SEM analysis of the MIC a) coarse clay (classic size), b) fine clay (fine milled)

3.2 Measuring of Kinematic Viscosity and Determination of Dynamic Viscosity of Enamel Slurry

Measuring of kinematic viscosity was carried out in compliance with ČSN EN ISO 2431. A standardized Ford cup with a standard discharge nozzle with the diameter of 6 mm was used; the time, during which the volume of the cup was discharged through a given hole, was determined in seconds. The measuring was performed at the temperature of 20 °C.

Viscosity of the fluid indicates a rate of tangential stress between layers of the flowing fluid and a velocity gradient. In addition to various factors (such as pressure, temperature), the viscosity value of suspensions depends on a shape and roughness of particles (see **Table. 1**).

The consistency of enamel slurry of both preliminary and surface vitreous enamel coatings is 1400 kg.m-3. Relation between dynamic and kinematic viscosity: $\nu = \eta / \rho$, where ν – kinematic viscosity, η – dynamic viscosity, ρ – consistency. On the basis of the performed experiment, it was found out that with usage of fine clay at the same weight content as classic clay, enamel slurry shows higher viscosity than enamel slurry with classic clay, and therefore its rheological properties are changed. It is necessary to take this found experience into account during application of enamel slurry in practice. Further works we are going to write will deal with monitoring of clay amount with respect to decrease in kinematic viscosity of slurry (see Table. 2).

Table 1 Kinematic Viscosity of Enamel Slurry

Vitreous enamel coating	Kinematic Viscosity [m^2/s]
Basic vitreous enamel coating with classic clay	5.10^{-6}
Basic vitreous enamel coating with fine clay	60.10^{-6}
Covering vitreous enamel coating with classic clay	10.10^{-6}
Covering vitreous enamel coating with fine clay	80.10^{-6}

Table 2 Dynamic Viscosity of Enamel Slurry

Vitreous enamel coating	Dynamic Viscosity [Pa.s]
Basic vitreous enamel coating with classic clay	7.10^{-3}
Basic vitreous enamel coating with fine clay	84.10^{-3}
Covering vitreous enamel coating with classic clay	14.10^{-3}
Covering vitreous enamel coating with fine clay	112.10^{-3}

3.3 MEASURING OF THE ROUGHNESS ON GLASS-CERAMIC COATINGS ČSN EN ISO 4287

Measuring of the roughness parameters of the samples with glass-ceramic coating according by ČSN EN ISO 4287. In the surface roughness measurements was found that samples containing fine clay show a smoother surface and the more uniform structure, which documents on **Fig. 2.**

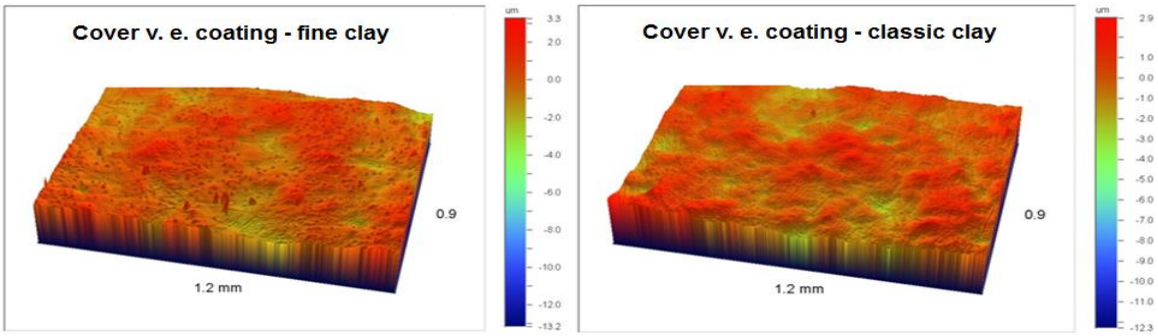

Fig. 2 Profilographs of the surface roughness

3.4 DETERMINATION OF MECHANICAL PROPERTIES

Enamel resistance to mechanical impact - ČSN ISO 4532 (945050)

In order to test adhesion of the vitreous enamel coating, a device according to Wegner in compliance with ČSN ISO 4532 (945050) was used. The test instrument according to Wegner consists of a firing pin, into which a steel ball with the diameter of 5 mm has been set. The steel ball is fired by means of a compressed spring towards an enamel surface. The impact force may be set within the range from 0 N to 90 N by a knurled nut according to a scale of graduation marks around the circumference. Testing is carried out at increasing power of the spring and always in a new place which is at least 20 mm far from the previous one. The test starts with a hit with the power of 10 N, which is gradually increased, and strength when the first impact to material occurs is determined. The assessment shall be carried out visually from the distance of 250 mm. Impacts to enamel shall be assessed (separation, peeling up to steel substrate). The final assessment is carried out in 24 hours. Vitreous enamel coatings showed higher resistance to mechanical impacts and higher adhesion to the steel substrate when fine clay was used in comparison with vitreous enamel coatings, for which classic clay was used.

Table 3 Average values bursting force by impact test, microhardness, fracture toughness

	Bursting force Fp [N]	$Hv_{0,1}$ [MPa]	K_{IC} [MPa.m$^{1/2}$]
Basic v. e. coating-classic clay	50	4042	0,88
Cover v. e. coating-classic clay	50	5136	1,01
Basic v. e. coating-fine clay	55	4227	0,87
Cover v. e. coating-fine clay	70	4376	1,04

Microhardness tests - ČSN EN ISO 4516

Material microhardness is defined as material resistance to local plastic deformation emerging under a loaded diamond cutting point (indenter). In order to measure microhardness, the Vickers method was used. The measuring was carried out by means of the Hanemann microhardness gauge (the NEOPHOT 2 optical microscope).

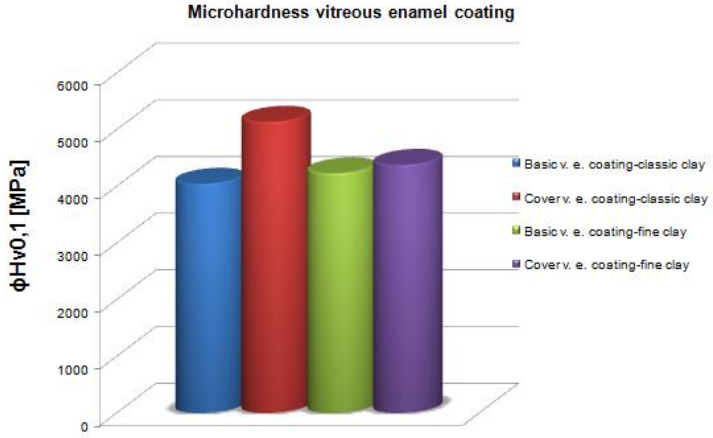

Graph 1 Average values of microhardness

Determination of vitreous enamel coating fracture toughness

Fracture toughness was determined on the basis of radial checks which emerged in diagonals of an indenter impression. Vitreous enamel coatings showed a change in microhardness and fracture toughness when fine clay was used in comparison with coatings with fine clay after time lag.

Measurements showed only Palmqvist cracks

$$\mathbf{K_{IC} = 0,035 \cdot \left(\frac{c}{r}\right)^{-\frac{1}{2}} \cdot \left(\frac{E \cdot k}{H_V}\right)^{\frac{2}{5}} \cdot \left(\frac{H_V \cdot r^{\frac{1}{2}}}{k}\right)} \quad (1)\ [1]$$

c – crack lenght
r – half the length of the indentation diagonal
E – Young's module elasticity
Hv – Vickers microhardness
k - constant

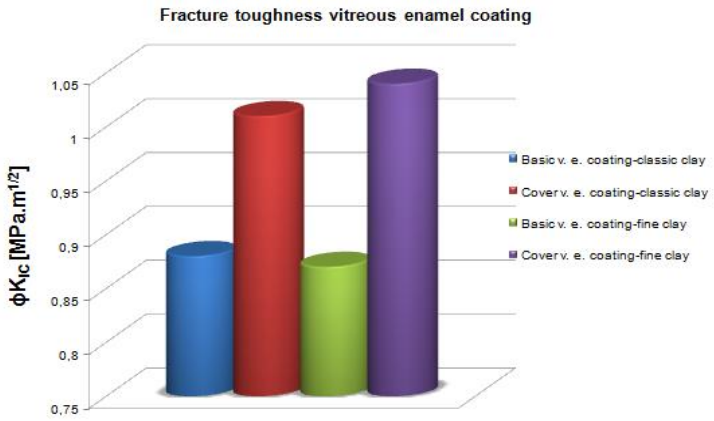

Graph 2 Average values of fracture toughness

4. CONCLUSION

The resulting value of these experiments showed that the fine clay demonstrated increased mechanical properties of glass-ceramic coatings opposite to coarse clay. This suggests a positive effect on brittle properties of enamels. On the basis of experimental tests have been shown positive affect of fine clay onto the brittle-fracture and functional properties of the coats. The nano dimension of the clay component, was positively influenced not only hardness but also the fracture toughness of enamel coatings. Tendency to defect formation is also substantially reduced. These benefits can be used in practice especially in assembling of enamelled segments.

5. LITERATURE

[1] Menčík, J.: Pevnost a lom skla a keramiky, SNTL, Praha, (1990)

Acknowledgement

This contribution was created within the project Creation of an international scientific team and incorporation to scientific networks in the area of nanotechnology and unconventional forming material. CZ.1.07/2.3.00/20.0038, which is financed by the European Social Fund and state budget of the Czech Republic.

european social fund in the czech republic
EUROPEAN UNION
MINISTRY OF EDUCATION, YOUTH AND SPORTS
OP Education for Competitiveness
INVESTMENTS IN EDUCATION DEVELOPMENT

Development of equipment for production of UFG materials at the Department of Mechanical Technology VSB – Technical University of Ostrava

Stanislav RUSZ

VSB – Technical university of Ostrava, 17. listopadu 15, CZ 708 33 Ostrava – Poruba, Czech Republic,

Abstract

Department of Mechanical Technology at VSB – Technical University of Ostrava conducts research and development of technology for production of UFG metallic materials for more than 7 years. In the first years of development influence of construction solution of ECAP tools with geometry of connecting channel (90°) and sample of the size of 8x8x34 mm, 10x10x42 mm and 15x15x60mm (final stage) was tested. The actual geometry of the channel is gradually changing. Angle of connection of channels ϕ = 90° (a constant), but design of horizontal channel was changed. New design was proposed - deflection of the channel around the vertical axis - by 10° and 20°. In the final stage a helix with pitch angle of 30° was built into the channel. This design solution created back pressure in the channel. A substantial increase efficiency of the process of grain refinement was achieved. The experiments were performed on hydraulic press of the type DP 1600 kN. Grain refinement was examined on Al and Mg alloys. The experimental results clearly confirmed achievement of the largest grain refinement and mechanical properties and high efficiency process for the ECAP channel with built-in helix. Mean values of grain size reached 300 to 500 nm in Al alloys after 5 passes through the ECAP tool. In the next stage of development work two prototype devices for semi-finished sheet metal and wire were developed. The device works on the principle of the SPD and it is similar to the device C2S2 (DCAP) and CONFORM. Extrusion of strip sheet of aluminium, copper, brass and low carbon steel was performed on the prototype machinery DRECE (Dual Rolls Extrusion Equal Channel). Remarkable results were achieved in brass and steel. Mechanical properties were increased (100% of R_e and R_m) already after 4 passes through DRECE machinery. The ductility values were reduced. In future development we want to modify the design of tools of DRECE machinery and propose the appropriate heat treatment to maintain the required elongation, while achieving high mechanical properties.

Keywords

Severe plastic deformation, grain refinement, extrusion process, mechanical properties, formability, forming equipment, new design of forming tool, strip of sheet

1. INTRODUCTION

At present numerous many scientific and research working sites in industrially developed countries deal with research and technology of ultra-fine grained (UFG) materials and nano-materials. Several principles of technological processes are examined and their influence on the micro-structure of materials and on operating conditions of the process. The cited literary sources indicate the best-known and the most frequently used severe plastic deformation (SPD) technologies. All research activities dealing with these technologies are in the state of basic and applied research. Possibility of their application in selected fields of industrial production is being verified. An integral trend of development works, regardless of the investigated technology, is to optimise the forming process in order to maximise the volume of processed material in combination possibility of its use in the industrial practice - as a continuous production process. For ensuring the general implementation of the UFG materials into industrial practice this direction of development is not only logical, but also highly desirable.

2. RESEARCH AREAS OF SPD PROCESSES – DEVELOPED AT THE DEPARTMENT OF MECHANICAL TECHNOLOGY VSB – TECHNICAL UNIVERSITY OF OSTRAVA

2.1 First area – Equal Channel Angular Pressing (ECAP process)

Figure 1 explains schematically the principle of the ECAP technology, where two rectangular channels intersect mutually at an oblique angle Φ. The pressing can be lead through a square configuration of the channel.

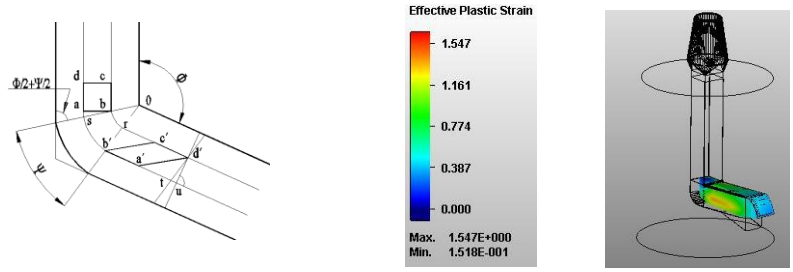

a) b)

Fig. 1. a) Principle of the ECAP, where Φ is the angle of transition of two channels and Ψ curvature of transition, b) FEM strain simulation for Al alloy (after the 1st pass through the ECAP tool)

This situation was considered already in the previous works of Inwahashi [5]. Quantity of friction against the channel wall was assigned to the angle Ψ. In practice this can be avoided by suitable lubricant. The sample is lubricated in such a way that friction effects are negligible. Figure 3 shows removal of small element of square section with dimensions given by the points a b c d, which changes after passage through the die due to effect of shear friction to the position defined by the points a´ b´ c´ d´. Under presumption that identical deformation is accumulated during each pass through the channel, it is possible to express the deformation intensity for N-cycles by the relation 1 [1, 2].

$$\varepsilon_N = N \cdot \left[\frac{2 \cdot \cot\left(\frac{\Phi}{2}+\frac{\Psi}{2}\right) + \Psi \operatorname{cosec}\left(\frac{\Phi}{2}+\frac{\Psi}{2}\right)}{\sqrt{3}} \right] \quad (1)$$

That's why it is possible to determine from the equation 6 magnitude of deformation at any conditions of pressing – subject to the condition that the angles Φ and Ψ are known. [3,4]

2.2 Second area - Dual Rolls Equal Channel Extrusion (DRECE process)

The process DRECE is similar to the DCAP process.

In spite of the fact that deformation is not achieved by perfect simple shear, both numerical analyses and experimental observations showed that simple shear is a dominant manner of deformation in the course of DCAP. Shear deformation input into the sample was distributed comparatively uniformly along the full width, with the exception of regions close to the lower surface of the strip. Experimental results agree completely with the results obtained by mathematical analyses with use of finite-element method. It is obvious from experimental results that different shear deformations occur near the lower surface. This uneven deformation occurs at the place, in which the work sample does not touch the tool.

The equation (2) gives an efficient deformation obtained by the DCAP, which is expressed in dependence on the number of passes (N) and relation of thicknesses (K). On the other hand the equation (3) represents rolling expressed in relation to the reduction ratio (R). Investigation of changes of hardness in dependence on efficient deformation established slightly lower hardness in the sample after DCAP than in the sample after cold rolling [5].

$$\varepsilon = 2N/\sqrt{3} \,.\, K2 \cot(\phi/2) \qquad \text{(for DCAP)} \qquad (2)$$

$$\varepsilon = 2/\sqrt{3} \,.\, / \ln(1-R) \qquad \text{(for rolling)}$$

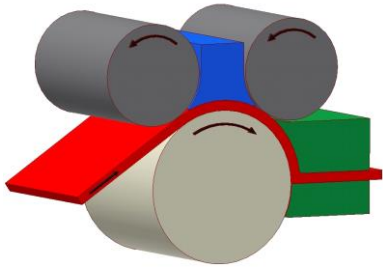

Fig. 2 Scheme of DRECE process

3. WORKING SITE FOR DEVELOPMENT OF THE ECAP METHOD AND NEW DIRECTIONS AT DESIGNING OF FORMING TOOLS ENABLING AN INCREASE OF EFFICIENCY OF THE SPD PROCESS

The working site at the VŠB - Technical University of Ostrava (VŠB-TUO) has at its disposal also a modified equipment for the ECAP method for bulk forming of prisms (blanks) from original dimensions (10 mm × 10 mm × 32 mm), which were at present enlarged to (15 mm × 15 mm × 60 mm), and which is placed on the hydraulic press DP 1600 kN – see Figs. 4-8. This equipment is used for investigation of influence of severe plastic deformation on refinement of structure in materials based on alloys of non-ferrous metals. In these materials we achieved ultra-fine grained (UFG) structure, which from the perspective of industrial use fully meets the requirements to substantial enhancement of mechanical properties with preservation of formability at the mean grain size within the interval of 300 nm ÷ 500 nm.

Fig.3 Hydraulic press 1 600 kN

Fig. 4 Detailed view of control panel

Fig. 5 Computer control of press

Fig. 6 New concept of the ECAP tool

At the Department of Mechanical Technology at the Faculty of Metallurgy and Materials Engineering of the VŠB – TU Ostrava we developed a new tool for the ECAP method (modification of channel geometry, enabling an increase of the amount of deformation at individual passes), which was placed on the press DP 1600 kN (see Fig. 3). Thanks to the newly designed geometry it was possible to reduce the number of passes in comparison with conventional tool with simultaneous increase of efficiency of the SPD process and thus also reduction of time necessary for achievement of the UFG structure in the investigated materials.

3.1 New geometry of forming tools (change of the deformation route) – substantial enhancement of the SPD process

Fig. 7 Classical geometry of the ECAP channel (90° angle between the horizontal and vertical part of the channel)

Fig. 8 New type of the ECAP tool with deflection (axle offset) of the horizontal part of the channel by 20°

Fig. 9 Detailed view of the tool with channel geometry in the form of built-in helix

The above photos illustrate progressive development of geometry of the ECAP tool. During the first experiments we used the classical channel geometry (90° angle between the horizontal and vertical part of the channel) – see Fig. 7. In order to increase the efficiency of the process of grain refinement (increase of the amount of deformation) the horizontal part of the channel was deflected in respect to the vertical axis by 10 and 20° - see Fig. 8. During the next experiments we built into the horizontal part of the channel a helix– see Fig. 9. In this was we achieved substantial increase of material deformation. During the forming process in principle a counter-pressure is created, which leads to substantial increase in efficiency of the forming process. From the viewpoint of the achieved results it is highly necessary to test and develop technological and forming conditions also for other types of materials (alloys based on Al, Cu, Mg and Zr), as well as to verify the influence of the strain rate and temperature on the forming process from the perspective of possibilities of further increase of its efficiency.

3.2 **DRECE Method**

During 2009 a prototype of this equipment was put into trial operation at the working site of the VSB-Technical University of Ostrava, Department of Mechanical Technology. Figure 10 a, b gives an overall view of the prototype of this equipment. It consists of the following main parts: gear of the type Nord with electric drive, disc clutch, feed roller and pressure rollers with regulation of thrust, forming tool made of the steel grade Dievar. Strip with dimensions 58 x 2 x 1000 mm was fed into the working space and it was pushed by the feed roller with help of pressure rollers through the forming tool without change of its cross section. Repeated plastic deformation realised in this manner brought substantial refinement of structure. During the trial operation the first experiments were made, followed by their evaluation. On the basis of these works some modifications of design were proposed.

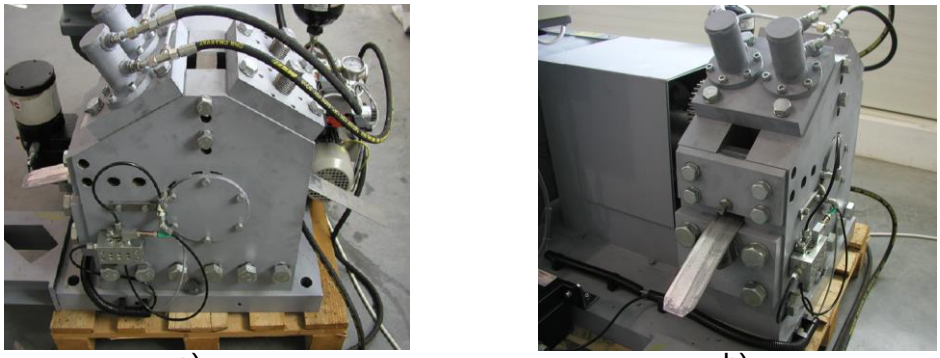

a) b)

Fig. 10 Prototype equipment DRECE for extrusion of strip sheet metal a) lateral view of the equipment b) front view

4. CONCLUSIONS

Both types of equipment mentioned above are suitable for experimental verification of structure refinement, bringing substantial enhancement of mechanical properties in all types of metallic materials, but particularly in the alloys of non-ferrous metals. The alloys of non-ferrous metals based on Al, Mg, Ti, etc. are at present broadly used namely in automotive industry, aerospace industry and lately also in medical practice (dental implants, prosthetics). The applications in power engineering bring an increase of conductivity in high-voltage transmission lines, increased resistance to corrosion resulting from structure refinement, and particularly the possibility of storage of hydrogen in UFG materials. The above mentioned devices will be fully usable also for laboratory verification of production of materials and blanks with such properties.

5. LITERATURE

[1] Inwahashi, Y.,Wang, J., Horita, M., Nemoto, Z. and Langdon, T. G Principle of equal–channel angular pressing for processing of ultra–fine grained materials, *Scripta Materialia*, vol.35, 1995, pp.143-147

[2] Delo, D.P., Semiatin, S.L. Finite-element modeling of nonisothermal equal-channel angular extrusion, *Metallurgical and Materials Transactions* A30 (1999) 1391-1402.

[3] Valiev,R. Recent developments of severe plastic deformations techniques for processing bulk nanostructured materials, Materials Science Forum A 579 (2008) 1–14.

[4] Lee, J.H., Son, I.H. and Im, Y.T. Finite element investigation of equal channel angular extrusion process, Materials Transactions, The Japan Institute of Metals 45 (2004) 2165-2171.

[5] Raghavan, S., Prabir, K., Balakrishna, Ch. and Swenson, D. Continuous Severe Plastic Deformation Processing of Aluminum Alloys, Final Technical Report, DOE Award Number: DE-FC36-01ID14022, 2006, April (2006) 33-39.

Acknowledgements

This paper was created within the project "**Creation of an international scientific team and incorporation to scientific networks in the area of nanotechnology and unconventional forming material. CZ.1.07/2.3.00/20.0038"**, which is financed by the European Social Fund and state budget of the Czech Republic.

european social fund in the czech republic
EUROPEAN UNION
MINISTRY OF EDUCATION, YOUTH AND SPORTS
OP Education for Competitiveness
INVESTMENTS IN EDUCATION DEVELOPMENT

Towards multifunctional bulk nanostructures: grain boundary structure and grain boundary diffusivity of severely strained alloys

G. Wilde

Institute of Materials Physics, University of Münster, 48149 Münster, Germany,

gwilde@uni-muenster.de

Abstract

Bulk nanostructured - or ultrafine-grained materials are often fabricated by severe plastic deformation (SPD) to break down the grain size by dislocation accumulation. Underlying the often observed property enhancement is a modification of the volume fraction of the grain boundaries. However, early concepts as well as recent results indicate that in addition to the increased volume fraction of grain boundaries in ultrafine grained materials, also the nature of at least a fraction of the grain boundaries is modified. Combined studies by radiotracer diffusion analyses and by high resolution transmission electron microscopy and geometric phase analysis indicate that these modifications can be far more complex as indicated in the picture of so-called “non-equilibrium” grain boundaries. These results also indicate that the modifications to the nature and characteristics of these grain boundaries can enhance or deteriorate the performance of the deformed materials and the comparison of differently deformed materials indicates further that the improvements or deteriorations are inherently coupled to the details of the deformation pathway.

1. INTRODUCTION

Nanostructured materials offer particular promise for new and potentially very useful products since they can have unique and often superior properties that crucially depend on the atomistic details of interior or exterior interfaces. The nanostructures may be used in a wide range of contexts; most of these are ones in which ensembles of nanostructures are assembled into complex, (multi)functional arrangements with high stability against detrimental coarsening. Likely examples include materials for extreme environments such as body implants or the off-shore industries [1]. However, today, most applications of nanostructured materials that are already on the market do not yet make use of the potential that lies within interface-design, but these applications are mostly based on nanoparticles. It is the reduced size of the structural entities alone that serves the purpose in most of these cases. However, in addition to materials that are to be structured by means that control the shape and feature size on the nanometer scale, an entire range of promising property modifications such as mechanical or magnetic properties generate the need to synthesize and stabilize *massive ultrafine grained materials*, i.e. polycrystalline materials with bulk shape consisting of a dense array of crystallites in the size range below a few 100 nm.

One way to obtain such materials and composite microstructures with extremely small average grain sizes is given by the application of severe plastic deformation treatments [2-4]. These recent methods and processing pathways extend the range of microstructures that are accessible towards much smaller grain sizes. In particular, sequentially combining different non-equilibrium processing pathways that are based on continuous strain energy input present new routes for nanostructure formation. The available permutations offer a wide range of options for tailoring the microstructure and the shape and quantity of the product nanostructure including the interfaces and – at the same time – present a wide field yet to be explored. First results on e.g. pure Ni indicate that the combination of repeated cold rolling (RCR) and high-pressure torsion (HPT) resulted in massive, nanocrystalline materials without texture and with the highest hardness observed ever for Ni [5, 6]. Other results have recently indicated that in addition to increased strength and ductility also other properties and property combinations can be significantly enhanced, such as strength and electrical conductivity or hydrogen storage capacity [1]. These results highlight the significant improvements concerning properties and performance that can be gained through nanostructuring by applying advanced deformation processing treatments.

Yet, along with the property enhancements, several important questions arise concerning the accommodation of external stresses if dislocation-based processes are not longer dominant at small grain sizes [7, 8]. One such aspect is given by the concept of so-called “non-equilibrium” grain boundaries [9, 10] that have been postulated to form during severe deformation and that might be of importance not only for the property enhancement known already today, but also might serve as internal transport pathways offering new applications in the context of e.g. gas permeation or fast matter transport for self-repairing structures [11]. Some of the underlying issues have recently been addressed by combining quantitative microstructure analysis at high resolution with grain boundary diffusion measurements [12, 13]. However, in another set of radiotracer diffusion experiments performed on SPD-treated pure metals and alloys including surface mechanical treatment, ball milling and compaction and “standard” SPD-methods, the development of a hierarchy of fast and ultra-fast diffusion pathways upon severe plastic deformation could be unambiguously proven. It is important to note that these diffusion pathways, which were observed in pure metals such as Cu and Ni but also in different alloys, such as nanocluster- strengthened ferritic steel or NiTi shape memory alloys, are percolating and that the fastest transport pathways are given by a network of open porosity [14-20].

With the desirable exploitation of the application potential of this new class of materials, several important questions arise, that are often concerned with the relation between the processing pathway and the resulting microstructure, including the defect structure on different length scales and the stability against detrimental coarsening under thermal or mechanical loading conditions. Some of these issues will be addressed by focusing on the comparison of two Ni-Ti alloys that have been SPD-processed via HPT or RCR and by analyzing the results obtained from grain boundary diffusion measurements and analyses of the local strain fields after severe deformation.

2. EXPERIMENTAL PROCEDURES

A NiTi alloy with a composition of $Ni_{50.6}Ti_{49.4}$ (at %) was investigated. The discs cut from the quenched rod were subjected to HPT under a pressure of 6 GPa to a true logarithmic strain of 6. Additionally, a slightly Ti-rich NiTi-alloy was investigated. The NiTi alloy with a nominal composition of Ni-50.1at.%Ti was produced by arc melting in cold crucibles using pure components (Ni, 5N and Ti, 4N) under an atmosphere of flowing argon. Sheets of 0.5 mm

thickness were cut from the homogenized samples and subjected to repeated cold rolling (RCR) at room temperature using a two-high rolling mill. Starting with an initial step of CR, up to 20 passes of RCR were applied. Each pass of RCR involves the application of two steps. Firstly, the CR NiTi sheet is cut into two pieces of similar size that are put on top of each other. Secondly, the stack is subjected to CR. To prevent fracture, CR is applied to the stack sandwiched between two plates made of hardened steel. CR is carried out several times until a final thickness of 0.25 mm of the stack is obtained. The degree of deformation achieved by a first step of CR followed by N passes of RCR calculated using the von Mises true strain yields $\varepsilon \approx 0.8 \cdot (N+1)$; $\varepsilon = 0.8$ after CR; $\varepsilon = 1.6$, 4.8, 8.8, 12.8 and 16.8 after CR followed by additional 1, 5, 10, 15 and 20 passes of RCR, respectively. Disc shaped specimens with a diameter of 2.3 mm were punched from the NiTi samples in their initial state, after RCR and after RCR followed by heating to a temperature of 500°C. Specimens used for X-ray analysis and calorimetry were mechanically polished. Specimens used for TEM were mechanically dimpled to a thickness of about 70 μm. This was followed by electropolishing using a Tenupol 3 (25 % nitritic acid and 75% methanol at a temperature of 22°C).

Calorimetric measurements were performed by DSC (Diamond DSC, Perkin-Elmer) under Ar atmosphere. The TEM measurements were performed on thermally treated samples using a Libra FE200 and a Tecnai F20, transmission electron microscope. TEM investigations of the Ti-rich samples were carried out using a Philips CM 200 and a CM 30ST operating at 200 kV and 250 kV, respectively. Specimens for transmission electron microscopy (TEM) were prepared by electropolishing using a solution of HNO_3 (65%) and CH_3OH in the ratio of 1:2 by volume. The electrolyte was cooled to –20 °C and the voltage applied for thinning was 10 V. Details concerning the geometric phase analysis method can be found in [8, 12].

The diffusion experiments were performed by applying the radiotracer technique using the ^{44}Ti, ^{59}Fe and ^{110m}Ag isotopes. The ^{44}Ti tracer was in the form of titanium chloride dissolved in 4 mol HCl. The commercial ^{59}Fe tracer was supplied by NEN Company in the form of iron chloride dissolved in 0.5 HCl. The original solution was highly diluted in double-distilled water. The ^{110m}Ag tracer was produced from the natural isotope ^{109}Ag by neutron irradiation at the research reactor in Geesthacht (Germany). The irradiated Ag chip was subsequently dissolved in nitric acid and diluted with double distilled water. More information on the radiotracer measurement methodology can be found e.g. in [11-20].

3. RESULTS AND DISCUSSION

3.1 Efficiency of giant straining processes

There have been several attempts to compare the true strain imparted by different methods of severe plastic deformation. So far, most of these comparisons target the minimum grain size or the grain size reduction as a function of strain. Yet, in terms of the performance of a material and also concerning the transfer capability of processing methodologies, the uniformity of the resulting microstructure plays a significant role.

As described in section 2, two NiTi alloys of slightly different compositions have been subjected to HPT or RCR []. While the strain metric might be calculated such that both processing treatments are comparable, the microstructures observed are not! In fact, RCR-processing up to a true strain of $\varepsilon = 16.8$ yields a uniform and mostly amorphous microstructure with some isolated nanocrystals of about 10 nm in diameter that are uniformly dispersed. In contrast, HPT treatment of NiTi leads to microstructures that are non-uniform even on a macroscopis scale.

Particularly, even after more than 10 revolutions under an applied pressure of 6 GPa, clusters of nanocrystals are abundant. Additionally, the comparison of the enthalpy releases of the samples treated by RCR and HPT until microstructural saturation was reached showed that the RCR-processed sample released almost two times the enthalpy that was released by the HPT-treated samples. This result clearly shows that the deformation-induced phase transformation was more pronounced in the RCR-treated sample.

3.2 "Non-equilibrium" grain boundaries?

In ultrafine-grained materials the possible existence of non-equilibrium grain boundaries is a long-standing issue. Recent results obtained by radiotracer diffusion measurements have clearly indicated that severe deformation leads to the formation of interconnected pathways for diffusion that have an increased specific mobility [11-19]. In order to analyze whether structural indications and indications from diffusion measurements for grain boundaries with significantly enhanced specific energy densities (and resulting enhanced mobility) can be found, the GPA method has been applied to high resolution TEM (HRTEM) images. Figure 1a shows a HRTEM image of a grain boundary joining <110>-oriented grains in a $Pd_{90}Ag_{10}$ alloy that has been severely deformed by the RCR method. Using two different g-vectors, atomic level strain maps of the grain boundary region were calculated by geometric phase analysis (GPA). Clearly, a "zipper-like" structure is visible in the in-plane rigid-body rotation (Fig. 1b) along the grain boundary, which is about 1.5 nm in width. This width, determined by the variation of the area-averaged strain with respect to a direction perpendicular to the grain boundary is considerably larger than the width of relaxed high angle grain boundaries as measured by structure sensitive methods, such as GPA or by diffusion analyses. Hot spots (red or yellow colors) refer to dislocation cores. This topology of the strain distribution at this grain boundary in the severely strained Pd-Ag alloy clearly serves to contribute an enhanced excess free energy density contribution to the grain boundary energy, supporting the existence of "non-equilibrium" grain boundaries after SPD processing.

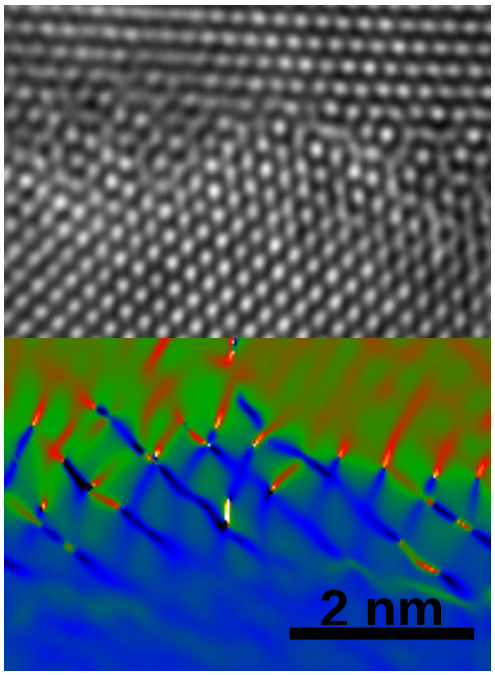

Fig. 1a (up) HRTEM image of a grain boundary in a Pd-Ag alloy after severe straining by RCR.

Fig. 1b (down) in-plane rigid-body rotation of the area shown in Fig. 1a. Rotations on a scale from -50° to +60° (anticlockwise positive) are displayed. Hot spots refer to dislocation cores. The greenish color of the upper grain represents the zero distortion taken as reference.

However, upon analyzing the diffusion data in detail, especially its time dependence, deviations from the linear dependence of the specific relative activity of the tracer with the diffusion depth squared are systematically observed. After analyzing this data for a range of pure metals and

alloys, it can be concluded that the defect accumulation during severe plastic deformation leads to the formation of a fraction of the grain boundaries with enhanced excess free energy density. Depending basically on the homologous temperature during processing, these high-energy grain boundaries, that might be termed “non-equilibrium” grain boundaries, are transformed to open porosity. In cases, where the material had not been exposed to higher homologous temperatures and where the relaxation time of the non-equilibrium grain boundaries had not been exceeded during processing, the characteristics of these high energy grain boundaries can still be observed. However, at increasing temperatures and/or times, these grain boundaries are likely to transform to percolating porosity.

4. CONCLUSIONS

Severe plastic deformation and particularly the combination of different SPD methods sequentially can yield new microstructures with extremely fine grain sizes and unique macroscopic properties. However, the processing routes affect strongly the resulting microstructure and particularly the occurrence of mesoscopic defects such as a percolating porosity network. From the limited data available, it seems that uniform shear with the activation of different glide systems during the repetition of the straining process, as present during the RCR process, provides conditions for extremely efficient microstructure refinement. Moreover, using radiotracer studies as sensitive probe for detecting interconnected porosity revealed that an increased hydrostatic component during the severe straining contributes to a reduction or even avoidance of percolating porosity after the deformation processing. Combined studies by high resolution TEM utilizing GPA to evaluate the local strain fields with radiotracer diffusion studies revealed the occurrence of a fraction of grain boundaries with increased residual strain. Along these grain boundaries in the adjacent grains, high dislocation densities were observed. These samples also showed a diffusion component with enhanced short circuit diffusivity that was attributed to grain boundaries with enhanced excess free energy density. The role of these “non-equilibrium” grain boundaries for the macroscopic performance is not known and neither is the role of the network of percolating porosity. However, indications from the present set of experiments exist, that the non-equilibrium grain boundaries might relax via thermally activated porosity formation. Such mesoscopic defects might act as classical stress concentrators, but might also serve to pin grain boundary motion such that an effective stabilization of the microstructure occurs. Additional scenarios involving the elution of agents for self-healing applications or for ultra rapid mass transport

In the end, however, it will be necessary to fully characterize and understand the relationship between processing pathways, microstructure evolution on all length scales and the resulting macroscopic properties and performance to utilize the full potential of the advanced materials that are available through giant straining processing.

5. REFERENCES

[1] R. Z. Valiev, M. J. Zehetbauer, Y. Estrin, H. W. Höppel, Y. Ivanisenko, H. Hahn, G. Wilde, X. Sauvage, H.J. Roven, T.G. Langdon: Adv. Eng. Mater. 9 (2007) 527-533.

[2] R. Z. Valiev, R. K. Islamgaliev, I. V. Alexandrov: Prog. Mater. Sci., 45 (2000) 103-189.

[3] G. P. Dinda, H. Rösner, G. Wilde: Scripta Materialia, 52 (2005) 577-582.

[4] G. Wilde, H. Rösner, G. P. Dinda: Adv. Eng. Mater. 7 (2005) 11-15.

[5] G. Wilde, N. Boucharat, G. P. Dinda, H. Rösner, R. Z. Valiev: Mater. Sci. Forum 503-504 (2006) 425-432.

[6] G. Wilde: Mater. Sci. Forum 579 (2008) 109-134.

[7] H. Rösner, N. Boucharat, J. Markmann, K. A. Padmanabhan, G. Wilde: Mater. Sci. Eng. A 525 (2009) 102-106.

[8] H. Rösner, N. Boucharat, K. A. Padmanabhan, J. Markmann, G. Wilde: Acta Mater. 58 (2010), 2610-2620.

[9] A. A. Nazarov, A. E. Romanov, R. Z. Valiev: Acta Metall. Mater. 41, (1993) 1033-1040.

[10] A. A. Nazarov, A. E. Romanov, R. Z. Valiev: Scripta Metall. Mater. 24, (1990) 1929-1934.

[11] S. V. Divinski, G. Wilde, E. Rabkin, Y. Estrin: Adv. Eng. Mater. 12 (2010) 779-785.

[12] G. Wilde, J. Ribbe, G. Reglitz, M. Wegner, H. Rösner, Y. Estrin, M. Zehetbauer, D. Setman, S. Divinski: Adv. Eng. Mater. 12 (2010) 758-764.

[13] S. V. Divinski, G. Reglitz, H. Rösner, G. Wilde: Acta Mater. submitted.

[14] Z. B. Wang, K. Lu, G. Wilde, S. Divinski: Appl. Phys. Lett. 93 (2008) 131904.

[15] S. V. Divinski, J. Ribbe, D. Baither, G. Schmitz, G. Reglitz, H. Rösner, K. Sato, Y. Estrin, G. Wilde: Acta Mater. 57 (2009) 5706-5717.

[16] S. V. Divinski, J. Ribbe, G. Reglitz, Y. Estrin, G. Wilde: J. Appl. Phy. 106 (2009), 063502.

[17] S. V. Divinski, G. Reglitz, G. Wilde: Acta Mater. 58 (2010) 386-395.

[18] Z. B. Wang, K. Lu, G. Wilde, S. Divinski: Acta Mater. 58 (2010) 2376-2386.

[19] S. V. Divinski, G. Reglitz, H. Rösner, G. Wilde, Y. Estrin: Acta Mater. submitted.

[20] R. Singh, S. V. Divinski, J. H. Schneibel, G. Wilde: Acta Mater. accepted.

[21] M. Peterlechner, J. Bokeloh, G. Wilde, T. Waitz: Acta Mater. 58 (2010) 6637-6648.

[22] R. Singh, S. V. Divinski, H. Rösner, E. A. Prokofyev, R. Z. Valiev, G. Wilde: Phil. Mag. accepted.

Acknowledgements

The author is grateful for severe plastic deformation treatments performed in the groups of Prof. R.Z. Valiev (USATU, Ufa, Russia), Prof. Y. Estrin (Monash University, Clayton, Australia), Prof. R. Pippan (Erich Schmid Institute, Leoben, Austria) and Prof. M. Zehetbauer (University of Vienna, Austria). The author also acknowledges the financial support by the Deutsche Forschungsgemeinschaft (DFG).

This contribution was created within the project Creation of an international scientific team and incorporation to scientific networks in the area of nanotechnology and unconventional forming material. CZ.1.07/2.3.00/20.0038, which is financed by the European Social Fund and state budget of the Czech Republic.

european social fund in the czech republic
EUROPEAN UNION
MINISTRY OF EDUCATION, YOUTH AND SPORTS
OP Education for Competitiveness
INVESTMENTS IN EDUCATION DEVELOPMENT

Strength and ductility improvement of ECAP processed aluminium alloy 7075

Jozef ZRNÍK [a], Martin FUJDA[b], Petr SLAMA [a], Libor KRAUS [a]

[a] *COMTES FHT Inc., Dobrany, Czech Republic, jzrnik@comtesfht.cz*

[b]*Technical University of Košice, Department of Materials Engineering, 04001 Košice, Slovak Republic, Martin.Fujda@tuke.sk*

Abstract

Strength of materials subjected to severe plastic deformation can be significantly improved due to ultrafine grain structure formation. The impact of various strain levels ε_{ef} on structure refinement and proportions different portions of grains with high angle boundaries and subgrains having low angle boundaries is present. Any severe plastic deformation procedure (ECAP, HPT, ARB, CGP) refines grains to size below 1000 nm and is usually accompanied by strength increase and reduction in ductility.

In order to improve the deformation behaviour of SPD prepared aluminium alloy AA7075 microstructure modification by ageing due to various holds at precipitation temperature prior to ECAP processing and post-deformation treatment were carried out. Over-aging process carried out prior severe deformation modified the characteristics of precipitates (intermetallic phases) present in alloy. The microstructure refined by intensive deformation was then altered by various annealing procedures. Ageing prior to ECAP contributed to a small increase in strength, as hardness results, as shown by results of hardness measurement and observation of microstructure. On the other hand, podt-deformation annealing of the ECAP-ed samples at various temperatures markedly modified the deformation response of the alloy as regards ductility. Evaluating the mechanical properties a small increase in strength was achieved at lower temperature of at lower temperatures of annealing (250°C, 300°C), whereas the highest temperature of annealing (350°C) preserved the strength at the same level as in samples without any additional post-deformation annealing. The microstructure analyses (TEM and EBSD) provided evidence about the ultrafine grain structure transformation towards bimodal structure. These preliminary results of purposeful structure modification will be further examined in regard to strength.

Keywords

Al alloy, microstructure, precipitation, ECAP deformation, annealing, EBSD, strength, ductility

1. INTRODUCTION

Severe plastic deformation (SPD) of metals and alloys leads to grain refinement and to formation of a nanocrystalline structure [1]. The structural changes caused by SPD are reflected in improved mechanical properties of pure metals and alloys [2]. The effects include increased

hardness and yield stress, while ductility drops. While a number of know methods of grain refinement, such as rapid solidification, vapor deposition, powder processing and thermomechanical processing, are employed and practiced, the process of SPD has proved to be an effective approach for manufacturing larger quantities of ultrafine grain metals and alloys. Equal channel angular pressing (ECAP) and other methods of SPD (HPT, CGP, ARB and others) proved to be effective methods for grain refinement down to hundreds of nm in range of 200 – 1000 nm. Repeating the SPD deformation to ensure overlapping of shear zones resulting from individual passes within the bulk material causes extensive strain value zones resulting from individual passes within the bulk material causes extensive grain subdivision and formation of fine grain microstructure, in dependence on the effective strain value introduced.

The first aim of this study was to assess the prior-precipitation effect in AA7075 Al alloy due to variation of annealing condition on UF grain structure formation and mechanical properties resulting from ECAP straining. Consequently, the thermal stability of resulted UFG structure, with aim of precipitation effect modification and then the effect of further post-deformation thermal treatment were evaluated with respect to modification of deformed ultrafine grain structure and with respect to retain the mechanical strength and to improve the plastic deformation properties.

Aluminium alloy AA7075 was used for severe plastic deformation experiment. Prior severe plastic deformation the alloy microstructre was conditioned with aim to obtain different initial precipitation characteristics of fine precipitates of intermetallic particles in matrix, due to various conditions of annealing executed prior annealing. The refined microstructure resulting from Equal Channel Angular Pressing (ECAP) exposed to effective strain εef – 4 was then altered by post-deformation annealing at different temperatures in range 250 – 350°C. A purpose of this annealing was to modify deformed structure with respect to balance strength and plasticity. Different ageing prior to ECAP contributed to a small increase in strength of initial alloy. Post deformation annealing of the ECAP bars markedly modified the deformation response of the alloy as regards ductility and strength. The microstructure analyses (TEM and EBSD) provided evidence on the ultrafine grain structure modification (degradation) and resulted mechanical properties. The first aim of this study was to assess the effect of prior precipitation in AA7075 aluminium alloy on formation of UFG.

2. PROCEDURES, RESULTS AND DISCUSSION.

A commercial aluminum alloy AA7075 was experimental materials employed for grain refining using severe plastic deformation with respect to evaluate the initial structural condition to modify deformation behaviour of resulted ultrafine grain structure. Four different initial structural states of alloy, characterized by different precipitates characteristics, were prepared by combination of solutioning at 500°C/1.5h/H_2O followed by ageing at temperature of 200°C varying hold time of ageing. The four quite long ageing holds of 107h, 180h, 300h and 515h were executed to modify the precipitates characteristics of various intermetallic phases (Mg_2Zn, $CuAl_2$, $Mg(Zn,Al,Cu)_2$), which used to be potential precipitates in specific alloy. Finalized this precipitation experimental a uniform precipitates distribution within grains and along the grain boundaries was observed in annealed structure of all states. However, the differences in precipitates morphology, size (coarsening), and volume fraction in aged structures resulted from different applied hold time were evident. The effect of long term annealing on mechanical strength and ductility was verified in condition of tensile test. The small drop in mechanical strength was observed, due to overageing, causes precipitates coarsening as the hold time increased.

2.1 The microstructure modification

In order to refine microstructure (grains) in annealed structures, large plastic deformation of bulk material was applied. The equal channel angular pressing deformation method (ECAP), with channel angle of 90° and with back pressure (100 tonnes), was carried out at room temperature. The Bc deformation route was employed and total effective deformation performing 4 passes was εef = 4. Considering the initial structure characteristics resulting from different long time of annealing at 200°C, prior applied ECAP deformation, the refined homogenous ultrafine grain structures for all thermal exposures of ageing was yielded, as presented in fig. 1a,b,c,d.

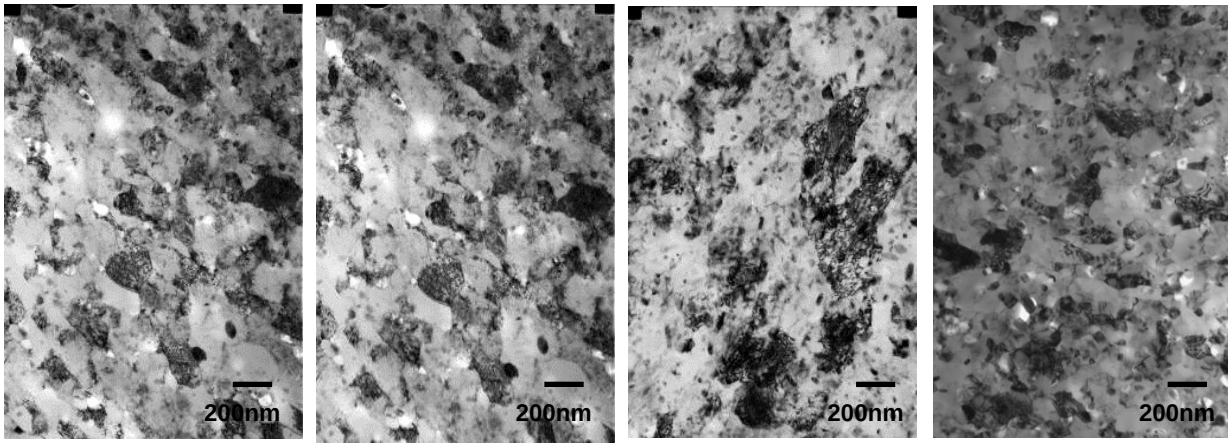

Fig. 1. TEM micrographs of ECAP deformed microstructures obtained from different initial structural conditions upon an effective strain ε_{ef} – 4

Microstructures of all specimens annealed for various times were examined using diverse investigation methods including light and transmission electron microscopy (TEM), diffraction analysis and electron back scattered diffraction (EBSD). The obtained results showed not too expressive difference in modification of grain refining characteristics with regards to different initial structural characteristics of alloy. The effect of different hold times at selected increased temperature to modify the initial structure, considering particular precipitation characteristics (coherency, size, distribution density of particles), showed indistinctive influence on microstructure resulting from ECAP refining. The refined microstructures characteristics resulted from ECAP condition were very similar for all initial structures conditions, resulting from prior long term annealing. The presence of secondary phase particles in the matrix prior refining, as results show, provided only negligible contribution to stabilize grain refinement by pinning effect. Also the there was negligible effect of particles to stabilize ultrafine structure when exposed to post-deformation annealing at different temperature. When increasing temperature the over to 250°C and above, polygonization and recovery processes were activated and resulted in UFG structure modification. At higher temperature of annealing (300°C) recrystallization process was then in progress and strongly modified the UFG structure.

2.2 Deformation behaviour and mechanical properties

The deformed structure and mechanical properties of ECAPed material can be modified in certain extent by structure modification prior ECAP and/or by modification of post-deformed ECAP microstructure. The thermal effect of structure modification prior ECAP deformation, as results for experimental alloy showed, modified the microstructure inexpressively as to UF grain formation. In case a post-deformation structure modification structure should be carried out a thermal effect for structure modification is the most accessible. In order to testify this option the

ECAP structure stability was testified in different condition of post-deformation heating. The structure modification and tensile properties were to evaluate in dependence of varying temperature while hold time was kept constant. From series of experimental the most convenient combination of strength and ductility was achieved for the highest temperature selected of 350°C. The achieved combination of mechanical strength and ductility appears to be the optimum and impressive result with respect to formation the bimodal structure, where residue of ultrafine grained structure and already recrystallized areas are co-existing in the microstructure. The deformation results and records are shown in Fig. 2. The effect of post-deform annealing appeared to be effective for plasticity improvement of alloy when still keeping high strength.

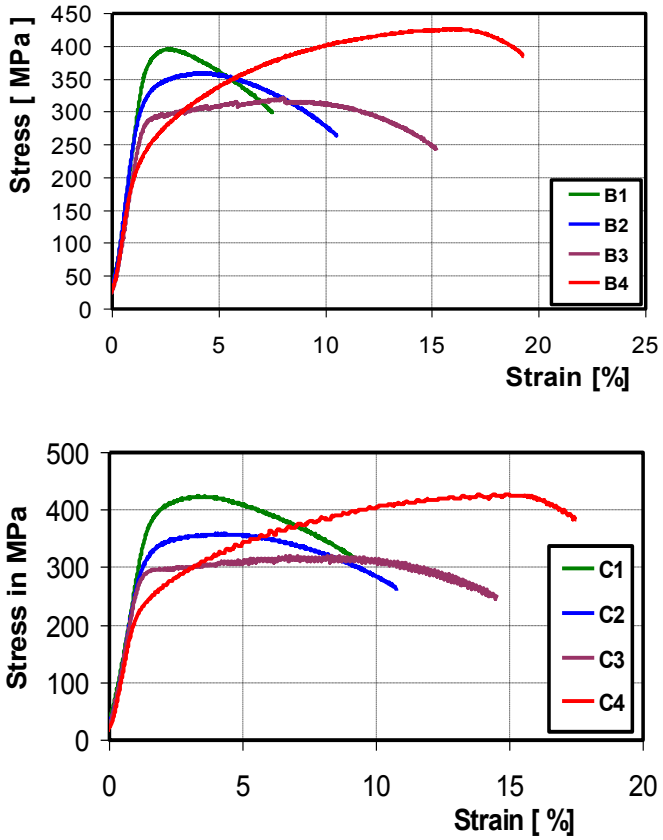

Fig. 2 Strength and ductility of ECAP-ed and post-deformed thermally exposed alloys B and C for different conditions of post deformation annealing 1h: B1, C1 – no anneling; B2,C2 - annealing 250°C/1h; B3, C3 – annealing 300°C/1h; B4, C4 – annealing 350°C/1h

3. CONCLUSIONS

1. Effect of prior ECAP alloy annealing to modify the characteristics of precipitates showed a negligible effect on modification of precipitates characteristics in matrix.

2. The bimodal structure resulting from post-deformation thermal exposure of ECAP structure showed improved both strength and plasticity.

4. LITERATURE

[1] Love T. C. and Valiev R. Z. (Eds.), “Investigation and Application of Severe Plastic Deformation, Kluwer, Dordrecht, 2000.

[2] Langdon T. G., Furakava M., Nemoto M., Horita Z., 2000, “Using Channel Angular Pressing for Refining Grain Size”, JOM, 52, 4, 30 – 33.

Acknowledgement

This contribution was created within the project **Creation of an international scientific team and incorporation to scientific networks in the area of nanotechnology and unconventional forming material. CZ.1.07/2.3.00/20.0038**, which is financed by the European Social Fund and state budget of the Czech Republic.